Programmable Assembly of Pi-Conjugated System Utilizing the Stereochemistry of Aromatic Tertiary Amide Unit

Ryohei Yamakado

2014

Field of Organic Materials, Department of Materials Science and Engineering,

Graduate School of Engineering, Nagoya Institute of Technology

Contents

Chapter 1

General Introduction

<Arrangement of π-Conjugated Molecules>

π-Conjugated molecules play an important role in various optoelectronic devices including light-emitting diodes (LED)s[1], field-effect transistors (FET)s[2], and solar cells[3]. π-Conjugated molecules normally have the highly planar structure leading to the self-aggregation such as the face-to-face π-π stacking and the edge-to-face herringbone packing. The large overlap of π-electron between neighboring molecules is crucial to enhance the charge carrier mobility of semiconducting materials. On the other hand, the dense packing of π-conjugated molecules decreases or quenches the light emission from compounds, and this is the shortcoming for applying to the luminescent devices. Accordingly, three-dimensional arrangement of π-conjugated molecules should be precisely designed in response to the application. The aggregation pattern between π-conjugated molecules has been studied intensively from over three quarter century. In 1937, Jelley et al. discovered that cyanine dyes in concentrated aqueous solution with molecular assemblies exhibit a large red-shift of their absorption band as compared with that in diluted solution. This phenomenon was named Jelley (*J*-) or Scheibe aggregate in honor of their discovery.[4] *H*-aggregate (H for hypsochromic) is another aggregation pattern of dyes, which leads to a blue-shift of their absorption band.[5] Thus the measurement of the absorption spectra is a powerful tool to investigate the aggregation pattern of π-conjugated molecules. In order to achieve the controlled arrangement of π-conjugated molecules, there are two possible strategies; (i) the chemical modification of π-conjugated molecules and (ii) the utilization of a well-defined tethering unit. For an example of the first approach, Kobayashi et al. introduced the thiomethyl groups at the 6- and 13-positions of pentacene (Figure 1a).[6] As a result of S-S and S-π interactions, the modified pentacene adopts the cofacial packing, although unmodified pentacene has the herringbone packing. Tohnai et al. succeeded in the modulation of π-stacked arrangement of anthracene-1,5-disulfonic acid by choosing the chemical structure of

co-crystallized aliphatic amines. The variation of the three-dimensional arrangement of anthracene skeletons in crystals including face-to-face slipped column, zigzag column, and brick-like arrangement showed multiple photoluminescence colors (Figure 1b and 1c).[7] In these methods, the three-dimensional structure of π-conjugated molecules relies on the non-covalent bond interactions and is difficult to be predicted. On the other hand, the second approach based on the covalent bond would be much reliable because the three-dimensional structure of π-conjugated molecules are determined by the shape of template molecules. In this PhD thesis, I have investigated the three-dimensional arrangement of various π-conjugated molecules using well-defined cyclic oligomers.

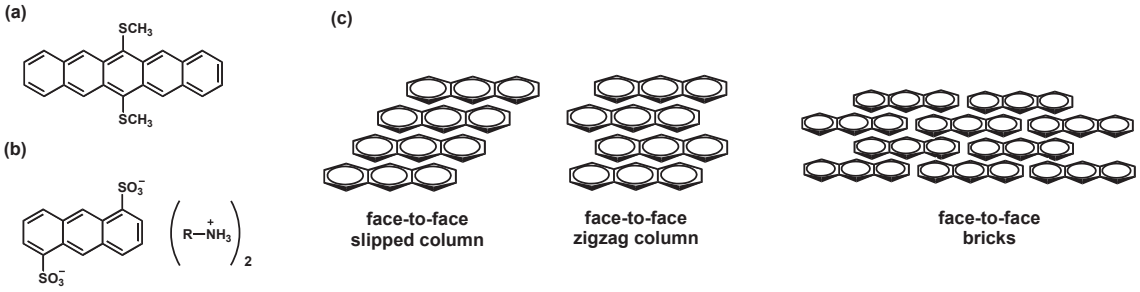

Figure 1. Chemical structures of (a) functionalized pentacene and (b) organic salt of an anthracene derivative. (c) Schematic representation of the different arrangement of anthracene; face-to-face slipped column, zigzag column, and brick-like arrangement.

<Three-Dimensional Arrangement of π-Conjugated Molecules Supported by Cyclic Oligomers>

Cyclic oligomers including calixarene, cyclophane, pillararene, and cyclodextrin have unique cavities and have been attracting much attention in the field of host-guest chemistry (Figure 2).[8] On the other hand, the definite conformations of these cyclic oligomers are useful as the template for the three-dimensional arrangement of various functional groups attached to the edge of the molecules.

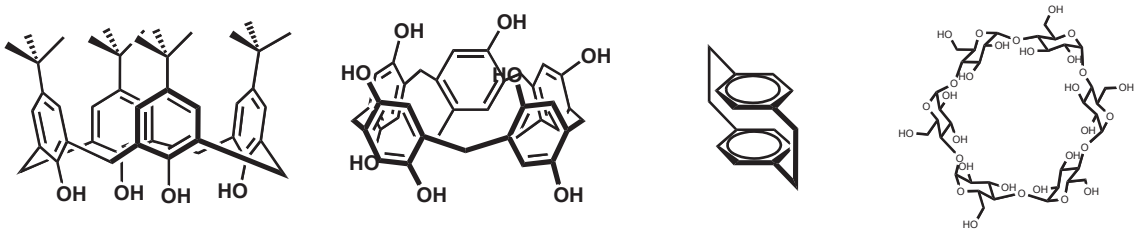

Figure 2. Chemical structures of calix[4]arene, pillar[5]arene, [2.2]paracyclophane, and α-cyclodextrin.

Since cyclophane compounds such as dithia[3.3]metacyclophane and [2.2]paracyclophane[9] prefer the face-to-face conformation of two benzene rings, these compounds can be used as the template for the three-dimensional arrangement of π-conjugated molecules. In particular, [2.2]paracyclophane forces two benzene rings in close proximity each other (ca. 3 Å), which enables the through-space π-electron interaction between appended π-conjugated molecules. Tsuge et al. achieved the spatial arrangement of oligothiophene chromophores (n=1~5) using dithia[3.3]metacyclophane (Figure 3).[10] The equilibrium between two conformers was studied by VT-NMR spectra, and the compound adopted the *syn* conformer in the crystalline state. As a result of the close arrangement of π-conjugated system, an excimer emission was observed even in the diluted solution.

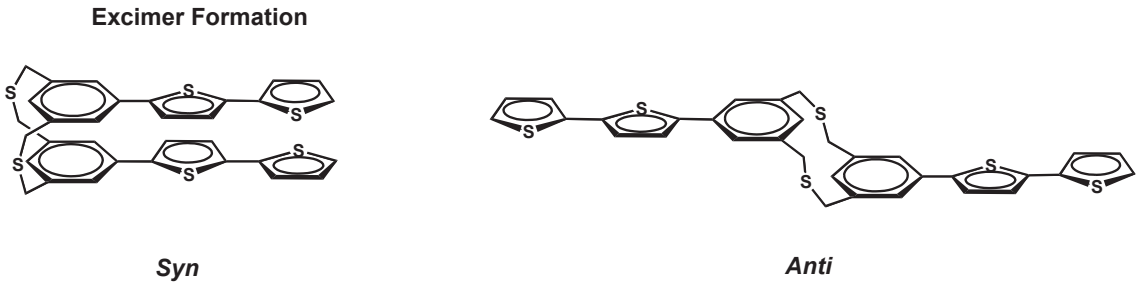

Figure 3. Chemical structures of *syn* and *anti* isomers of dithia[3.3]metacyclophane bearing oligothiophene chromophores.

Through-space π-conjugated polymers containing the [2.2]paracyclophane units were prepared by Morisaki et al. through the palladium-catalyzed cross-coupling reaction (Figure 4).[11] From the measurement of UV-vis absorption and fluorescence spectra, these polymers showed excellent charge and energy transfer properties. The high quantum yields were obtained despite the π-stacked structure.

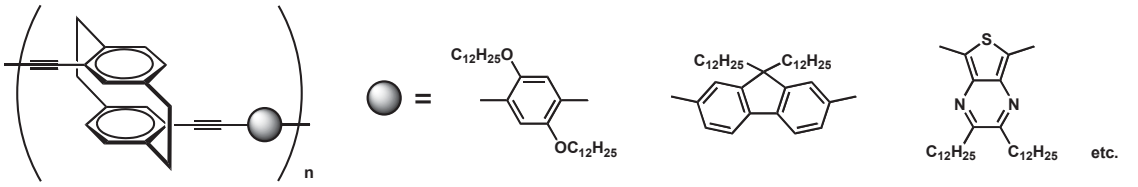

Figure 4. Chemical structures of [2.2]paracyclophane-containing through-space conjugated polymers.

Calix[4]arene is a cyclic tetramer made up of alternating phenol and methylene units.[12] The rotation of phenol moiety allows various conformations. Among them, "cone isomer" would be suitable for the template as the three-dimensional arrangement of π-conjugated molecules, because the substituents on the upper rim are positioned at the same side.[13] Wong et al. introduced oligothiophene chromophores into the calix[4]arene (Figure 5).[14] The close proximity of the tetra-oligothiophenes lead to the blue-shift in

the absorption and red-shift in the emission spectra. The fluorescence quantum yield was decreased as compared with that of the model compound corresponding to the repeating unit. These phenomena can be interpreted as a result of the intramolecular chromophore interaction .

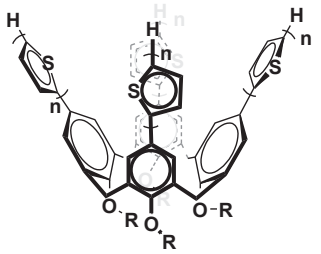

Figure 5. Chemical structure of calix[4]arene bearing oligothiophene chromophores

Würthner et al. prepared the zigzag array of three different perylene bisimide chromophores using the calix[4]arene scaffold, and demonstrated sequential energy and electron transfer cascades.[15] The Calix[4]arene plays an important role for providing defined distance and angle between the chromophores to inhibit the fluorescence quenching and energy loss.

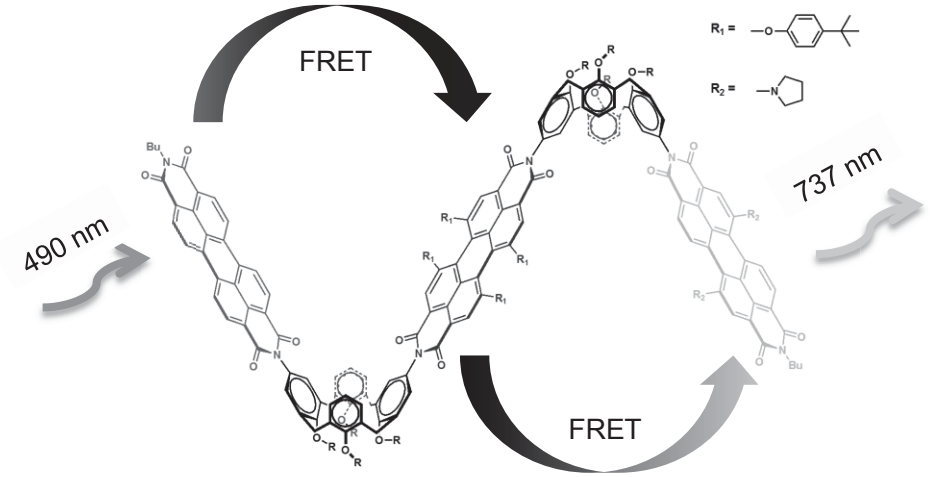

Figure 6. Sequence-controlled perylene bisimides array using calix[4]arene scaffold.

As shown in above, cyclic oligomers are suitable templates for the three-dimensional arrangement of π-conjugated moieties, and the conformation and optoelectronic properties of π-conjugated moieties depend on the character of the template. Accordingly, the precision arrangement of π-conjugated molecules using novel cyclic oligomer is quite interesting to obtain novel photophysical and electronic properties of π-conjugated molecules.

<Stereochemistry of Aromatic Tertiary Amide>

***N*-Methylbenzanilide**

The crystal structure of *N*-methylbenzanilide was initially revealed by Shudo et al. in 1989.[16] *N*-Methylbenzanilide exists in the *cis* form in the crystal state, although *N*-unsubstituted benzanilide exists in the *trans* form both in the crystal and solution states.[17, 18] The *cis* preference of *N*-methylbenzanilide in solution was also confirmed by the ^{1}H NMR spectroscopy. Moreover, Shudo et al. showed the steric influence of the ortho-substituent on the conformation (Table 1).[19] *N*-Methylbenzanilide derivatives mostly exist in the *cis* forms in the crystal state. In solution, the *trans/cis* ratio was increased with increasing the number of methyl substituents.

Table 1. *Trans*/*cis* ratio of *N*-methylbenzanilide derivatives **1**–**7**.

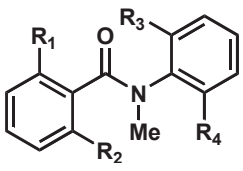

Compound	R^1	R^2	R^3	R^4	*trans* : *cis*
1	H	H	H	H	1 : 99
2	Me	H	H	H	10 : 90
3	Me	Me	H	H	33 : 67
4	H	H	Me	H	6 : 94
5	H	H	Me	Me	8 : 92
6	Me	H	Me	H	22 : 78
7	Me	Me	Me	Me	100 : 0

Character of Cyclic Amide Trimer; Calix[3]amide

The stepwise synthesis of *meta*-cyclic amide trimer (calix[3]amide) was first reported by Stoddart et al. in 1982 (Scheme 1).[20] In 1996, Shudo et al. developed the one-step formation of calix[3]amide (Scheme 1).[21] Due to the *cis* preference of the *N*-alkylbenzanilide skeleton (vide supra),[16] calix[3]amide can be efficiently synthesized by the condensation reaction of *meta*-(*N*-methylamino)benzoic acid with tetrachlorosilane or dichlorotriphenylphosphorane.[22] Yokozawa et al. also reported the synthesis of the cyclic amide trimer with the large inner cavity from monomers bearing 4-alkylamino and 4'-methoxycarbonyl groups using lithium bis(trimethylsilyl)amide (LiHMDS) (Scheme 1).[23]

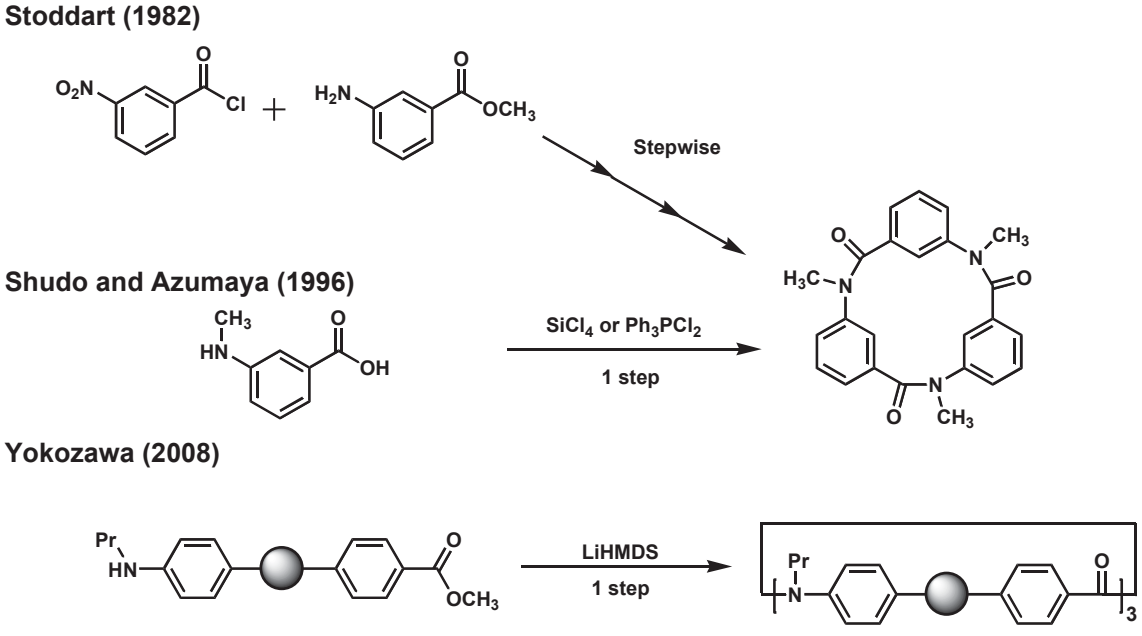

Scheme 1. Synthetic routes to cyclic amide trimers.

Calix[3]amide has two conformers, in which the *syn* conformer has three benzene rings in the same orientation relative to the amide bond and the *anti* conformer has one

benzene ring turning in other direction. The equilibrium between two conformers was investigated by VT-NMR spectra,[21] and the *syn* conformer generally prefers to the *anti* conformer (Figure 7). The influence of the substituent at the 5-position on the energy barrier between the *syn* and *anti* conformers in solution was discussed (Figure 8; **8**~**12**).[24] The *syn*/*anti* ratio of each compound was dependent on the temperature. The percentage of the *syn* conformer increased with increasing the solvent polarity because of the larger dipole moment of the *syn* conformer. Functionalization of calix[3]amide was also reported. For example, the calix[3]amide bearing the carboxylic acid group was synthesized (Figure 8; **13**).[25] The hydrogen bonding interaction with chiral amines resulted in the chiral induction on the calix[3]amide skeleton in solution, and the capsule-type homo-dimer was obtained in the crystalline state.

Interestingly, calix[3]amide has a planar chirality based on the direction of the amide bond. However, the optical resolution of enantiomers was impossible owing to the easy racemization through the conformational exchange in solution (Figure 7; *syn* and *syn'*). In order to suppress the conformational exchange, the spherical aromatic amide compound consisting of four calix[3]amide rings was synthesized, and the optical resolution was successfully achieved by chiral HPLC (Figure 8; **14** and **14'**).[26]

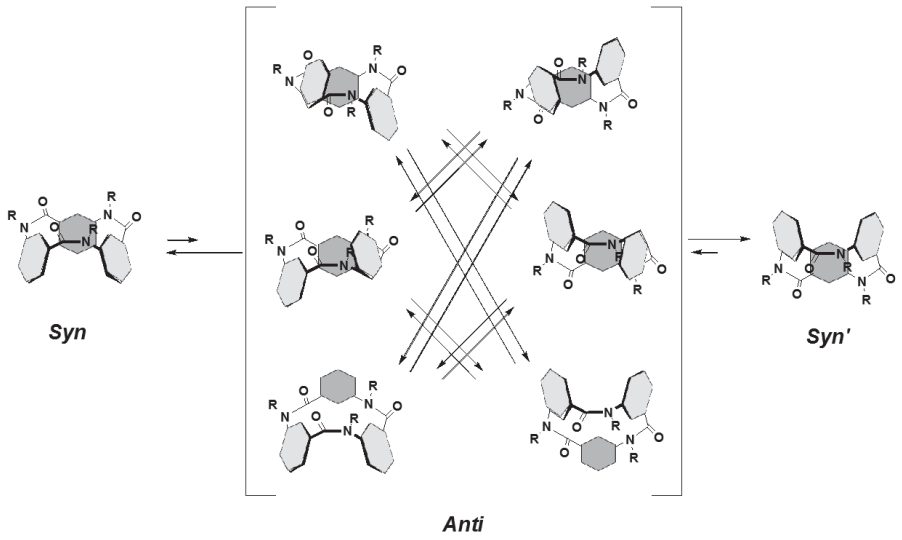

Figure 7. Schematic representation of equilibria of calix[3]amide.

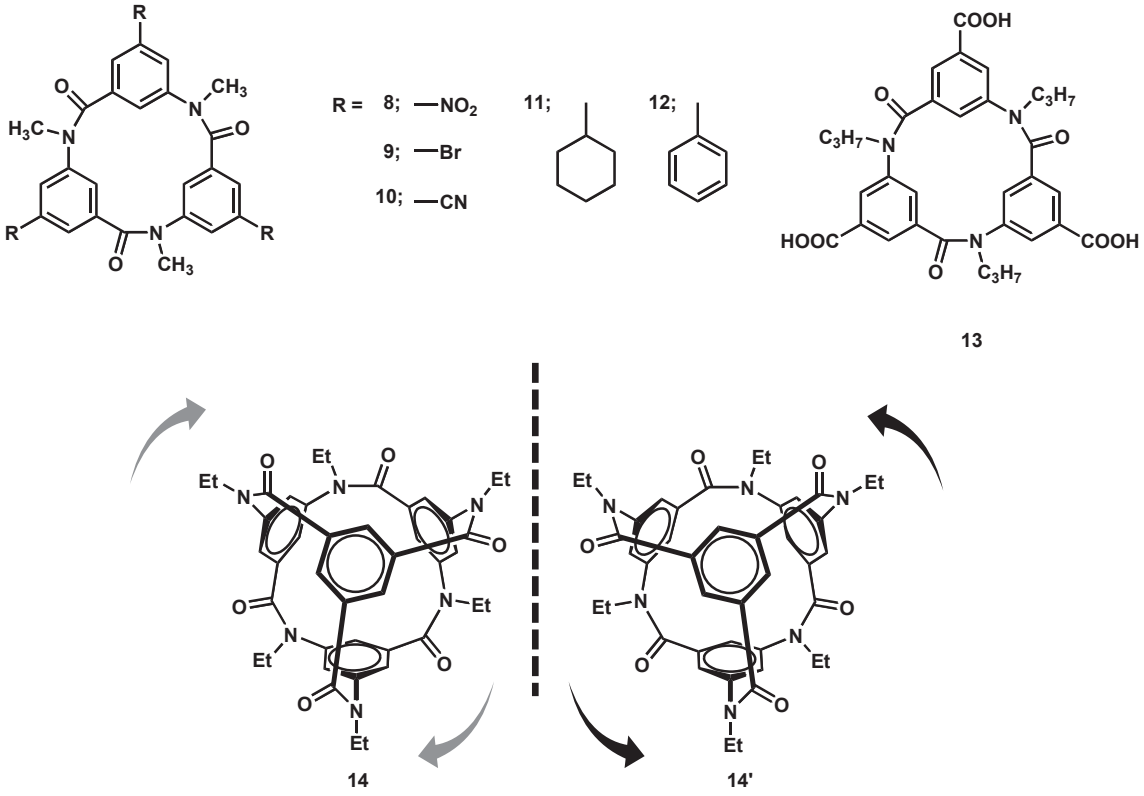

Figure 8. Chemical structures of calix[3]amide derivatives **8**~**13** and enantiomeric structure of **14**.

Although the conformation analysis and the host-guest chemistry were investigated, calix[3]amide has not been used as the template for the three-dimensional arrangement of π-conjugated molecules yet. The author focused on three exclusive properties of calix[3]amide; 1) facile introduction of substituents, 2) conformation character depending on the solvents, 3) molecular chirality based on the direction of the amide bond. Based on the stereochemistry of the aromatic tertiary amide, it would be possible to carry out the precision arrangement of π-conjugated molecules.

Survey of This Thesis

On the basis of these backgrounds, this thesis deals with a development of programmable assembly of π-conjugated systems by the stereochemistry of the aromatic amide.

In Chapter 2, the preparation of the molecular cage composed with calix[3]amide through pyridine-palladium interaction is described. The calix[3]amide having pyridine moieties on the benzene rings was prepared. The conformation was studied using ^{1}H NMR spectra to find out the conformational preference in the solution. The molecular cage was prepared from the 2:3 mixture of the calix[3]amide and [Pd(dppp)(OTf)$_2$] in $CDCl_3$/CD_3OD (5/1 in volume) via pyridine-palladium coordination. The effect of the solvent character on the formation of this molecular cage was discussed.

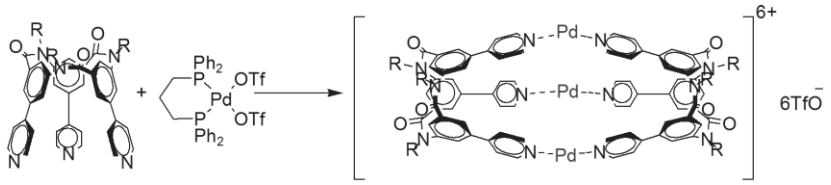

In Chapter 3, the screw-shaped arrangement of pyrene moieties by the conformation of calix[3]amide is described. The calix[3]amide bearing three pyrenes was prepared by the condensation reaction. The structure was investigated in the crystalline and solution states by the single X-ray crystallography and ^{1}H NMR spectroscopy, respectively. The origin for unique optical properties is discussed.

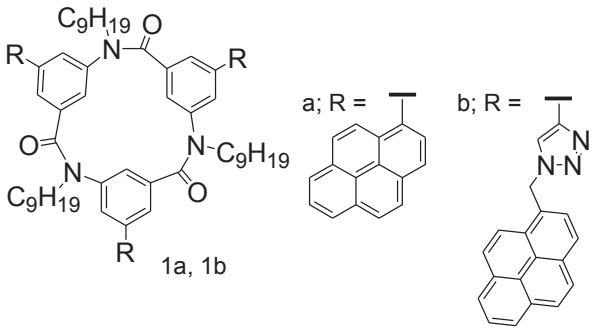

In Chapter 4, the triple-stranded arrangement of bithiophene moieties by the conformation of calix[3]amide is described. The tubular molecule was obtained, in which three bithiophene moieties were covalently connect to two calix[3]amide. The mechanism of chirality transmission from the calix[3]amide to three bithiophenes is discussed.

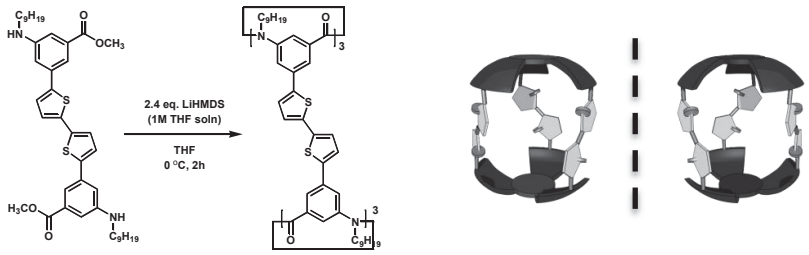

In Chapter 5, the triangular arrangement of anthracene moieties based on the cyclic triamide skeleton is described. The cyclic amide trimer containing 9,10-diphenylanthracene was prepared by the condensation reaction. The reduction of the carbonyl groups gave the cyclic amine trimer. The electronic state before and after the reduction is discussed.

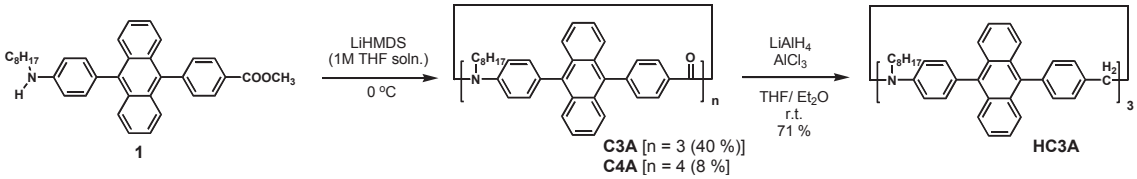

Reference and Notes

1. (a) Tang, C. W.; Vanslyke, S. A. *Appl. Phys. Lett.* **1987**, *51*, 913 – 915. (b) Burroughes, J. H.; Bradley, D. D. C.; Brown, A. R.; Marks, R. N.; Mackay, K.; Friend, R. H.;Burns, P. L.; Holmes, A. B. *Nature* **1990**, *347*, 539 – 541.
2. (a) De Silva, A.P.; Gunaratne, H. Q. N.; Gunnlaugsson, T,; Huxley, A. J. M.; McCoy, C. P.; Rademacher, J. T.; Rice, T. E. *Chem. Rev.* **1997**, *97*, 1515 – 1566. (b) Chabincy, M. L.; Salleo, A. *Chem. Mater.* **2004**, *16*, 4509 – 4521.
3. (a) Tang, C. W. *Appl. Phys. Lett*. **1986**, *48*, 183 – 185. (b) Hoppe, H.; Sariciftci, N. S. *J. Mater. Res*. **2004**, *19*, 1924 – 1945. (c) Günes, S.; Neugebauer, H.; Sariciftci, N. S. *Chem. Rev.* **2007**, *107*, 1324 – 1338.
4. (a) Jelley, E. E. *Nature* **1936**, *138*, 1009, (b) Jelley, E. E. *Nature* **1937**, *139*, 631, (c) Scheibe, G. *Angew. Chem.* **1937**, *50*, 51.
5. Brooker, L. G. S.; White, F. L.; Heseltine, D. W.; Keyes, G. H.; Dent S. G.; VanLare E. J. *J. Photogr. Sci.* **1953**, *1*, 173.
6. Kobayashi, K.; Shimaoka, R.; Kawahata, M.; Yamanaka, M.; Yamaguchi, K. *Org. Lett.* **2006**, *8*, 2385 – 2388.
7. Hinoue, T.; Shigenoi, Y.; Sugino, M.; Mizobe, Y.; Hisaki, I.; Miyata, M.; Tohnai, N. *Chem. Eur. J.* **2012**, *18*, 4634 – 4643.
8. Lehn, L. M. *Supramolecular Chemistry-Concepts and Perspective*; VCH: Weinheim, 1995.
9. Brown, C. J.; Farthing, A. C. *Nature* **1949**, *164*, 915.
10. (a) Tsuge, A.; Hara, T.; Motiguchi, T.; Yamaji, M. *Chem. Lett.* **2008**, *37*, 870 – 871. (b) Tsuge, A.; Hara, T.; Motiguchi, T. *Tetrahedron Lett.* **2009**, *50*, 4509 – 4511. (c) Tsuge, A. *J. Synth. Org. Chem., Jpn.* **2010**, *68*, 247 – 261.
11. (a) Morisaki, Y.; Chujo, Y. *Angew. Chem. Int. Ed.* **2006**, *45*, 6430 – 6437. (b) Morisaki, Y.; Chujo, Y. *Prog. Polym. Sci.* **2008**, *33*, 346 – 364. (c) Hopf, H. *Angew.*

Chem. Int. Ed. **2008**, 47, 9808 – 9812. (d) Morisaki, Y.; Chujo, Y. *Bull. Chem. Soc. Jpn.* **2009**, *82*, 1070 – 1082. (e) Morisaki, Y.; Chujo, Y. *Polym. Chem.* **2011**, *2* 1249 – 1257.

12. Ikeda, A.; Shinkai, S. *Chem. Rev.* **1997**, *97*, 1713 – 1734.
13. (a) Larsen, M.; Krebs, F. C.; Jørgensen, M.; Harrit, N. *J. Org. Chem.* **1998**, *63*, 4420 – 4424. (b) Alemán, A.; Zanuy, D.; Casanovas, J. *J. Org. Chem.* **2006**, *71*, 6952 – 6957.
14. Sun, X. H.; Chan, C. S.; Wong, M. S.; Wong, W. Y. *Tetrahedron* **2006**, *62*, 7846 – 7853.
15. Hippius, C.; van Stokkum, I. H. M.; Gsänger, M.; Groeneveld, M. M.; Williams, R. M.; Würthner, F. *J. Phys. Chem. C* **2008**, *112*, 2476 – 2486.
16. (a) Kagechika, H.; Himi, T.; Kawauchi, E.; Shudo, K. *J. Med. Chem.* **1989**, *32*, 2292 – 2296. (b) Itai, A.; Toriumi, Y.; Tomioka, N.; Kagechika, H.; Azumaya, I.; Shudo, K. *Tetrahedron Lett.* **1989**, *30*, 6177 – 6180. (c) Toriumi Y.; Kasuya, A.; Itai, A. *J. Org. Chem.* **1990**, *55*, 259 – 263. (d) Azumaya, I.; Kagechika, H.; Yamaguchi, K.; Shudo, K. *Tetrahedron* **1995**, *51*, 5277 – 5290.
17. The terms "*cis*" and "*trans*" are conventionally used to show the relative positions of aromatic groups connected to the amide unit.
18. Kashino, S.; Ito, K.; Haisa, M.; *Bull. Chem. Soc. Jpn.* **1979**, *52*, 365 – 369.
19. Azumaya, I.; Yamaguchi, K.; Kagechika, H.; Saito, S.; Itai, A.; Shudo, K. *Yakugaku Zasshi* **1994**, *114*, 414 – 430.
20. (a) Elhadi, F. E.; Ollis, W. D.; Stoddart, J. F.; Williams, D. J.; Woode, K. A. *Tetrahedron Lett.* **1980**, *21*, 4215 – 4218. (b) Elhadi, F. E.; Ollis, W. D.; Stoddart, J. F. *J. Chem. Soc. Perkin Trans. I* **1982**, 1727 – 1732.
21. Azumaya, I.; Kagechika, H.; Yamaguchi, K.; Shudo, K.; *Tetrahedron Lett.* **1996**, *37*, 5003 – 5006.

22. (a) Azumaya, I.; Okamoto, T.; Imabeppu, F.; Takayanagi, H. *Tetrahedron* **2003**, *59*, 2325 – 2331. (b) Imabeppu, F.; Katagiri, K.; Masu, H.; Kato, T.; Tominaga, M.; Therrien, B.; Takayanagi, H.; Kaji, E.; Yamaguchi, K.; Kagechika, H.; Azumaya, I. *Tetrahedron Lett.* **2006**, *47*, 413 – 416. (c) Katagiri, K.; Sawano, K.; Okada, M.; Yoshiyasu, S.; Shiroyama, R.; Ikejima, N.; Masu, H.; Kato, T.; Tominaga, M.; Azumaya, I. *J. Mol. Struct.* **2008**, *891*, 346 – 350.
23. Yokoyama, A.; Maruyama, K.; Tagami, K.; Masu, H.; Katagiri, K.; Azumaya, I.; Yokozawa, T. *Org. Lett.* **2008**, *10*, 3207 – 3210.
24. Kakuta H.; Azumaya, I; Masu, H.; Matsumura, M; Yamaguchi, K.; Kagechika, H.; Tanatani, A. *Tetrahedron* **2010**, *66*, 8254 – 8260.
25. Fujimoto, N.; Matsumura, M.; Azumaya, I.; Nishiyama, S.; Masu, H.; Kagechika, H.; Tanatani, A. *Chem. Commun.* **2012**, *48*, 4809 – 4811.
26. Masu, H.; Katagiri, K.; Kato, T.; Kagechika, H.; Tominaga, M.; Azumaya, I. *J. Org. Chem.* **2008**, *73*, 5143 – 5146.

Chapter 2

Preparation of Molecular Cage by Coordination of *m*-Calix[3]amide Bearing Pyridine with Palladium Complex

Abstract: *m*-Calix[3]amide having pyridine on the benzene ring (**PyC3A**) was synthesized by the cyclization of methyl 3-nonylamino-5-(pyridin-4'-yl)benzoate using lithium 1,1,1,3,3,3-hexamethyldisilazide (LiHMDS). The molecular cage **3Pd·2PyC3A** was prepared from a 2:3 mixture of **PyC3A** and [**Pd(dppp)(OTf)$_2$**] in $CDCl_3/CD_3OD$ (5/1 in volume). On the other hand, in $CDCl_3$, the formation of a polymeric mixture was confirmed.

Introduction

The noncovalent bond self-assembly of chemically-designed components proceeds under thermodynamic equilibrium and thus permits the generation of supramolecular cages or capsules more easily than with covalent bond approaches. The size and dimension control of supramolecular objects depends on the shape of the building blocks. Stang[1] and Fujita[2] hitherto reported many fantastic examples of self-assembled supramolecular objects using the coordination of the pyridine nitrogen to palladium complexes. They synthesized two- or three-dimensional supramolecular objects with modified building blocks. For example, ditopic building blocks with a predetermined angle gave cyclic molecules, and the combination of ditopic and tritopic building blocks afforded three-dimensional supramolecular cages. On the other hand, Shinkai and co-workers prepared molecular capsules using bowl-shaped calix[n]arenes as the building block through similar pyridine coordination to palladium complexes.[3 - 7] Molecular capsules constructed from two bowl-shaped calix[n]arenes provided the large cavity, which could be utilized as the host of fullerene encapsulation. In this methodology, however, the immobilization of the cone conformation by the chemical bonding was necessary for building the molecular capsules and the 1,3-alternate conformation gave uncharacterizable oligomers.

Calix[3]amide classified by Azumaya[8] is a cyclic trimer having *N*-alkyl benzanilide skeletons. In particular, calix[3]amide linked at the meta-position (*m*-calix[3]amide) likely adopts a bowl-shaped structure. A *m*-calix[3]amide was first synthesized by Azumaya in one step using 3-alkylaminobenzoic acid as a substrate and tetrachlorosilane[9,10] or dichlorotriphenylphosphorane[8,11] as condensation reagents. On the other hand, Yokozawa investigated the cyclic trimerization of a diphenylacetylene monomer bearing 4-propylamino and 4'-methoxycarbonyl groups using lithium 1,1,1,3,3,3-hexamethyldisilazide (LiHMDS) as the base.[12] In both methods, the

cyclization proceeded efficiently and cyclic trimers were obtained as the main product, owing to the *cis* preference around the amide bond of *N*-alkyl benzanilide units.[13] *m*-Calix[3]amide is known to have two conformers in solution. The *syn*-conformer has three benzene rings in the same orientation relative to the amide bond, and the *anti* -conformer has one benzene ring turning in the other direction. It is found that the preferable conformation depends on the solvent character ([*syn*] / [*anti*] = 74/26 in $CDCl_3$ and 96/4 in CD_3OD).[9]

In our previous work, *m*-calix[3]amide derivatives carrying oligothiophene chromophore on the benzene ring were synthesized and the self-assembly of π-conjugated system influenced by the solvent character was reported.[14] Despite extensive research[8 - 11] on the conformation of calix[3]amides in crystal and solution states, only a minimal effort[15] has been devoted for the application as functional molecules. As mentioned above, the shape of the building block is of importance to obtain self-assembled molecular capsules. With the fact that *m*-calix[3]amide prefers the *syn*-conformer in CH_3OH in mind, we investigated the construction of *m*-calix[3]amide-based molecular cage not by covalently fixing the conformation but by tuning the conformation with the solvent character. In this article, we will describe the synthesis and conformation analysis of a new *m*-calix[3]amide having pyridine on the benzene ring by using variable temperature (VT)-NMR, and the formation of molecular cage with palladium complexes.

Result and Discussion

3-Nonylaminobenzoic acid and its methyl ester bearing pyridine at the 5-position were prepared as monomers. Following our previous report,[14] methyl 3-bromo-5-nonylaminobenzoate was synthesized in three steps starting from 3-bromo-5-nitrobenzoic acid. The subsequent Suzuki coupling reaction with

4-pyridineboronic acid in the presence of tetrakis(triphenylphosphine)palladium(0) afforded methyl 3-nonylamino-5-(pyridin-4'-yl)benzoate (**1**) in 58 % yield. The hydrolysis of methyl ester **1** under the acidic condition gave 3-nonylamino-5-(pyridin-4'-yl)benzoic acid (**2**) in 68 % yield. Cyclic oligomerization was initially carried out using acid **2** based on the procedure reported by Azumaya et al. using $SiCl_4$ as the condensation reagent (Scheme 1, Path A).[9,10] The preparative GPC profile of crude products gave a multimodal curve ranging from the oligomeric region to the high-molecular-weight region. The MALDI-TOF MS also indicated the formation of macrocyclic oligomers in addition to the target cyclic trimer. In the cyclic oligomerization of 3-nonylamino-5-phenyl benzoic acid, however, the cyclic trimer could be selectively formed (not shown here). Thus the introduction of the pyridine group in the monomer structure might interrupt the effective cyclic trimerization. The cyclic oligomerization of methyl ester **1** was then performed using LiHMDS following to the method developed by Yokozawa et al. (Scheme 1, Path B).[12] In contrast to the result through Path A, the preparative GPC profile showed a good peak separation of the oligomeric product from the high-molecular-weight product. *m*-Calix[3]amide (**PyC3A**) was successfully isolated by the preparative GPC in 16 % yield. The MALDI-TOF MS showed a signal at *m/z* 967.6075 assignable to the proton adduct of **PyC3A**.

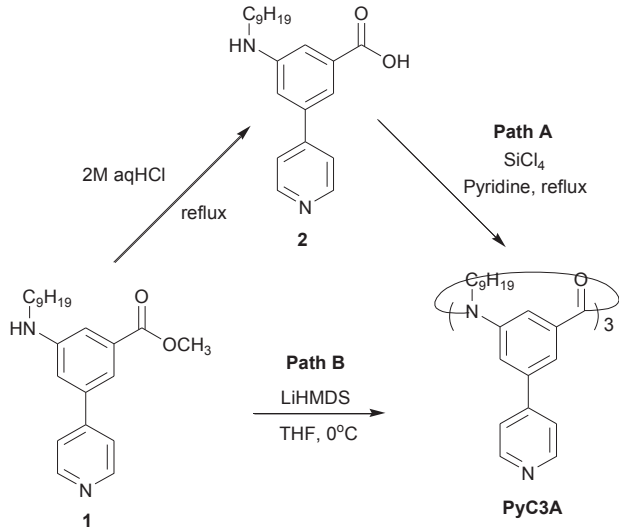

Scheme 1. Cyclic oligomerization of monomers **1** and **2**.

Figure 1 shows the single-crystal X-ray structure of *N*-methyl analog of **PyC3A**, abbreviated hereafter as **PyC3A'**. The X-ray quality single crystals of **PyC3A'** were grown by slow evaporation in mixed solvents containing chloroform and hexane. The *syn*-conformer was observed similarly to *m*-calix[3]amide having the benzene group.[10] **PyC3A'** is obtained as a racemic crystal, in which one enantiomer has a right-handed amide skeleton and another has a left-handed amide skeleton. The X-ray data indicated an almost planar structure around the amide bond (an averaged dihedral angle Me-N-C-O was 2.3°) comparable to that of *m*-calix[3]amide having the benzene group (1.5°).[10] From the IR spectroscopic study (carbonyl stretching vibration signal) of **PyC3A** in the solid state, the dihedral angle around the amide bond might not be affected by the electron density of the π-conjugated system (bithiophene; 1650 cm^{-1}, phenyl ; 1650 cm^{-1}, and pyridine; 1644 cm^{-1}).[10,14] The bowl-shaped structure of **PyC3A'** is suggested from the evidence of that the averaged distance between C(2) carbon atoms (3.78Å) is shorter than that between pyridine nitrogen atoms (5.02 Å).

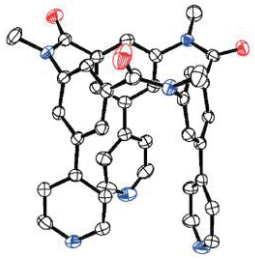

Figure 1. ORTEP view of **PyC3A'** with thermal elliosoids

In a $CDCl_3$ solution at 293 K, ^1H NMR spectrum gave many signals indicating the existence of *syn*- and *anti*-conformers. The VT-NMR measurement was investigated to gain insight into the equilibrium between two conformers. **PyC3A** existed in the rapid equilibrium at above 318 ± 5 K because a pyridyl α-proton signal of the *syn*-conformer (8.46 ppm) was coalesced with that of the *anti*-conformer (8.66 ppm) (Figure 2). On the other hand, these signals were separated at below 318 K. Following the report by Azumaya et al.,[9] an observed minor signal can be assigned to a proton of the *anti*-conformer. The [*syn*]/[*anti*] ratio at 293 K was calculated from the integral ratio of these pyridyl α-proton signals to be [*syn*]/[*anti*] = 69/31. The [*syn*]/[*anti*] ratio was dependent on the temperature in which the *syn*-population increased with the rise of temperature ([*syn*]/[*anti*] = 70/30 at 313 K and 66/34 at 233 K). The conformation was also influenced by the solvent character. **PyC3A** existed as largely the *syn*-conformer in pure CD_3OD and the *anti* population increased with decreasing the percentage of CD_3OD in $CDCl_3/CD_3OD$ mixed solvents.

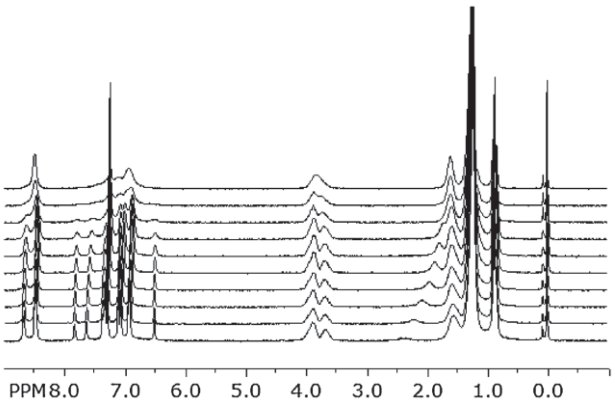

Figure 2. VT-NMR spectra of **PyC3A** in $CDCl_3$ (From top to bottom: 323 – 233 K with interval of 10 K).

For the preparation of the molecular cage (**3Pd·2PyC3A**), **PyC3A** and [Pd(dppp)Cl_2] or [Pd(dppp)$(OTf)_2$] was mixed with the molar ratio of 2:3 in $CDCl_3$ /CD_3OD (5/1 in volume, 19 mM).

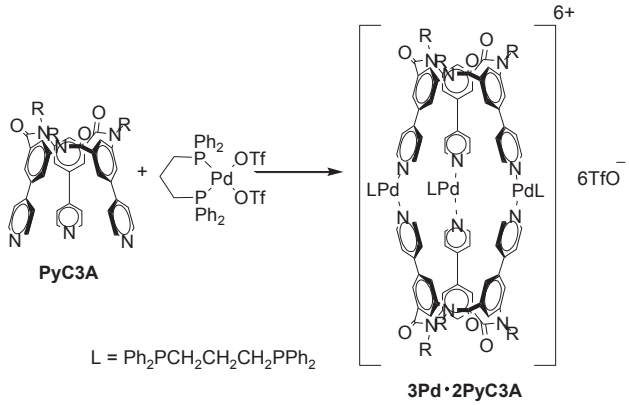

Scheme 2. Preparation of **3Pd·2PyC3A** from **PyC3A** and [Pd(dppp)$(OTf)_2$].

In the ESI-MS of the mixture using [Pd(dppp)Cl_2] as the palladium complex, no peak ascribed to the target molecular cage was detected though incomplete coordinated products were detected. Thus [Pd(dppp)Cl_2] has a poor coordination ability with pyridine due to the lack of the cationic character of palladium center. On the other hand, the ESI-MS of the 2:3 mixture of **PyC3A** and [Pd(dppp)$(OTf)_2$] showed strong peaks at

m/z 2043.6100 for [**3Pd·2PyC3A**-2OTf]$^{2+}$ and *m/z* 1312.4136 for [**3Pd·2PyC3A**-3OTf]$^{3+}$ (Figure 3) indicating the formation of an ideal molecular cage (Scheme 2). In addition, the ^{31}P NMR and the diffusion-ordered NMR spectroscopy (DOSY) were investigated to confirm the efficiency of capsule formation. The phosphorous signal at 15.0 ppm for the original [Pd(dppp)(OTf)$_2$] completely disappeared and only one signal was observed at 5.21 ppm by adding [Pd(dppp)(OTf)$_2$] to a $CDCl_3/CD_3OD$ (5/1 in volume) solution of **PyC3A**. The DOSY experiments for **PyC3A** and the 2:3 mixture of **PyC3A** and [Pd(dppp)(OTf)$_2$] showed different diffusion coefficients (D = 5.89 ± 0.3 × 10^{-10} m^2s^{-1} and D = 3.74 ± 0.6 × 10^{-10} m^2s^{-1}) (Table 1) indicating the quantitative capsule formation. From the results, we estimated the hydrodynamic radii (R_H) by the Einstein-Stokes equation (R_H = 0.60 nm for **PyC3A** and R_H = 0.96 nm for **3Pd·2PyC3A**).[16] The increase in R_H indicated the change of molecular shape. In contrast, 2:1 mixture showed a complicated ^{1}H- and ^{31}P NMR spectrum and DOSY experiments gave several diffusion coefficients. The ^{1}H NMR spectrum of the 2:3 mixture in $CDCl_3/CD_3OD$ (5/1 in volume) showed a new set of signals (Figure 4). The pyridyl α-proton signals at 8.43 ppm for the *syn*-conformer and 8.61 ppm for the *anti*-conformer observed in the original **PyC3A** vanished and a new proton signal was detected only at 8.90 ppm. Accordingly, *m*-calix[3]amide included in molecular cage **3Pd·2PyC3A** would be fixed as the *syn*-conformer. Finally, the solvent dependency on the cage formation was investigated. The 2:3 mixture of **PyC3A** and [Pd(dppp)(OTf)$_2$] in $CDCl_3$ gave a broad ^{1}H NMR[17] and DOSY spectra which indicated the formation of polymeric mixture. Two pyridyl α-proton signals (8.99 and 9.17 ppm) still remained implying the existence of both the *syn*- and *anti*-conformers. The presence of the *anti*–conformer in $CDCl_3$ may be responsible for the interruption of the effective cage formation. These findings indicate that the conformation change of **PyC3A** induced by the solvent character dramatically affects the formation of molecular cage

3Pd·2PyC3A.

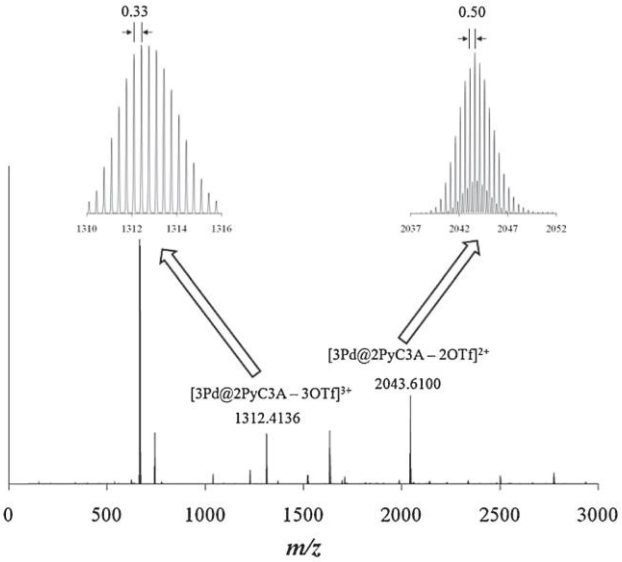

Figure 3. ESI-MS of 2:3 mixture of **PyC3A** and $[Pd(dppp)(OTf)_2]$.

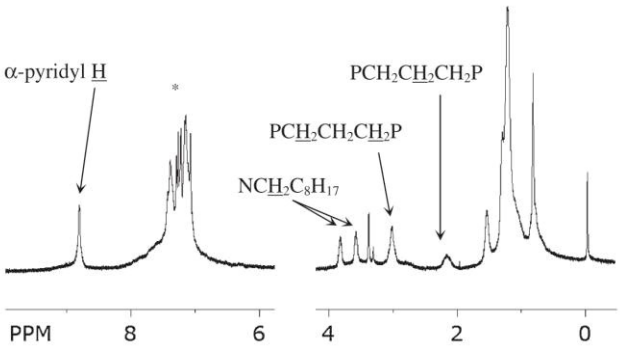

Figure 4. Expanded ^1H NMR spectra of **3Pd·2PyC3A** in $CDCl_3/CD_3OD$ (5/1 in volume).

Table 1. Spectral data for **PyC3A**, $Pd(dppp)(OTf)_2$, 2:1 and 2:3 mixture of **PyC3A** and $Pd(dppp)(OTf)_2$ in $CDCl_3/CD_3OD$ (5/1 in volume) at 293 K.

Compound	^1H (ppm)[a]	^{31}P (ppm)[b]	Diffusion coefficient ($\times 10^{-10}$ m^2s^{-1})
PyC3A	8.43 and 8.61	NA	5.89 ± 0.3
$Pd(dppp)(OTf)_2$	NA	15.0	NA
2:1 mixture of **PyC3A** and $Pd(dppp)(OTf)_2$	NA	6.8, 6.6, 6.1, 6.0, 5.8, 5.6	3.81 ± 0.3, 4.79 ± 0.3, 5.37 ± 0.3
2:3 mixture of **PyC3A** and $Pd(dppp)(OTf)_2$	8.90	5.21	3.74 ± 0.6

[a] Chemical shifts of pyridyl α-proton signal in $CDCl_3/CD_3OD$ (5/1 in volume).

[b] Relative to phosphorous signal using 85% H_3PO_4 as external standard.

Conclusion

In conclusion, *m*-calix[3]amide having pyridine on the benzene ring was synthesized to obtain a molecular cage by the coordination to palladium complexes. The conformation study was carried out using ^1H NMR spectra to find out that *m*-calix[3]amide bearing pyridine preferred the *syn*-conformer in CD_3OD. The 2:3 mixture of **PyC3A** and $[Pd(dppp)(OTf)_2]$ in $CDCl_3/CD_3OD$ = 5/1 (in volume) gave molecular cage (**3Pd·2PyC3A**), which was supported by ESI-MS, DOSY, ^1H NMR, and ^{31}P NMR spectra. On the other hand, in $CDCl_3$, the formation of polymeric mixture was indicated. Accordingly, the conformation change of **PyC3A** triggered by solvent character has a large impact on the formation of molecular cage.

Experimental

Material

All reactions were performed under the dry nitrogen atmosphere. Dry tetrahydrofuran (THF) was purchased from Kanto Chemical Co. Lithium 1,1,1,3,3,3-hexamethyldisilazide solution (LiHMDS, 1.0 M in THF) and tetrakis(triphenylphosphine)palladium(0) ($Pd(PPh_3)_4$) were purchased from Aldrich Chemical Co. 4-Pyridineboronic acid and tetrachrolosilane ($SiCl_4$) were purchased from TCI Co.

Instrumentation

^1H and ^{13}C nuclear magnetic resonance (^1H-NMR and ^{13}C-NMR) spectra were recorded on Bruker Avance 200 and 600 FT-NMR spectrometers using tetramethylsilane (^1H-NMR, δ 0.00) and $CDCl_3$ (^{13}C-NMR, δ 77.0) as internal reference peaks. Infrared (IR) spectra were recorded on a JASCO FT-IR 460Plus spectrophotometer in the attenuated total reflectance (ATR) method. Melting points (Mp) were determined on a Yanaco micro melting point apparatus MP-500D. High resolution mass (HRMS) spectra were obtained on a Hitachi M-200S in the electron ionization mode. Matrix-assisted laser desorption/ionization time-of-fright mass (MALDI-TOF-MS) spectra were obtained on a Shimadzu Axima CFRplus (s/w version 2.4) in the reflection and liner modes using dithranol as a matrix. Electrospray ionization mass (ESI-MS) spectra were performed on a Waters Synapt G2 HDMS quadrupole orthogonal acceleration time-of-flight (oa-TOF) instrument in the positive ion mode. Purification with the preparative GPC was carried out on a Japan analytical industry LC-9201 system using tandem JAIGEL 1H, 2H, and 2.5H columns ($CHCl_3$ as an eluent, flow rate = 3.5 mL/min) equipped with the ultraviolet (UV) detector (254 nm).

Synthesis

Methyl 3-nonylamino-5-(pyridine-4'-yl)benzoate (**1**)

To a mixture of methyl 3-bromo-5-nonylaminobenzoate[14] (2.2 g, 6.0 mmol) and 4-pyridineboronic acid (0.90 g, 7.0 mmol) in THF (60 mL) were added 2 M aq. K_2CO_3 (24 mL) and $Pd(PPh_3)_4$ (72 mg, 60 μmol), and the system was heated to reflux overnight. After an aqueous phase was extracted with ethyl acetate, the combined organic phase was washed with saturated aq. Na_2CO_3. After drying over $MgSO_4$, solvents were removed by the rotary evaporator. The crude product was purified by the SiO_2 chromatography (acetone:CH_2Cl_2 = 1:39, Rf = 0.6) followed by the recrystallization from hexane to obtain yellow crystals in 1.3 g (58% yield). Mp. 114 – 115 ˚C. ^{1}H NMR (δ, 200 MHz, ppm, $CDCl_3$) 8.65 (d, *J* = 4.1 Hz, 2H), 7.60 (s, 1H), 7.49 (d, *J* = 4.2 Hz, 2H), 7.31 (s, 1H), 6.97 (s, 1H), 3.92 (s, 3H), 3.16 (t, *J* = 6.8 Hz, 2H), 1.62 (m, 2H), 1.45 – 1.18 (12H), 0.88 (t, *J* = 6.5 Hz, 3H). ^{13}C NMR (δ, 50 MHz, ppm, $CDCl_3$) 167.1, 150.2, 149.2, 148.1, 139.3, 131.9, 121.7, 116.7, 115.0, 113.8, 52.2, 43.9, 31.9, 29.5, 29.4, 29.3, 29.2, 27.1, 22.7, 14.1. IR (cm^{-1}) 3915, 3753, 2382.62, 2349, 2301, 1715, 1550, 1438, 1242, 1114, 997, 917, 819, 769, 743, 819, 634, 608. HRMS (M^+) calcd. 354.2307, obsd. 354.2333.

Methyl 3-nonylamino-5-(pyridine-4'-yl)benzoic acid (**2**)

A solution of **2** (0.09 g, 0.25 mmol) in 4 M aq. HCl (3.0 mL) was heated to reflux for 2 h. After neutralized by 4 M aq NaOH, the mixture was extracted with ethyl acetate. The organic phase was dried over $MgSO_4$ and a solvent was removed by the rotary evaporator. The crude product was washed with hexane to obtain white powder in 0.058 g (68% yield). ^{1}H NMR (δ, 200 MHz, $CDCl_3$) 8.72 (d, *J* = 5.2 Hz, 2H), 7.72 (s, 1H), 7.60 (d, *J* = 5.2 Hz, 2H), 7.43 (s, 1H), 7.02 (s, 1H), 3.23 (t, *J* = 7.0 Hz, 2H), 1.68 (m, 2H), 1.40 ~ 1.25 (12 H), 0.89 (t, *J* = 6.4 Hz, 3H). ^{13}C NMR (δ, 50 MHz, $CDCl_3$) 170.3,

149.3, 149.2, 149.0, 138.9, 132.3, 132.2, 132.0, 128.6, 128.4, 122.1, 117.3, 115.2, 114.5, 43.9, 31.8, 29.5, 29.4, 29.4, 29.2, 27.1, 22.6, 14.1. IR (cm^{-1}) 3289, 2925, 2852, 1684, 1597, 1553, 1455, 1410, 1357, 1262, 1119, 997, 817, 772, 723, 694. Anal. Calcd for $C_{21}H_{28}N_2O_2$: C, 74.08; H, 8.29; N,8.23. Found: C, 73.86; H, 8.31; N, 7.81.

m-Calix[3]amide having pyridine (**PyC3A**)

Path A: To a solution of 3-nonylamino-5-(pyridine-4'-yl)benzoic acid **2** (0.17 g, 0.50 mmol) in pyridine (4.0 mL) was added $SiCl_4$ (86 mL, 0.75 mmol), and the system was heated to reflux overnight. After solvents were removed, CH_2Cl_2 was added that was washed with 1.0 M aq. HCl and brine. The organic phase was dried over $MgSO_4$ and solvents were removed by rotary evaporator.

Path B: To a solution of methyl 3-nonylamino-5-(pyridine-4'-yl)benzoate **1** (0.71 g, 2.0 mmol) in THF (2.0 mL) was added dropwise LiHMDS solution (1.0 M in THF) (2.4 mL, 2.4 mmol) at 0 ˚C, and the system was stirred overnight. After saturated aq. NH_4Cl was added, an aqueous phase was extracted with CH_2Cl_2. The combined organic phase was dried over $MgSO_4$ and solvents were removed by the rotary evaporator. The crude product was purified by the preparative GPC ($CHCl_3$ as an eluent) to obtain yellow solid (28 mg, 16%). Mp. > 300 ˚C. ^{1}H NMR (δ, 600 MHz, ppm, $CDCl_3$, 293 K) 8.66 (s, 6H × 0.30), 8.46 (s, 6H × 0.70), 7.82 (s, 3H × 0.30), 7.58 (s, 3H × 0.30), 7.33 (s, 6H × 0.30), 7.26 (s, 3H × 0.70), 7.09 (s, 3H × 0.70), 7.02 (s, 3H × 0.70), 6.89 (s, 6H × 0.70), 6.51 (s, 3H × 0.30), 3.91 (m, 3H ×0.70), 3.86 (m, 6H × 0.30), 3.69 (m, 3H × 0.70) 1.67 – 1.48 (6H), 1.37 – 1.13 (m, 36 H), 0.97 – 0.87 (t, J = 6.9 Hz, 9H). ^{13}C NMR (d, 150 MHz, ppm, $CDCl_3$) 169.2, 150.4, 145.8, 143.3, 139.9, 139.8, 128.8, 127.1, 125.6, 121.0, 49.9, 31.7, 29.4, 29.2, 29.1, 27.5, 26.7, 22.6, 14.0. IR (cm^{-1}) 3871, 3854, 3743, 3437, 2922, 2850, 1645, 1590, 1550, 1442, 1393, 1340, 1266, 1132, 822, 712. HRMALDI-TOF-MS calcd for $C_{63}H_{79}N_6O_3$ ($M + H^+$): 967.6214. Found: 967.6075.

Formation of molecular capsule (**3Pd·PyC3A**)

In an NMR tube, a solution of Pd(dppp)$(OTf)_2$ (5.68 mg, 6.90 μmol) in $CDCl_3/CD_3OD$ (0.12mL , 5/1 in volume) was added to a solution of **PyC3A** (4.48 mg, 4.60 μmol) in $CDCl_3/CD_3OD$ (0.12 mL, 5/1 in volume), and the solution was mixed by vigorously shaking for 3 min at room temperature. ^{1}H NMR (δ, 600 MHz, ppm, $CDCl_3/CD_3OD$ = 5/1, 293 K) 8.90 (s, 12H), 7.70 – 6.70 (90 H), 3.88 (s, 6H), 3.75 (s, 6H), 3.10 (bs, 12H), 2.20 (bs, 6H), 1.75 – 0.59 (102 H).

Reference and Notes

27. Leininger, S.; Olenyuk, B.; Stang, J. P. *Chem. Rev.* **2000**, *100*, 853.

28. Fujita, M.; Tominaga, M.; Hori, A.; Therrien, B. *Acc Chem Res*. **2005**, *38*, 369.

29. Ikeda, A.; Yoshimura, M.; Udzu, H.; Fukuhara, C.; Shinkai, S.; *J. Am. Chem. Soc.* **1999**, *121*, 4296.

30. Ikeda, A.; Yoshimura, M.; Tani, F.; Naruta, Y.; Shinkai, S.; *Chem. Lett*. **1998**, 587.

31. Ikeda, A.; Sonoda, K.; Shinkai, S. *Chem. Lett.* **2000**, 1220.

32. Zhong, Z.; Ikeda, A.; Ayabe, M.; Shinkai, S.; Sakamoto, S.; Yamaguchi, K. *J. Org. Chem.* **2001**, *66*, 1002.

33. Ikeda, A.; Udzu, H.; Zhong, Z.; Shinkai, S.; Sakamoto, S.; Yamaguchi, K. *J. Am. Chem. Soc.* **2001**, *123*, 3872.

34. Imabeppu, F.; Katagiri, K.; Masu, H.; Kato, T.; Tominaga, M.; Therrien, B.; Takayanagi, M.; Kaji, E.; Yamaguchi, K.; Kagechika, H.; Azumaya, I. *Tetrahedron Lett.* **2006**, *47*, 413.

35. Azumaya, I.; Kagechika, H.; Yamaguchi, K.; Shudo, K. *Tetrahedron Lett.* **1996**, *37*, 5003.

36. Kakuta, H.; Azumaya, I.; Masu, H.; Matsumura, M.; Yamaguchi, K.; Kagechika, H.; Tanatani, A. *Tetrahedron* **2010**, *66*, 8254.

37. Azumaya, I.; Okamoto, T.; Imabeppu, F.; Takayanagi, H.; *Tetrahedron* **2003**, *59*, 2325.

38. Yokoyama, A.; Maruyama, T.; Tagami, K.; Masu, H.; Katagiri, K.; Azumaya, I.; Yokozawa, T. *Org. Lett.* **2008**, *10*, 3207.

39. Itai, A.; Toriumi, Y.; Tomioka, N.; Kagechika, H.; Azumaya, I.; Shudo, K. *Tetrahedron Lett*. **1989**, *30*, 6177.

40. Takagi, K.; Sugimoto, S.; Yamakado, R.; Nobuke, K. *J. Org. Chem.* **2011**, *76*, 2471.

41. Katagiri, K.; Furuyama, T.; Masu, H.; Kato, T.; Matsumura, M.; Uchiyama, M.;

Tanatani, A.; Tominaga, M.; H. Kagechika, H.; Yamaguchi, K.; Azumaya, I. *Supramol. Chem.* **2011**, *23*, 125.

42. For related review, see: P. T. Callaghan, *Aust. J. Phys.* **1984**, *37*, 359.
43. The pyridyl α-proton signals (8.46 ppm for *syn* and 8.66 ppm for *anti*) disappeared owing to the coordination to palladium cation.

Chapter 2. Preparation of Molecular Cage by Coordination of *m*-Calix[3]amide Bearing Pyridine with Palladium Complex

Chapter 3

A Screw-Shaped Alignment of Pyrene Using *m*-Calix[3]amide

Abstract: *m*-Calix[3]amide bearing three pyrenes (**1a**) was prepared by the condensation reaction of 3-nonylaminobenzoic acid derivative using Ph_3PCl_2. Pyrenyl groups were found to be aligned in the screw-like fashion by *m*-calix[3]amide as confirmed by the X-ray crystallography. Aromatic proton signals observed at the up-field region in the ^1H NMR spectrum at low temperature indicated that pyrenyl groups in **1a** are aligned in close proximity in THF solution. UV-vis absorption and fluorescence emission spectra did not show marked peak shift nor concentration fluorescence quenching compared with reference compounds implying no significant electronic interaction between pyrenyl groups. These results can be explained by the steric effect of the *m*-calix[3]amide platform. On the other hand, an excimer emission was observed for *m*-calix[3]amide having a flexible spacer between pyrene and *m*-calix[3]amide (**1b**).

Introduction

π-Conjugated molecules play a central role in organic optoelectronic materials. It is well known that not only the chemical structure but also the three dimensional alignment structure of π-conjugated molecules contributes largely to the performance of materials. Thus the programmable arrangement of π-conjugated molecules in space and the understanding of structure-properties relationship are of much importance. However, the three dimensional alignment structure is generally governed by the chemical structure of molecules, as represented by the herringbone packing of pentacene. One possible strategy to tune-up the alignment structure is the chemical modification at the periphery of π-conjugated molecules (Method 1). Kobayashi et al. succeeded in the cofacial packing of bis(methylthio)acenes by using S-S and S-π interactions.[1,2] Other groups also proposed the molecular design for the cofacial crystal packing of acene derivatives.[3,4] Another technique to control the alignment structure of π-conjugated molecules is the utilization of well-defined tethering unit (Method 2). Yoshizawa et al. recently reported a tubular macrocycle containing four anthracenes covalently connected by the meta-phenylene unit.[5] The covalent bond approach (Method 2) would be much reliable since the three dimensional alignment structure of π-conjugated molecules can be maintained both in the solid state and diluted solution. Pyrene having the high fluorescence quantum yield shows two characteristic luminescence behaviors,[6] namely a monomer emission observed in the diluted solution and an excimer emission derived from the associated dimer in the concentrated solution. The excimer emission can be also detected when pyrenes are forced into the confined space even in the diluted condition. Consequently, pyrene is a useful probe as the DNA fluorescence label to investigate their distance and chain conformation.[7] We will herein describe a novel alignment of three pyrenes using Method 2 and report optical properties of pyrene-carrying macrocycles in order to figure out the structure-properties relationship.

Cyclic meta-benzamide trimer (*m*-calix[3]amide) is efficiently synthesized by the condensation reaction of 3-alkylaminobenzoic acid derivatives due to the *cis* preference of the *N*-alkyl benzanilide skeleton.[8e13] *m*-Calix[3]amide has two conformers, in which the *syn* conformer has three benzene rings in the same orientation relative to the amide bond and the *anti* conformer has one benzene ring turning in other direction. The *syn* conformer prefers to the *anti* conformer both in the solid phase and solution. As a consequence, appended substituents on the benzene ring are positioned closely in the *syn* conformer of *m*-calix[3]amide. We have reported the synthesis and characterization of *m*-calix[3]amides bearing pyridine[14] and bithiophene[15] to reveal that *m*-calix[3]amide is suitable candidate for assembling functional groups in close proximity. In this paper, *m*-calix[3]amide was chosen as the platform to align pyrenes in the screw-like fashion. The synthesis of *m*-calix[3] amides having three pyrenes (**1a** and **1b**), *m*-calix[3]amide having one pyrene (**2**), and model compound (**3**) (Figure 1) along with the conformational characteristics of **1a** in solid and solution states, and optical properties in solution will be described.

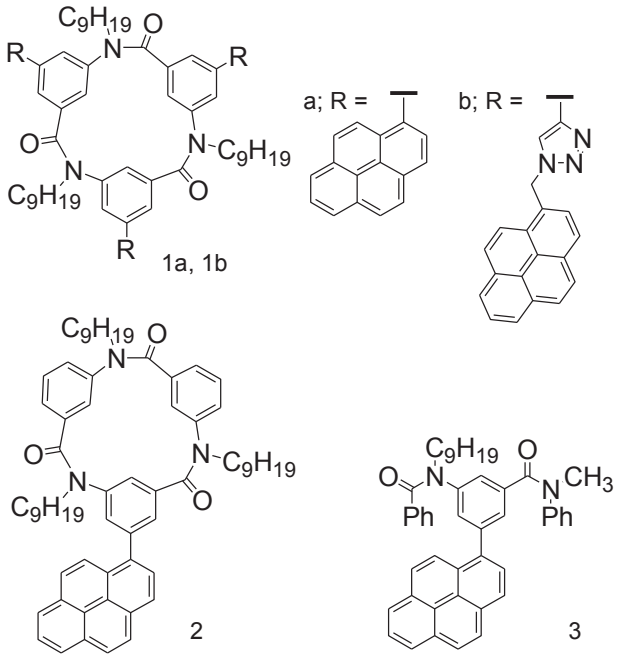

Figure 1. Structure of *m*-calix[3]amides (**1a**, **1b**, and **2**) and model compound (**3**).

Results and Discussion

Following to our previous report,[15] methyl 3-bromo-5-nonylaminobenzoate (**4**) was synthesized in three steps from 3-bromo-5-nitrobenzoic acid. *m*-Calix[3]amide bearing three pyrenes (**1a**) was synthesized from **4** as shown in Scheme1. The synthetic route consists of the Suzuki-Miyaura cross coupling of **4** with pyrene-1-boronic acid, the hydrolysis of methyl ester by NaOH, and the cyclic oligomerization using Ph_3PCl_2 as the condensation reagent. Cyclic trimer **1a** was isolated by preparative GPC in 17% yield. The low yield of the product is likely due to the steric hindrance of the pyrenyl group. *m*-Calix[3]amide (**1b**) having a flexible spacer between pyrene and *m*-calix[3]amide was prepared for comparison and the synthetic route is shown in Scheme 2. Methyl 3-iodo-5-nonylaminobenzoate (**7**) was prepared from 3-iodo-5-nitrobenzoic acid. *m*-Calix[3]amide bearing three ethynyl groups (**10**) was obtained in three steps from **7** by the Sonogashira-Hagihara cross coupling with trimethylsilylacetylene, the concomitant de-silylation and ester hydrolysis by NaOH, and the cyclic oligomerization using $SiCl_4$. Finally, the Huisgen cycloaddition of **10** with 1-azidomethylpyrene in the presence of copper(I) iodide afforded **1b** in 70% yield. The cyclic oligomerization of 3-alkylaminobenzoic acid carrying the triazole ring with pyrene using Ph_3PCl_2 or $SiCl_4$ met with no success probably due to the basic character of the heterocycle.

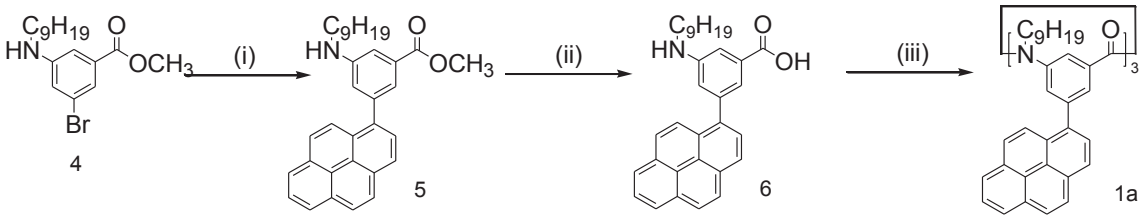

Scheme 1. Synthetic route to **1a**, Reagents and conditions: (i) pyrene-1-boronic acid, K_2CO_3, $Pd(PPh_3)_4$, THF, H_2O, reflux,; (ii) NaOH, H_2O, THF, MeOH, 40 ºC; (iii) Ph_3PCl_2, $(CHCl_2)_2$, reflux.

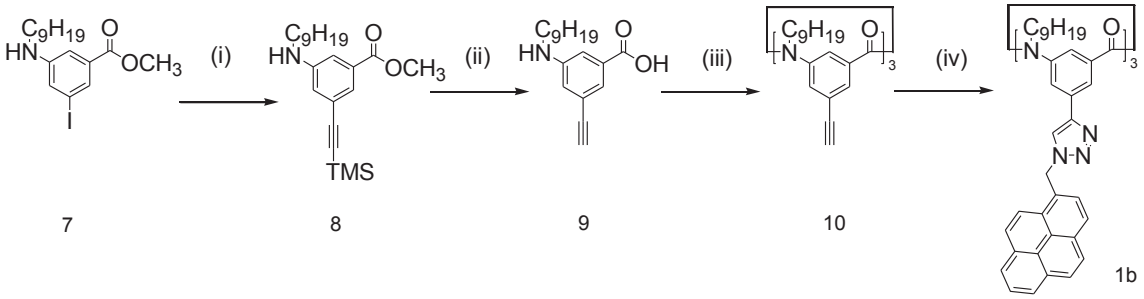

Scheme 2. Synthetic route to **1b**. Reagents and conditions: (i) trimethylsilylacetylene, CuI, $Pd(PPh_3)_4$, Et_3N, 50 ºC; (ii) NaOH, H_2O, THF, MeOH, rt; (iii) $SiCl_4$, pyridine, reflux; (iv) 1-azidomethylpyrene, CuI, DMF, 90 ºC.

To investigate the optical properties of *m*-calix[3]amide in detail, *m*-calix[3]amide having one pyrene (**2**) and acyclic model compound (**3**) were prepared. The synthesis of **2** was carried out by the cyclic co-oligomerization of **6** and 3-nonylaminobenzoic acid using Ph_3PCl_2 as the condensation reagent, and the purification by preparative GPC afforded the desired compound **2** in 6% yield. On the other hand, **3** was prepared in three steps from **4**, which consists of the benzoylation of the *N*-nonylamino group, the ester-amide exchange of methyl ester, and the Suzuki-Miyaura cross coupling with pyrene-1-boronic acid.

The alignment structure of three pyrenyl groups was determined by the single crystal X-ray crystallography using *m*-calix[3]amide bearing the ethyl substituent on the amide nitrogen (**1a'**) instead of **1a** (Figure 2). **1a'** adopts the *syn* conformation and three pyrenyl groups are arranged on the same side of the *m*-calix[3]amide skeleton. The tertiary amide bond has the nearly planer structure as judged by the dihedral angle Me-N-C-O to be 6.0º on average. The averaged dihedral angle formed between the benzene ring and the amide plane is 110.3º. Owing to the large steric hindrance induced by three pyrenyl groups, this value is larger than that observed for *m*-calix[3]amide

bearing three phenyl groups (the corresponding dihedral angle is 100.0º).[12] The center-to-center distances between adjacent pyrenyl groups are approximately 6.2 Å and the dihedral angle between three pyrenyl groups is about 61º.

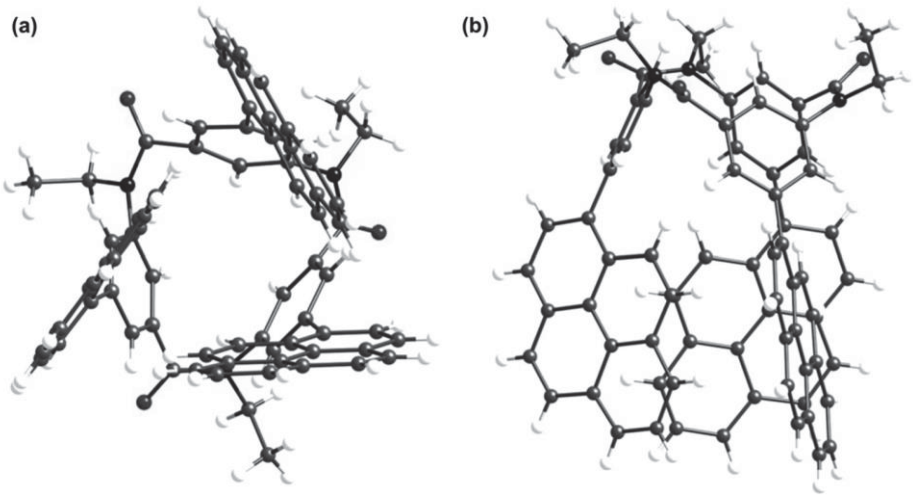

Figure 2. Crystal structure of **1a'** depicted as a ball and stick model. (a) Top view and (b) side view. Chloroform molecules are omitted for clarity. One of the pyrene groups is disordered to two positions and the occupancies are refined (about 0.60 and 0.40). Disordered atoms of pyrene rings, which have minor occupancy are omitted for clarity.

The close arrangement of three pyrenyl groups in **1a** was also evident in the ^{1}H NMR spectra (Figure 3). At 293 K, the ^{1}H NMR spectrum showed broad signals and the position of aromatic proton signals was not much different from that of **6**. When the spectrum was measured at 233 K, proton signals become sharp and several new signals were appeared due to the slow rotation around the carbon(benzene)-carbon(pyrene) bond relative to the NMR time scale. The doublet signal at 6.48 ppm can be assigned to the proton derived from the *anti* conformer.[16] Although the complete signal assignment is impossible, the proton signals observed at the up-field region (6.8-4.5 ppm) seem to be originated from pyrene protons, which are strongly shielded by the adjacent pyrenyl group. On the other hand, ^{1}H NMR spectra of **2** and **3** showed no proton signals around

the same region. These results indicate that *m*-calix[3]amide is a suitable platform to realize the screw-like arrangement of three pyrenyl groups.

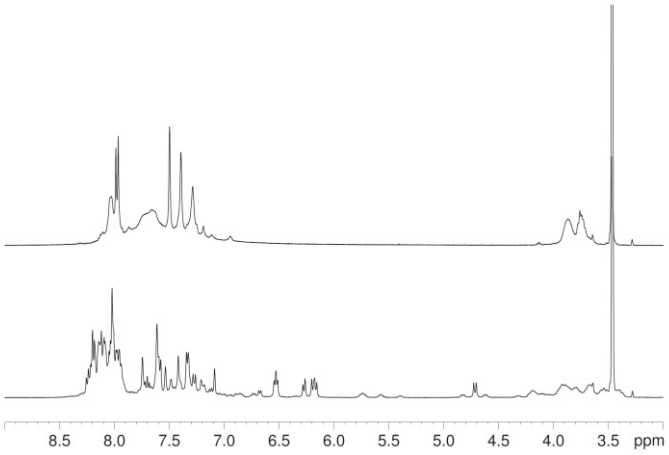

Figure 3. ^{1}H NMR spectra of **1a** in THF-d_8 at 293 K (top) and 233 K (bottom).

The UV-vis absorption and fluorescence emission spectra were measured in THF solution. Prior to the measurement, the solution was purged with nitrogen in order to avoid the fluorescence quenching by oxygen. The concentration of the solution are kept low ($<10^{-5}$ M) to prevent the intermolecular interaction. As shown in Figure 4a, the absorption maximum wavelengths were similar between **1a**, **2**, and **3**, which indicates that they have comparable effective conjugation length. In our previous report,[15] the absorption maximum wavelength of *m*-calix[3]amide bearing three bithiophenes was blue-shifted by 9 nm from that of acyclic model compound to imply the intramolecular electronic interaction between bithiophenes. Hence three pyrenes included in **1a** have negligible interaction in the ground state. The absorption spectrum of **1b** showed the vibronic fine structure characteristic to pyrene (Figure 4b). Fluorescence maximum wavelength of **1a** was red-shifted by 3-5 nm from those of **2** and **3**, and the tailing to the longer wavelength region was observed (Figure 4c). The fluorescence emission from the associated state (excimer emission) was not observed from **1a**. These results indicate

that three pyrenes in **1a** have very weak electronic interaction in the excited state because they cannot form the face-to-face stacked structure. In contrast, the fluorescence emission of **1b** appeared as a broad featureless band at the longer wavelength region (476 nm) having the quantum yield of 0.06. The flexible methylene spacer reduces the steric hindrance to permit the excimer emission. The fluorescence quantum yield of **3** was quite low (Φ_{fl}=0.04), which might be resulted from the twisted intramolecular charge transfer (TICT) by the rotation of the amide bonds.[17] On the other hand, the quantum yields of **1a** (Φ_{fl}=0.36) and **2** (Φ_{fl}=0.34) were high probably because the cyclic structure suppresses the rotation of the amide bond. It should be noted that the fluorescence quantum yield of **1a** and **2** are almost similar even though the chromophores are closely located in **1a**. This is also a consequence of the tilted alignment of three pyrenes in the *m*-calix[3]amide platform.

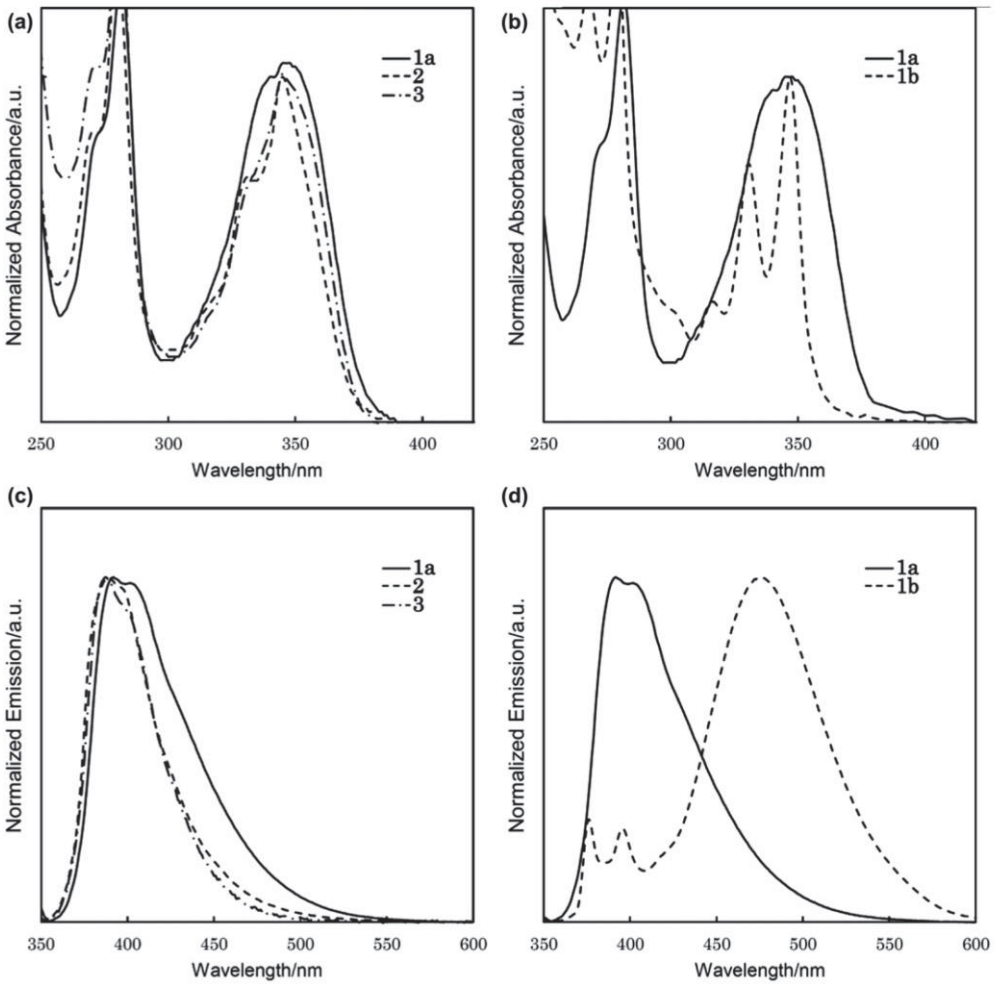

Figure 4. Normalized absorption and emission spectra of **1a**, **1b**, **2**, and **3** in THF solution ($\lambda_{ex} = \lambda_{abs}$, room temperature).

Conclusion

m-Calix[3]amides bearing three pyrenes (**1a** and **1b**), *m*-calix[3]amide having one pyrene (**2**), and model compound (**3**) were synthesized. The structure was investigated in the solid and solution states by the single crystal X-ray crystallography and ^{1}H NMR spectroscopy to find out that three pyrenyl groups in **1a** are arranged closely in space by the *m*-calix[3]amide platform. Optical properties in THF solution were investigated by UV-vis and fluorescence spectroscopy. The absorption and emission maximum wavelengths were similar between **1a**, **2**, and **3**. In contrast to **1b** having the flexible spacer between pyrene and *m*-calix[3]amide, **1a** showed monomer emission and no excimer emission was observed. **1a** had a high fluorescence quantum yield compared to **3** and the concentration quenching did not occur. These results indicate that *m*-calix[3]amide is an excellent platform to align conjugated molecules in close proximity and screw-like fashion. We believe that this new strategy for the programmable arrangement of π-conjugated molecules in space leads to the better understanding of structure-properties relationship of π-conjugated molecules.

Experimental

Synthesis of 5

To a mixture of methyl 3-bromo-5-nonylaminobenzoate (**4**)[15] (0.70 g, 2.0 mmol) and pyrene-1-boronic acid (0.50 g, 2.0 mmol) in THF (20 mL) were added 2 M aq K_2CO_3 (8.0 mL) and $Pd(PPh_3)_4$ (26 mg, 20 mmol), and the system was heated to reflux overnight. After an aqueous phase was extracted with DCM, the combined organic phase was washed with saturated aq Na_2CO_3. After drying over $MgSO_4$, solvents were removed by rotary evaporator. The crude product was purified by recrystallization from DCM/hexane to obtain yellow crystal in 0.55 g (57% yield). Mp 102-103 ºC. ^{1}H NMR (δ, 200 MHz, ppm, $CDCl_3$) 8.47-7.91 (9H), 7.62 (s, 1H), 7.37 (s, 1H), 6.95 (s, 1H), 3.90 (s, 3H), 3.14 (t, *J*=7.0 Hz, 2H), 1.60 (m, 2H), 1.40-1.20 (12H), 0.87 (t, *J*=6.8 Hz, 3H). ^{13}C NMR (δ, 50 MHz, ppm, $CDCl_3$) 167.5, 148.5, 142.2, 137.3, 131.4, 131.1, 130.9, 130.6, 128.4, 127.5, 127.5, 127.4, 127.3, 127.3, 125.9, 125.2, 125.1, 124.8, 124.8, 124.5, 120.4, 119.2, 112.2, 52.0, 44.0, 31.8, 29.5, 29.4, 29.4, 29.2, 27.1, 22.6,14.1. IR (ν, cm^{-1}) 3395, 2921, 2847,1708, 1597,1523,1435,1352, 1307, 1239, 1187, 1104, 987, 840, 772, 722. Anal. Calcd for $C_{33}H_{35}NO_2$: C, 82.98; H, 7.39; N, 2.93. Found: C, 81.89; H, 7.65; N,2.85.

Synthesis of 6

To a solution of **5** (0.40 g, 0.84 mmol) in THF/MeOH (4 mL/4 mL) was added 2 M aq NaOH (4 mL), and the system was stirred for 10 h at 40 ºC. The solution was acidified to pH 3-4 with 1 M aq HCl and the precipitate was collected to obtain yellow powder in 0.36 g (93% yield).

^{1}H NMR (δ, 200 MHz, ppm, $CDCl_3$) 7.56 (s, 1H), 7.30 (s, 1H), 6.94 (s, 1H), 3.14 (t, *J*=7.1 Hz, 2H), 3.06 (s, 1H), 1.63 (brm, 2H), 1.43-1.21 (12H), 0.89 (t, *J*=6.7 Hz, 3H). ^{13}C NMR (δ, 50 MHz, ppm, $CDCl_3$) 171.1, 147.7, 130.6, 123.3, 123.2, 121.1, 115.2,

83.1, 77.2, 44.4, 31.8, 29.5, 29.3, 29.2, 29.1, 27.0, 22.6, 14.0. IR (ν, cm^{-1}) 3734, 3628, 3422, 3275, 2925, 2850, 1682, 1597, 1506, 1429, 1344, 1305, 1270, 873, 773, 654.

Synthesis of 1a

To a solution of **6** (0.27 g, 0.74 mmol) in $(CHCl_2)_2$ (30.0 mL) was added Ph_3PCl_2 (0.87 mL, 2.6 mmol), and the mixture was heated to reflux for 12 h. After removal of $(CHCl_2)_2$, ethylacetate was added and washed with water. The organic phase was dried over $MgSO_4$ and solvents were removed by rotary evaporator. The crude product was purified by the preparative GPC ($CHCl_3$ as an eluent) to obtain white solid (72 mg, 17%). Mp>300 ºC. ^{1}H NMR (δ, 600 MHz, ppm, $CDCl_3$) 8.40-6.81 (brm, 36H), 4.15-3.62 (brm, 6H), 1.84-1.60 (brs, 6H), 1.50-1.10 (brm, 36 H), 0.94-0.73 (brs, 9H). ^{13}C NMR (δ, 150 MHz, ppm, $CDCl_3$) 170.2, 142.7, 134.3, 131.0, 128.7, 128.3, 127.9, 127.8, 127.6, 127.1, 126.0, 125.3, 124.8, 31.8, 29.5, 29.4, 29.2, 27.8, 26.9, 22.6, 14.1. IR (ν, cm^{-1}) 2923, 2853, 1651, 1586, 1456, 843, 721. HR MALDI-TOF MS calcd for $C_{96}H_{94}N_3O_3$ $(M+H)^+$: 1336.7295. Found: 1336.8346.

Synthesis of 8

To a mixture of methyl 3-iodo-5-nonylaminobenzoate (**7**)[15] (0.40 g, 1.0 mmol), CuI (12 mg, 0.06 mmol), and $Pd(PPh_3)_4$ (34 mg, 0.03 mmol) in Et_3N (10 mL) was added trimethylsilylacetylene (0.28 mL, 2.0 mmol), and the system was heated to 50 ºC for 6 h. After removal of solvents, DCM was added and washed with 1M aq HCl. The organic phase was dried over $MgSO_4$ and solvents were removed by rotary evaporator. The crude product was purified by SiO_2 chromatography (DCM, R_f =0.7) followed by recrystallization from DCM/hexane to obtain yellow powder in 0.27 g (73% yield). Mp 112-113 ºC. ^{1}H NMR (δ, 200 MHz, ppm, $CDCl_3$) 7.44 (s, 1H), 7.20 (s, 1H), 6.83 (s, 1H), 3.88 (s, 3H), 3.73 (s, 1H), 3.11 (t, *J*=7.4, 2H), 1.60 (brm, 2H), 1.41-1.23 (12H), 0.88 (t,

J=6.7 Hz, 3H), 0.24 (s, 9H). ^{13}C NMR (δ, 50 MHz, ppm, $CDCl_3$) 166.8, 148.3, 131.0, 123.9, 121.8, 119.3, 113.9, 104.8, 93.9, 52.1, 43.8, 31.8, 29.5, 29.4, 29.3, 29.2, 27.0, 22.6, 14.1, -0.09. IR (ν, cm^{-1}) 3396, 2954, 2923, 2849, 2149, 1706, 1595, 1518, 1436, 1344, 1308, 1237, 1178, 1105, 996, 843, 771. Anal. Calcd for $C_{22}H_{35}NO_2Si$: C, 70.73; H, 9.44; N, 3.75. Found: C, 70.42; H, 9.57; N, 3.62.

Synthesis of 9

To a solution of **8** (0.20 g, 0.48 mmol) in THF/MeOH (2 mL/2 mL) was added 2 M aq NaOH (2 mL), and the system was stirred for 48 h at room temperature. The solution was acidified to pH 3-4 with 1 M aq HCl and the precipitate was collected to obtain white powder in 0.14 g (93% yield). Mp 112-113 ºC. ^{1}H NMR (δ, 200 MHz, ppm, $CDCl_3$) 7.56 (s, 1H), 7.30 (s, 1H), 6.94 (s, 1H), 3.14 (t, *J*=7.1 Hz, 2H), 3.06 (s, 1H), 1.63 (brm, 2H), 1.43-1.21 (12H), 0.89 (t, *J*=6.7 Hz, 3H). ^{13}C NMR (δ, 50 MHz, ppm, $CDCl_3$) 171.1, 147.7, 130.6, 123.3, 123.2, 121.1, 115.2, 83.1, 77.2, 44.4, 31.8, 29.5, 29.3, 29.2, 29.1, 27.0, 22.6, 14.0. IR (ν, cm^{-1}) 3734, 3628, 3422, 3276, 2925, 2850, 1682, 1597, 1506, 1429, 1344, 1305, 1270, 873, 773, 654.

Synthesis of 10

To a solution of **9** (0.17 g, 0.60 mmol) in dry pyridine (4.0 mL) was added dropwise $SiCl_4$ (0.12 mL, 0.90 mmol) at 0 ºC, and the mixture was heated to reflux for 12 h. After removal of pyridine, DCM was added and washed with 1 M aq HCl. The organic phase was dried over $MgSO_4$ and solvents were removed by rotary evaporator. The crude product was purified by the preparative GPC ($CHCl_3$ as an eluent) to obtain brown solid (16 mg, 10%). Mp>300 ºC. ^{1}H NMR (δ, 600 MHz, ppm, $CDCl_3$) 7.62 (s, minor 3H×0.25), 7.35 (s, minor 3H×0.25), 7.15 (s, major 3H×0.75), 7.02 (s, major 3H×0.75), 6.84 (s, major 3H×0.75), 6.32 (s, minor 3H×0.25), 3.77 (m, major 3H×0.75 and minor

6H×0.25), 3.60 (m, major 3H×0.75), 3.12 (s, major and minor 3H), 1.60-1.48 (6H), 1.36-1.14 (36H), 0.88 (t, *J*=7.1 Hz, 9H). ^{13}C NMR (δ, 150 MHz, ppm, $CDCl_3$), 168.9, 142.3, 139.2, 133.0, 130.1, 127.1, 124.0, 81.1, 79.7, 50.1, 31.8, 29.5, 29.2, 29.1, 27.4, 26.7, 22.6, 14.1. IR (ν, cm^{-1}) 3734, 3306, 3235, 2924, 2853, 1648, 1581, 1433, 1389, 1328, 1261, 1127, 887, 802, 703, 652. HR MALDI-TOF MS calcd for $C_{54}H_{70}N_3O_3$ $(M+H)^+$: 808.5417. Found: 808.5050.

Synthesis of 1b

To a solution of **10** (16 mg, 0.02 mmol) and 1-azidomethylpyrene[18] (30 mg, 0.12 mmol) in DMF (2 mL) was added CuI (2.0 mg, 0.01 mmol), and the system was stirred for 6 h at 90 ºC. After removal of solvents, DCM was added and washed with brine. The organic phase was dried over $MgSO_4$ and solvents were removed by rotary evaporator. The crude product was purified by SiO_2 chromatography (DCM then ethylacetate (R_f = 0.9)) to obtain brown solid (23 mg, 70%). ^{1}H NMR (δ, 600 MHz, ppm, $CDCl_3$) 8.16-7.76 (24H×0.75, 27H×0.25), 7.71-7.66 (6H×0.25), 7.64 (s, 3H×0.75), 7.49 (s, 3H×0.25), 7.46 (3H×0.75), 7.19 (s, 3H×0.75), 7.13 (d, *J*=8.1 Hz, 3H×0.75), 6.69 (s, 3H×0.75), 6.23 (s, 3H×0.25), 5.85 (s, 6H×0.25), 5.55 (d, *J*×15.0 Hz, 3H×0.75), 5.38 (d, *J*=15.0 Hz, 3H×0.75), 3.77 (s, 3H×0.75), 3.67 (6H×0.25), 3.54(3H×0.75), 1.60-1.50 (6H), 1.30-1.05 (36H), 0.84 (t, *J*=7.3 Hz, 9H). ^{13}C NMR (d, 150 MHz, ppm, $CDCl_3$) 169.5, 145.6, 142.9, 139.3, 131.4, 130.9, 130.3, 128.6, 128.3, 127.9, 127.2, 127.0, 126.7, 126.2, 126.0, 125.7, 125.6, 124.7, 124.4, 124.1, 121.5, 107.9, 67.6, 51.5, 49.6, 31.7, 29.7, 29.4, 29.2, 29.1, 27.5, 26.7, 23.9, 22.6, 14.1. IR (ν, cm^{-1}) 3868, 3044, 2922, 2851, 1651,1590,1453,1391, 1304,1185,1129,1044, 881, 845, 756, 706. HR MALDI-TOF MS calcd for $C_{105}H_{102}N_{12}NaO_3$ $(M+Na)^+$: 1602.8129. Found: 1602.8812.

Reference and Notes

44. Kobayashi, K.; Masu, H.; Shuto, A.; Yamaguchi, K. *Chem. Mater.* **2005**, *17*, 6666.
45. Kobayashi, K.; Shimaoka, R.; Kawahata, M.; Yamanaka, M.; Yamaguchi, K. *Org. Lett.* **2006**, *8*, 2385.
46. Anthony, J. E.; Brooks, J. S.; Eaton, D. L.; Parkin, S. R. *J. Am. Chem. Soc.* **2001**, *123*, 9482.
47. Sundar, V. C.; Zaumeil, J.; Podzorov, V.; Menard, E.; Willett, R. L.; Someya, T.; Gershenson, M. E.; Rogers, J. A. *Science* **2004**, *303*, 1644.
48. Hagiwara, K.; Sei, Y.; Akita, M.; Yoshizawa, M. *Chem. Commun.* **2012**, 7678.
49. Winnik, F. M. *Chem. Rev*. **1993**, *93*, 587.
50. Isied, S. S.; Ogawa, M. Y.; Wishart, J. F. *Chem. Rev.* **1992**, *92*, 381.
51. Azumaya, I.; Kagechika, H.; Yamaguchi, K.; Shudo, K. *Tetrahedron* **1995**, *51*, 5277.
52. Azumaya, I.; Kagechika, H.; Yamaguchi, K.; Shudo, K. *Tetrahedron Lett.* **1996**, *37*, 5003.
53. Imabeppu, F.; Katagiri, K.; Masu, H.; Kato, T.; Tominaga, M.; Therrien, B.; Takayanagi, H.; Kaji, E.; Yamaguchi, K.; Kagechika, H.; Azumaya, I. *Tetrahedron Lett.* **2006**, *47*, 413.
54. Azumaya, I.; Okamoto, T.; Imabeppu, F.; Takayanagi, H. *Tetrahedron* **2003**, *59*, 2325.
55. Kakuta, H.; Azumaya, I.; Masu, H.; Matsumura, M.; Yamaguchi; Kagechika, H.; Tanatani, A. *Tetrahedron* **2010**, *66*, 8254.
56. Katagiri, K.; Furuyama, T.; Masu, H.; Kato, T.; Matsumura, M.; Uchiyama, M.; Tanatani, A.; Tominaga, M.; Kagechika, H.; Yamaguchi, K.; Azumaya, I. *Supramol. Chem.* **2011**, *23*, 125.
57. Yamakado, R.; Sugimoto, S.; Matsuoka, S.; Suzuki, M.; Funahashi, Y.; Takagi, K.

Chem. Lett. **2012**, *41*, 249.

58. Takagi, K.; Sugimoto, S.; Yamakado, R.; Nobuke, K. *J. Org. Chem.* **2011**, *76*, 2471.
59. The *syn/anti* ratio in **1a** could not be determined due to the complicated NMR signals.
60. Azumaya, I.; Kagechika, H.; Fujiwara, Y.; Itoh, M.; Yamaguchi, K.; Shudo, K. *J. Am. Chem. Soc.* **1991**, *113*, 2833.
61. Wang, X.-N.-S.; Tao, X.-Z.-Z.; Yamamoto, T. *Org. Lett.* **2011**, *13*, 552.

Chapter 4

Helicity Induction in Three π-Conjugated Chromophores by Planar Chirality of Calixamide

Abstract: Three-dimensional arrangement of π-conjugated chromophores with triple-stranded helicity was achieved by using the planar chirality of *m*-calix[3]amide. Based on spectroscopic data and theoretical calculations, the dynamic and preferred helical characters of bithiophene units embedded in the tubular molecule were elucidated, and the absolute configuration was determined.

Introduction

The construction of well-arranged π-conjugated chromophores has been attracting much attention because the relative orientations and distances of the chromophores play crucial roles in determining their photophysical properties. Calixarenes,[1] cyclophanes,[2] pillararenes,[3] and calixamides[4] have been used as scaffolds to control the spatial relationships of π-conjugated chromophores. Among these, *m*-calix[3]amide,[5] which is a cyclic trimer consisting of benzamide units, has a planar chirality based on the direction of the amide bond, and is therefore considered to be a good candidate as a chiral scaffold (Figure 1A). We have recently reported *m*-calix[3]amides with three oligothiophene chromophores (**1**).[4a] Although the π-conjugated chromophores were successfully aligned by a single *m*-calix[3]amide, the system did not show any chiroptical properties because of racemization by rapid flipping of benzene units in solution. In this study, we report helicity induction in three bithiophene units by two chiral *m*-calix[3]amide scaffolds (Figure 1B). To suppress the flipping of benzene units, we designed a tubular molecule (**2**), in which three π-conjugated chromophores were covalently connected by twin *m*-calix[3]amides.[6] Interestingly, the helicity induction depended strongly on the experimental conditions, such as solvent character and temperature. The three-dimensional (3D) structure of the bithiophene chromophores and absolute configuration were determined by comprehensive spectroscopic and theoretical analyses.

Result and Discussion

The synthetic route to **2** is shown in Scheme 1. The bis(nonylaminobenzoate) derivative **5**, connected by 2,2'-bithiophene, was synthesized in 28% yield from methyl 3-bromo-5-nonylaminobenzoate (**4**) and 5,5'-bis(trimethylstannyl)-2,2'-bithiophene under Migita–Kosugi–Stille cross-coupling conditions. The cyclic oligomerization was

carried out by the dropwise addition of lithium bis(trimethylsilyl)amide (LiHMDS) to a dilute THF solution of **5**. [4,7] Since **5** is the A2 B2 -type multifunctional monomer, a branched polymer was produced as the major products in the final step. Purification by preparative thin-layer chromatography followed by preparative gel-permeation chromatography gave the target molecule **2** in 5% yield as a diastereomeric mixture. Matrix-assisted laser desorption/ionization time-of-flight mass spectrometry showed a signal at *m/z* 1959.00, which can be assigned to the proton adduct of **2**. Elemental analysis was also in good agreement with the theoretical value. As expected, **2** consisted of three optical isomers in the ratio of 1:2:1, generated by the direction of the amide bond of *m*-calix[3]amide: one set of enantiomers having the same planar chirality (Figure 1B) and a meso compound that has two different planar chiralities (Figure 1C). Each compound was successfully separated by chiral high-performance liquid chromatography. The specific rotations ($[\alpha]_D^{25}$; c=10^{-3} in THF) of the first and third eluates were –24.8º [(–)-**2**] and +27.6º [(+)-**2**], respectively. The circular dichroism (CD) spectra of (–)-**2** and (+)-**2** showed a Cotton effect in the mirror image. In contrast, the second eluate [(*meso*)-**2**] did not show a specific rotation and a Cotton effect. Compared with the ^{1}H NMR spectrum of single *m*-calix[3]amide **1**, that of (–)-**2** showed a very simple signal pattern, implying that (–)-**2** adopts a well-defined and highly symmetric geometry. In contrast to the case of **1**, no obvious peak coalescence of (–)-**2** was observed when the ^{1}H NMR spectrum was measured at 50ºC. This result originates from the suppression of the flipping of benzene units by the covalent connections of two *m*-calix[3]amides with three bithiophene units.

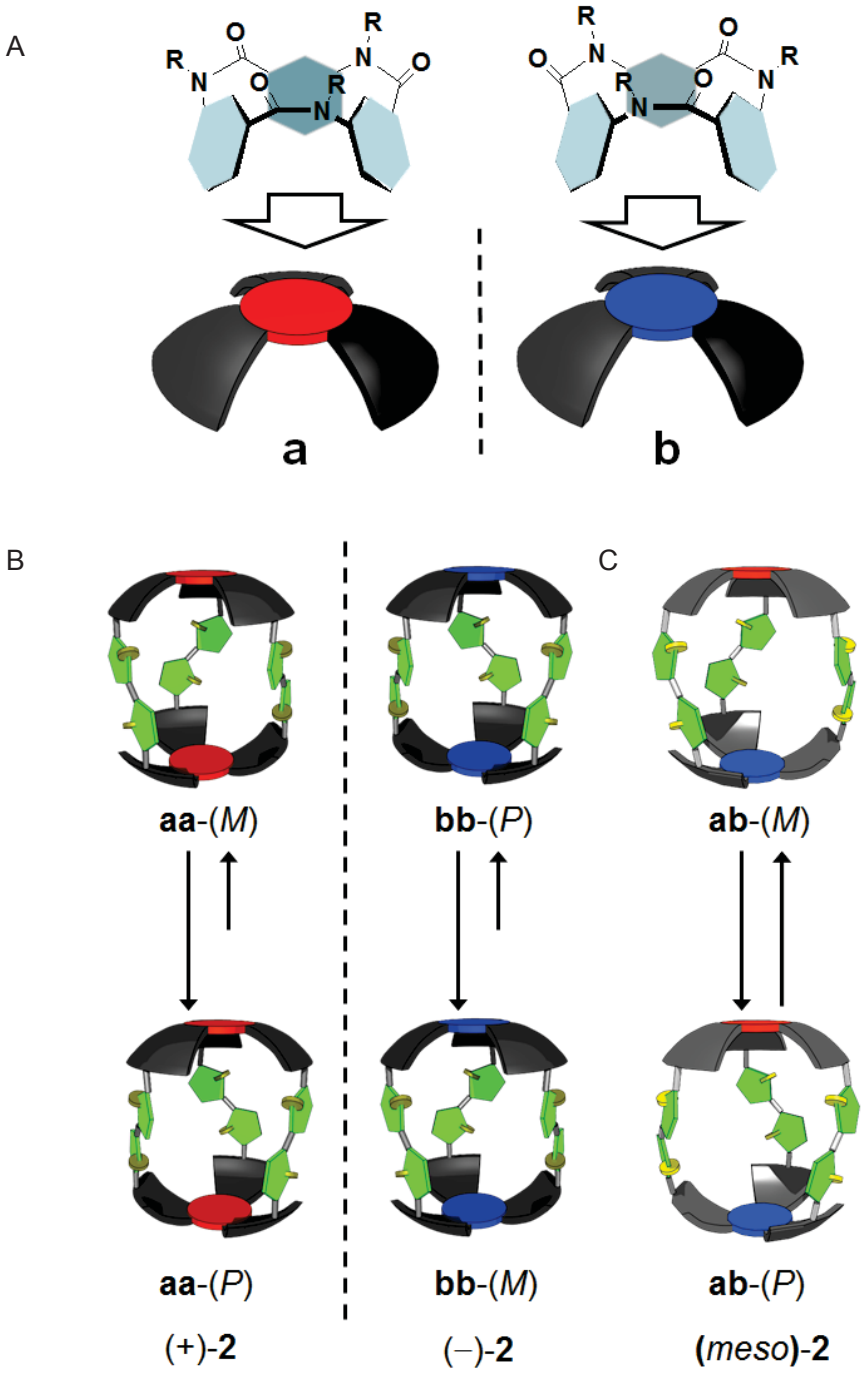

Figure 1. Overview and schematic illustrations of the present system with triple-stranded helicity: A) enantiomers of *m*-calix[3]amide (**a** and **b**); B) equilibria of chiral triple-stranded helical biases of (+)-**2** and (–)-**2**; C) equilibrium of (*meso*)-**2**. *P* and *M* indicate right- and left-handed helicities of the chromophores, respectively.

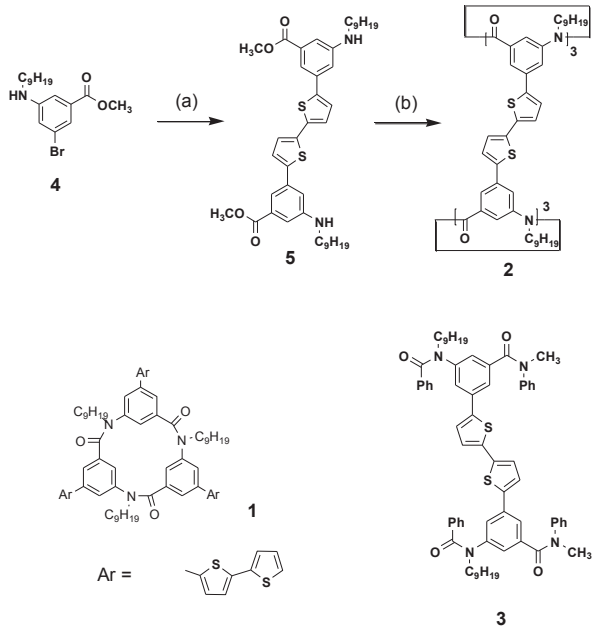

Scheme 1. Synthetic route to tubular molecule **2** and chemical structures of **1** and **3**. Reagents and conditions: a) 5,5'-bis(trimethylstannyl)-2,2'-bithiophene, $Pd(PPh_3)_4$, toluene, reflux; b) LiHMDS, THF, 0 °C.

The UV spectrum of (–)-**2** in chloroform is shown in Figure 2. The tubular molecule (–)-**2** exhibited a large absorption band at 364 nm with a broad shoulder peak at around 420 nm. The observed spectral features can be explained on the basis of Kasha's exciton model.[8] As shown in Figure 3, the formation of a cyclic arrangement of the transition dipole moments results in three exciton states as a result of its symmetry; the lower exciton state, which has one nodal plane, is doubly degenerate and optically forbidden as a result of cancellation of the net transition dipole moment, whereas the higher energy state is optically allowed. This model reasonably accounts for the experimental observation that the peak position of **3** (386 nm) is in between the peak maximum (364 nm) and the shoulder (ca. 420 nm) of the tubular molecule (–)-**2**. The fluorescence spectrum of (–)-**2** showed a larger Stokes shift than that of **3**, and the relative quantum yield of (–)-**2** (2.4%) was about one-sixth smaller than that of **3** (13.4%). Since the

internal conversion from the higher exciton state to the lower exciton state is generally much faster than emission, the observed emission of (–)-**2** would have occurred from the doubly degenerate forbidden transition state, resulting in weak fluorescence. [8]

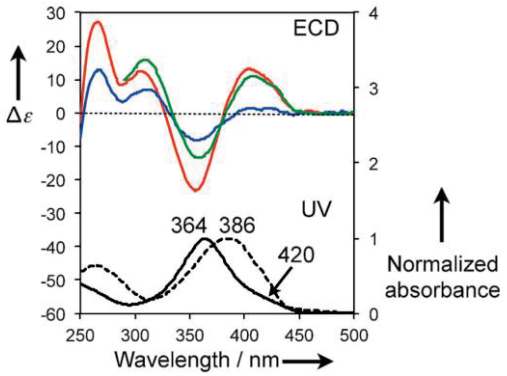

Figure 2. UV spectra of **3** (black dotted line) and (−)-**2** (black solid line) in chloroform and ECD spectra of (−)-**2** at room temperature (blue line: in THF, green line: in toluene, red line: in chloroform).

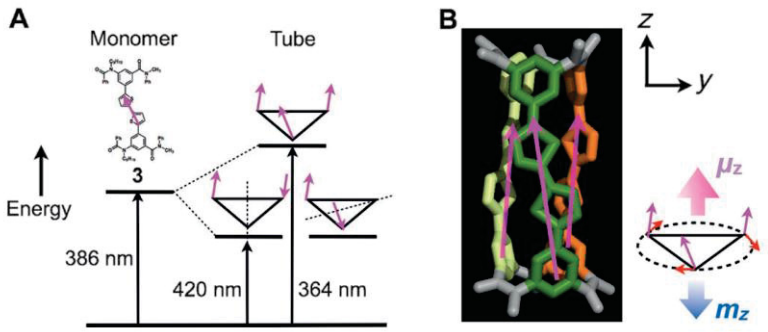

Figure 3. A) Schematic exciton band energy diagram for a tube molecule with three light-absorbing units. B) Optically allowed exciton state of the tube compound with *M* helicity. The pink solid arrows indicate the electric transition dipole moments (μ) of each monomer unit. The red solid arrows indicate the *x,y* components of μ. The pink and blue semitransparent arrows indicate the net electric and magnetic transition dipole moments, respectively.

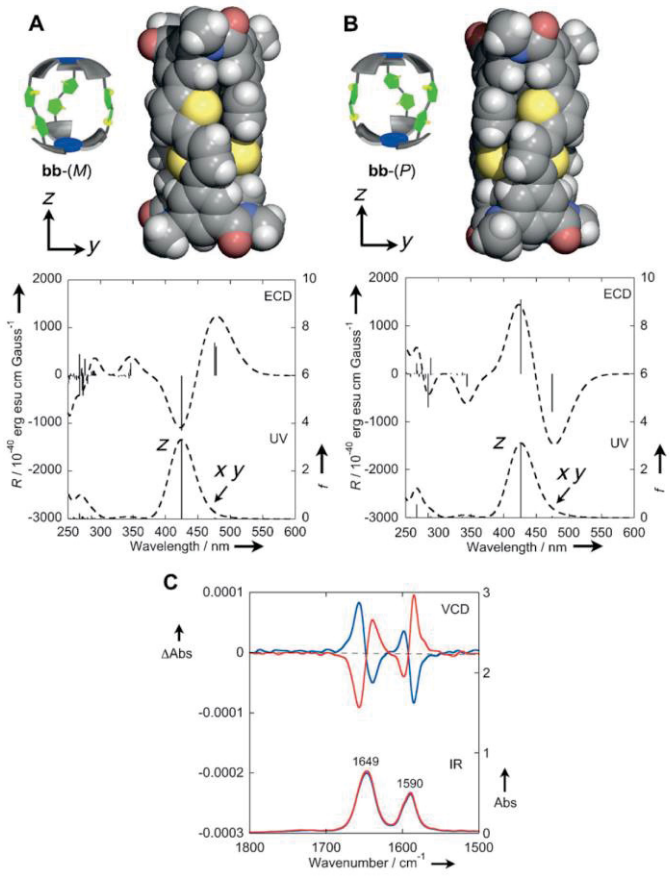

Figure 4. Energy-minimized structures adopting: A) **bb**-(*M*), and B) **bb**-(*P*) at B97D/6-31G(d) level and stick UV and ECD spectra obtained by ZINDO/S calculation. The nonyl side chains were replaced by methyl groups to reduce the computational cost. Gaussian band-shape with 2500 cm^{-1} as a half-height width was applied to produce the spectra. C) IR and VCD spectra of (+)-**2** (red line) and (−)-**2** (blue line) in chloroform

The electronic CD spectra (ECD) of (–)-**2** are shown in Figure 2. Strong bisignate ECD signals corresponding to transitions to the exciton states were observed in chloroform and toluene. This clearly indicates that the chiral information of the ordered *m*-calix[3]amide has been effectively transferred to the π-conjugated system through the covalent linkage, resulting in a twisted chiral structure of the bithiophene chromophores. Although the ECD intensity in THF was considerably weaker than those in chloroform and toluene, we found that the intensity increased significantly with decreasing temperature and completely recovered at room temperature. Since the increase in the ECD intensity in the longer wavelength region was significantly more than that in the shorter wavelength region, the bithiophene chromophores were considered to be aligned in a chiral fashion under low-temperature conditions. These results indicate that (–)-**2** can adopt a dynamic chiral structure between two diastereomeric isomers (Figure 1). The equilibrium constant, *K*, for the interconversion of these isomers in THF was roughly estimated by comparing the experimental specific rotation (–24.8º) with the computed one. Based on the DFT calculation with B3LYP level of theory with the 6-31G(d) basis set, *K* was 1.6, suggesting that substantial amounts of both isomers must be present at the room temperature. [9]

The preferred chiral structure of the tubular molecule (–)-**2** can be determined by considering the excitonic interactions among three transition dipole moments. According to the Rosenfeld equation [$R=Im(\boldsymbol{\mu}\cdot\boldsymbol{m})$], the ECD sign is readily determined by the relative arrangement of the electric transition dipole moment ($\boldsymbol{\mu}$) and the magnetic transition dipole moment ($\boldsymbol{m}$).[10] In the case of the *M* structure (Figure 3), the ECD signal corresponding to the higher exciton state is negative, whereas a positive ECD is predicted for the lower exciton state. As a consequence, it can be concluded that (–)-**2** preferentially adopts a left-handed helicity [**aa**-(*M*) or **bb**-(*M*)] in chloroform and toluene at room temperature, and in THF at low temperature. It is noted that a positive

bisignate ECD signal was observed even though (–)-**2** has chromophores in the *M* helical arrangement.

In order to confirm the qualitative analysis, the UV and ECD spectra were calculated by using the ZINDO/S method.[11,12] Geometry optimization calculations of one enantiomer (**bb**) were performed by using B97D, M06-2X, and B3LYP functionals. The nonyl side chains were replaced by methyl groups to reduce the computational cost. These DFT calculations provided two energy-minimized structures; one has a left-handed helical conformation [**bb**-(*M*)], whereas the other is right-handed [**bb**-(*P*)]. Figure 4A and B show the theoretical ECD and UV spectra of the energy-minimized structures obtained at the B97D/6-31G(d) level. The results reproduced the doubly degenerate lower energy state and the optically allowed higher energy state. The polarizations of the transition to the lower energy state were along the x and y axes, whereas the transition to the higher energy state was polarized along the z axis. In the case of the **bb**-(*M*), the plus-to-minus CD pattern, in ascending energy, was calculated. These results are in good agreement with the above qualitative exciton analysis. Almost the same results were obtained when the M06-2X and B3LYP structures were used. Surprisingly, mirror-image ECD spectra were predicted for these conformers in the range of 250–600 nm, although they are not enantiomers (Figure 1). This implies that the ECD signal associated with the *m*-calix[3]amide moiety is weak and that its absolute configuration is not unambiguously assigned by the ECD spectral analysis.

We successfully determined the absolute configuration using vibrational CD (VCD) spectroscopy (Figure 4C). The VCD spectra of (–)-**2** (blue line) in chloroform showed two dispersion-type signals at 1649 and 1590 cm^{-1}. The former and latter signals were associated with the C=O stretching of carbonyl groups and C=C stretching of benzene rings, respectively. The mirror-image spectrum was observed for (+)-**2** (red line). The theoretical VCD profiles of the two energy-minimized **bb** isomers [**bb**-(*P*) and **bb**-(*M*)]

were calculated.[13] Interestingly, the VCD signal pattern of the *P* conformer was the same as that of the *M* conformer, which indicates that the VCD spectra were associated with the planar chirality of *m*-calix[3]amide and independent of the twisted chirality of chromophores. The experimental pattern of (–)-**2** was consistent with the calculated patterns of **bb**-(*M*) and **bb**-(*P*). The absolute configurations of *m*-calix[3]amides of (+)-**2** and (–)-**2** were, therefore, assigned as **aa** and **bb**, respectively. The VCD and ECD results allowed us to conclude that the planar chiralities of **aa** and **bb** induce, respectively, the *P* and *M* helicities in the three bithiophene units in chloroform. The present VCD assignment agrees with the determination of the absolute configuration on the basis of coupling of C=O stretching by using VCD spectroscopy. [13c]

.

Conclusion

In summary, we achieved chiral 3D alignment of π-conjugated chromophores with triple-stranded helicity. The inherent chirality of *m*-calix[3]amide induced a predominantly one-handed helicity to the arrangement of π-conjugated chromophores, without the help of chiral guests or chiral centers. The absolute configuration of *m*-calix[3]amide and the preferred helicity of the bithiophene units were determined by combined experimental and theoretical studies. It is worth mentioning that ECD and VCD analyses were mutually complementary in aiding the interpretation of the chiral structure in the present system; ECD spectroscopy was sensitive to the helicity of the bithiophene chromophores, whereas VCD spectroscopy was sensitive to the planar chirality of *m*-calix[3]amide. The determination of the solid state structure and the activation energy barrier for the diastereomeric conformation changes between (+)-**2** and (–)-**2** are currently under way.

Experimental

Materials and instruments

All materials were obtained from commercial suppliers and used without purification. 5,5'-Bis(trimethylstannyl)-2,2'-bithiophene,[14] methyl-3-(nonylamino)-5-bromoben--zoate(**4**),[4a] and 3-(*N*-nonyl-*N*-benzoylamino)-5-bromo-*N*'-methylbenzanilide (**6**)[4a] were synthesized following to the previous reports. ^{1}H- and ^{13}C-nuclear magnetic resonance (NMR) spectroscopy and H-H correlation spectroscopy (COSY) were investigated on Bruker Avance 200, 500, and 600 FT-NMR spectrometers using tetramethylsilane (^{1}H-NMR, δ 0.00) and solvent residual peaks as the internal standards (^{1}H-NMR and ^{13}C-NMR). Infrared (IR) spectra were recorded on a JASCO FT-IR 460Plus spectrophotometer in the attenuated total reflectance (ATR) method. Melting points (Mp) were determined on a Yanaco micro melting point apparatus MP-J3. Matrix-assisted laser desorption/ionization time-of-fright mass spectra (MALDI TOF-MS) were performed on a JEOL JMS-S3000 in the spiral mode using dithranol as a matrix. Purifications with preparative gel permeation chromatography (GPC) were carried out on a Japan analytical industry LC-9210 system using tandem JAIGEL 1H, 2H, and 2.5H columns ($CHCl_3$ as an eluent, flow rate = 3.8 mL/min) equipped with an ultraviolet (UV) detector monitored at 254 nm. UV and photoluminescence (PL) spectra were recorded on a Shimadzu UV-1650PC spectrophotometer and a Shimadzu RF-5300PC spectrofluorometer, respectively, using a 10 mm quartz cell. Fluorescence quantum yields (QY) in solution were determined relative to quinine sulfate in 0.05 M H_2SO_4 having a QY of 0.55. The circular dichroism (CD) spectra were measured in 5 mm and 10 mm quartz cells on a JASCO J-820 spectropolarimeter. The temperature was controlled with a liquid nitrogen-controlled quartz cell (5.0 mm) in a cryostat from +25 °C to –90 °C. Optical rotations were measured in a 10 mm quartz cell using a JASCO P-1010 polarimeter at a wavelength of 589 nm in THF at 25 °C. The chiral high

performance liquid chromatography (HPLC) analysis was performed on a Shimadzu LC-10AT liquid chromatograph equipped with a UV detector (TOSOH UV-8020) using a CHIRALPAK IA column (Daicel Chemical Industries, Ltd) (0.46 cm (i.d.) × 25 cm). The VCD spectra were recorded with a spectrometer JASCO FVS-6000, using a 150 μm BaF_2 cell. The absorption signals were detected using a MCT infrared detector. Spectra were recorded at 4 cm^{-1} resolution. Signals were accumulated for 6000 scans.

2,5'-Bis(3-methoxycarbonyl-5-nonylaminobenzene-1-yl)-[5,2']bithiophene (5).

To a toluene (15 mL) solution of **4** (1.4 g, 6.0 mmol) and 5,5'-bis(trimethylstannyl)-2,2'-bithiophene (1.0 g, 2.0 mmol) was added $Pd(PPh_3)_4$ (84 mg, 68 μmol), and the system was heated to reflux overnight. After water was added, an aqueous phase was extracted with CH_2Cl_2. A combined organic phase was dried over $MgSO_4$ and solvents were removed by rotary evaporator. The crude product was purified by SiO_2 chromatography (CH_2Cl_2:acetone=3:1, Rf=0.6) followed by recrystallization from hexane to obtain brown crystals in 0.42 g (28% yield). Mp. 136–137 °C. ^{1}H-NMR (δ, 200 MHz, ppm, $CDCl_3$) 7.59 (s, 2H), 7.42–7.05 (6H), 6.94 (s, 2H), 3.92 (s, 6H), 3.84 (s, 2H), 3.17 (m, 4H), 1.67 (m, 4H), 1.48–1.15 (24H), 0.89 (brs, 6H). ^{13}C-NMR (δ, 50 MHz, ppm, $CDCl_3$) 167.1, 149.0, 142.8, 136.8, 135.0, 131.7, 124.3, 124.1, 115.6, 113.6, 112.6, 51.9, 43.9, 31.8, 29.5, 29.4, 29.2, 27.1, 22.6, 13.9 IR (cm-1) 3399, 2920, 2852, 1702, 1597, 1446, 1349, 1255, 786, 763. Anal. Calcd for $C_{42}H_{56}N_2O_4S_2$: C, 70.35; H, 7.87; N, 3.91; S, 8.94. Found: C, 70.27; H, 7.62; N, 3.86; S, 8.92.

Tubular molecule consisting of twin m-calix[3]amide and three bithiophenes (2).

To a THF (3 mL) solution of **5** (0.22 g, 0.30 mmol) was added dropwise LiHMDS (1.0 M in THF, 2.0 mL, 2.0 mmol) at 0 °C, and the system was stirred for 6 h. After

saturated aq. NH_4Cl was added, an aqueous phase was extracted with $CHCl_3$. A combined organic phase was dried over $MgSO_4$ and solvents were removed by rotary evaporator. The crude product was purified by preparative TLC (CH_2Cl_2:acetone=4:1, Rf=0.6) followed by preparative GPC ($CHCl_3$ as an eluent) to obtain yellow solid in 10 mg (5% yield). Optical resolution was carried out by chiral HPLC with a Daicel CHIRALPAK IA column (0.46 cm (i.d.) × 25 cm) using hexane/THF (50/50 in volume ratio) as an eluent at a flow rate of 1.0 mL/min (elution time (–)**2**=2.9 min, (***meso***)**2**=5.9 min, and (+)**2**=7.6 min). MALDI TOF-MS Calcd for $C_{120}H_{145}N_6O_6S_6$ ($M+H^+$): 1958.96. Found: 1959.00. Anal. Calcd % for $C_{120}H_{144}N_6O_6S_6$; C, 73.58; H, 7.41; N, 4.29; S, 9.82. Found: C, 73.43; H, 7.29; N, 4.23; S, 9.72.

(+) and **(–)2**

Mp. 163–164 °C. ^{1}H-NMR (δ, 600 MHz, ppm, $CDCl_3$) 7.25 (s, 6H), 7.04 (s, 6H), 7.03 (d, *J*=3.7Hz, 6H), 6.80 (t, *J*=3.7Hz, 6H), 6.78 (s, 6H), 4.01 (m, 6H), 3.57 (m, 6H), 1.70–1.58 (12H), 1.39–1.20 (72H), 0.87 (t, *J*=7.2Hz, 18H). ^{13}C-NMR (δ, 150 MHz, ppm, $CDCl_3$) 169.5, 142.8, 140.6, 139.3, 137.8, 134.7, 128.4, 124.9, 124.7, 124.6, 124.5, 49.2, 31.8, 29.5, 29.3, 29.2, 27.7, 26.8, 22.6, 14.1. IR (cm^{-1}) 2923, 1650, 1587, 1389.

(*meso*)2

Mp. 164–165 °C, ^{1}H-NMR (δ, 600 MHz, ppm, $CDCl_3$) 7.22 (s, 6H), 7.09 (s, 6H), 6.98 (d, *J*=3.7Hz, 6H), 6.80 (d, *J*=3.7Hz, 6H), 6.78 (s, 6H), 4.01 (m, 6H), 3.57 (m, 6H), 1.70–1.58 (12H), 1.39–1.20 (72H), 0.87 (t, *J*=7.2Hz, 18H). ^{13}C-NMR (δ, 150 MHz, ppm, $CDCl_3$) 169.6, 142.8, 140.5, 139.3, 137.8, 134.7, 128.4, 124.8, 124.6, 124.5, 124.4, 49.2, 31.8, 29.5, 29.3, 29.2, 27.7, 26.8, 22.6, 14.1. IR (cm^{-1}) 2923, 1650, 1587, 1389.

2,5'-Bis(3-(N-nonyl-N-benzoylamino)-5-(N'-methyl-N'-phenylaminocarbonyl)benzene-1-yl)-[5, 2']bithiophene (3).

To a THF (2.5 mL) solution of 6 (0.14 g, 0.25 mmol) and 2,2'-bithiophene-5,5'-bis(boronic acid) (0.02 g, 0.13 mmol) were added 2 M aq. K_2CO_3 (1 mL) and $Pd(PPh_3)_4$ (2.8 mg, 2.0 μmol), and the system was heated to reflux overnight. After an aqueous phase was extracted with CH_2Cl_2, a combined organic phase was dried over $MgSO_4$. Solvents were removed by rotary evaporator. The crude product was purified by SiO_2 chromatography (CH_2Cl_2:acetone=4:1, Rf=0.6) followed by washed with hexane to obtain brown solid in 50 mg (19% yield). Mp. 75–77 °C. ^{1}H-NMR (δ, 600 MHz, ppm, $CDCl_3$) 7.40 (s, 2H), 7.30 (t, *J*=7.6Hz, 4H), 7.26–7.19 (4H), 7.18–7.10 (8H), 7.03 (s, 2H), 7.01 (s, 2H), 7.00 (d, 2H, *J*=2.9 Hz), 6.90 (s, 2H), 6.88 (s, 2H), 6.84 (s, 2H), 3.67 (t, *J*=7.6Hz, 4H), 3.49 (s, 6H), 1.42 (m, 4H), 1.33–1.18 (24H), 0.87 (t, *J*=6.2Hz, 6H). ^{13}C-NMR (δ, 150 MHz, ppm, $CDCl_3$) 170.0, 168.9, 144.5, 143.4, 141.1, 137.4, 137.0, 135.8, 134.3, 129.6, 129.4, 128.5, 127.8, 127.0, 126.9, 126.4, 125.8, 124.7, 124.6, 123.9, 50.1, 38.3, 31.7, 29.5, 29.3, 29.2, 27.6, 26.8, 22.6, 14.1. IR (cm^{-1}) 2924, 2360, 1645, 1585, 1376, 695. HR ESI-MS Calcd for $C_{68}H_{74}N_4NaO_4S_2$ (M+Na+): 1097.5049. Found: 1097.5040.

Computation Detail

All computations were performed using the Gaussian 09 package of programs.[15] Geometry optimizations of **3** and (–)-**2** were executed with the DFT method employing the B3LYP functional. M06-2X and B97D functionals were also used for (-)-**2**. The 6-31G(d) basis sets were used for all atoms. The C_9H_{19} group was omitted and replaced with a methyl group for these calculations. The time-dependent DFT method at the B3LYP/6-31G(d) level or the ZINDO/S method was used to calculate the oscillator strengths and rotatory strengths. Rotatory strengths were reported here based on the

dipole-length expression. Gaussian band-shape with 2500 cm^{-1} as a half-height width was applied to produce the spectra. The IR and VCD spectra were calculated at the same level as the optimization calculation.

Reference and Notes

62. (a) H.-H. Yu, B. Xu, T. M. Swager, *J. Am. Chem. Soc.* **2003**, *125*, 1142–1143; (b) H.-H. Yu, A. E. Pullen, M. G. Büschel, T. M. Swager, *Angew. Chem.* **2004**, *116*, 3786–3789; *Angew. Chem. Int. Ed.* **2004**, *43*, 3700–3703; (c) X.-H. Sun, C.-S. Chan, M.-S. Wong, W.-Y. Wong, *Tetrahedron* **2006**, *62*, 7846–7853; (d) C. Hippius, I. H. M. van Stokkum, M. Gsänger, M. M. Groeneveld, R. M. Williams, F. Würthner, *J. Phys. Chem. C* **2008**, *112*, 2476–2486.

63. (a) G. P. Bartholomew, G. C. Bazan, *J. Am. Chem. Soc.* **2002**, *124*, 5183–5196; (b) A. Tsuge, T. Hara, T. Moriguchi, M. Yamaji, *Chem. Lett.* **2008**, *37*, 870–871; (c) A. Tsuge, T. Hara, T. Moriguchi, *Tetrahedron Lett.* **2009**, *50*, 4509–4511; (d) Y. Morisaki, Y. Chujo, *Polym. Chem.* **2011**, *2*, 1249–1257; (e) Y. Morisaki, R. Hifumi, L. Lin, K. Inoshita, Y. Chujo, *Polym. Chem.* **2012**, *3*, 2727–2730.

64. (a) T. Ogoshi, K. Umeda, T. Yamagishi, Y. Nakamoto, *Chem. Commun.* **2009**, 4874–4876; (b) T. Ogoshi, R. Shiga, M. Hashizume, T. Yamagishi, *Chem. Commun.* **2011**, *47*, 6927–6929.

65. (a) K. Takagi, S. Sugimoto, R. Yamakado, K. Nobuke, *J. Org. Chem.* **2011**, *76*, 2471–2478; (b) R. Yamakado, S. Matsuoka, M. Suzuki, K. Takagi, K. Katagiri, I. Azumaya, *Tetrahedron* **2013**, *69*, 1516–1520.

66. (a) F. E. Elhadi, W. D. Ollis, J. F. Stoddart, D. J. Williams, K. A. Woode, *Tetrahedron Lett.* **1980**, *21*, 4215–4218; (b) F. E. Elhadi, W. D. Ollis, J. F. Stoddart, *J. Chem. Soc. Perkin Trans*. *1* **1982**, 1727–1732; (c) I. Azumaya, H. Kagechika, K. Yamaguchi, K. Shudo, *Tetrahedron Lett.* **1996**, *37*, 5003–5006; (d) I. Azumaya, T. Okamoto, F. Imabeppu, H. Takayanagi, *Tetrahedron* **2003**, *59*, 2325–2331; (e) F. Imabeppu, K. Katagiri, H. Masu, T. Kato, M. Tominaga, B. Therrien, H. Takayanagi, E. Kaji, K. Yamaguchi, H. Kagechika, I. Azumaya, *Tetrahedron Lett.* **2006**, *47*, 413–416; (f) H. Masu, K. Katagiri, T. Kato, H. Kagechika, M. Tominaga, I.

Azumaya, *J. Org. Chem.* **2008**, *73*, 5143–5146; (g) H. Kakuta, I. Azumaya, H. Masu, M. Matsumura, K. Yamaguchi, H. Kagechika, A. Tanatani, *Tetrahedron* **2010**, *66*, 8254–8260; (h) K. Katagiri, T. Furuyama, H. Masu, T. Kato, M. Matsumura, M. Uchiyama, A. Tanatani, M. Tominaga, H. Kagechika, K. Yamaguchi, I. Azumaya, *Supramol. Chem.* **2011**, *23*, 125–130; (i) N. Fujimoto, M. Matsumura, I. Azumaya, S. Nishiyama, H. Masu, H. Kagechika, A. Tanatani, *Chem. Commun.* **2012**, *48*, 4809–4811; (j) R. Yamakado, S. Sugimoto, S. Matsuoka, M. Suzuki, Y. Funahashi, K. Takagi, *Chem. Lett.* **2012**, *41*, 249–251.

67. Higuchi et al. have recently reported chiral phenylazomethine cages with covalently-connected three 1,4-phenylene units arranged in the twisted manner. See: R. Shomura, S. Higashibayashi, H. Sakurai, Y. Matsushita, A. Sato, M. Higuchi, *Tetrahedron Lett.* **2012**, *53*, 783–785.
68. (a) A. Yokoyama, T. Maruyama, K. Tagami, H. Masu, K. Katagiri, I. Azumaya, T. Yokozawa, *Org. Lett.* **2008**, *10*, 3207–3210; (b) T. Ohishi, T. Suzuki, T. Niiyama, K. Mikami, A. Yokoyama, K. Katagari, I. Azumaya, T. Yokozawa, *Tetrahedron Lett.* **2011**, *52*, 7067–7070.
69. (a) M. Kasha, H. R. Rawls, M. A. El-Bayoumi, *Pure Appl. Chem.* **1965**, *11*, 371–392; (b) M. Kasha, in *Spectroscopy of the Excited State* (Ed.: B. Bartolo), Plenum, New York, **1976**, pp. 337–363.
70. It is to be noted that the computed specific rotation and the estimated equilibrium constant were affected by the calculation method (K=0.4 with M06-2X and K=1.2 with B97D).
71. (a) A. Rodger, B. Nordén, in *Circular Dichroism and Linear Dichroism*, Oxford University Press, Oxford, **1997**; (b) N. Kobayashi, A. Muranaka, J. Mack, in *Circular Dichroism and Magnetic Circular Dichroism Spectroscopy for Organic Chemists*, RSC Publishing, Cambridge, **2012**.

72. Recent ECD analysis using ZINDO/S method: (a) J. L. Alonso-Gómez, P. Rivera-Fuentes, N. Harada, N. Berobe, F. Diederich, *Angew. Chem.* **2009**, *121*, 5653–5656; *Angew. Chem. Int. Ed.* **2009**, *48*, 5545–5548; (b) M. Kudo, T. Hanashima, A. Muranaka, H. Sato, M. Uchiyama, I. Azumaya, T. Hirano, H. Kagechika, A. Tanatani, *J. Org. Chem.* **2009**, *74*, 8154–8163; (c) P. Rivera-Fuentes, J. L. Alonso-Gómez, A. G. Petrovic, F. Santoro, N. Harada, N. Berova, F. Diederich, *Angew. Chem.* **2010**, *122*, 2296–2300; *Angew. Chem. Int. Ed.* **2010**, *49*, 2247–2250; (d) H. Maeda, T. Nishimura, R. Akuta, K. Takaishi, M. Uchiyama, A. Muranaka, *Chem. Sci.* **2013**, *4*, 1204–1211.

73. TDDFT calculation also provided almost the same result as the ZINDO/S calculation.

74. Recent structural analysis using VCD. (a) H.-Z. Tang, B. M. Novak, J. He, P. L. Polavarapu, *Angew. Chem.* **2005**, *117*, 7464–7467; *Angew. Chem. Int. Ed.* **2005**, *44*, 7298–7301; (b) T. Kawauchi, J. Kumaki, A. Kitaura, K. Okoshi, H. Kusanagi, K. Kobayashi, T. Sugai, H. Shinohara, E. Yashima, *Angew. Chem.* **2008**, *120*, 525–529; *Angew. Chem. Int. Ed.* **2008**, *47*, 515–519; (c) T. Taniguchi, K. Monde, *J. Am. Chem. Soc.* **2012**, *134*, 3695–3698; (d) F. Torricelli, J. Bosson, C. Besnard, M. Chekini, T. Bürgi, J. Lacour, *Angew. Chem.* **2013**, *125*, 1840–1844; *Angew. Chem. Int. Ed.* **2013**, *52*, 1796–1800.

75. E. Kozma, D. Kotowski, F. Bertini, S. Luzzati, and M. Catellani, *Polymer*, **2010**, *51*, 2264–2270. Gaussian 09, Revision C.01, M. J. Frisch, G. W. Trucks, H. B. Schlegel, G. E. Scuseria, M. A. Robb, J. R. Cheeseman, G. Scalmani, V. Barone, B. Mennucci, G. A. Petersson, H. Nakatsuji, M. Caricato, X. Li, H. P. Hratchi, A. F. Izmaylov, J. Bloino, G. Zheng, J. L. Sonnenberg, M. Hada, M. Ehara, K. Toyota, R. Fukuda, J. Hasegawa, M. Ishida, T. Nakaj, Y. Honda, O. Kitao, H. Nakai, T. Vreven, J. A. Montgomery, Jr., J. E. Peralta, F. Ogliaro, M. Bearpark, J. J. Heyd, E.

Brothers, K. N. Kudin, V. N. Staroverov, T. Keith, R. Kobayashi, J. Norman, K. Raghavachari, A. Rendell, J. C. Burant, S. S. Iyengar, J. Tom, M. Cossi, N. Rega, J. M. Millam, M. Klene, J. E. Knox, J. B. Cro, V. Bakken, C. Adamo, J. Jaramillo, R. Gomperts, R. E. Stratmann, O. Yazyev, A. J. Austin, R. Cammi, C. Pomelli, J. W. Ochterski, R. L. Martin, K. Morokuma, V. G. Zakrzewski, G. A. Voth, P. Salvador, J. J. Dannenberg, S. Dapprich, A. D. Daniels, O. Farkas, J. B. Foresman, J. V. Ortiz, J. Cioslowski, and D. J. Fox, Gaussian, Inc., allingford CT, 2010.

Chapter 4. Helicity Induction in Three π-Conjugated Chromophores by Planner Chirality of Calixamide

Chapter 5

Synthesis and Optical Properties of Cyclic Trimer Bearing 9,10-Diphenylanthracene Based on an Aromatic Tertiary Amide Unit

Abstract: Novel cyclic aromatic amide oligomers containing highly fluorescent 9,10-diphenylanthracene units were prepared by condensation of a monomer with amino and ester functional groups using lithium bis(trimethylsilyl)amide. The cyclic trimer (**C3A**, 40%) and tetramer (**C4A**, 8%) were isolated using preparative gel permeation chromatography. Some of the aromatic proton signals derived from anthracene were observed in the upfield region (6.96–6.87 ppm) in the ^{1}H nuclear magnetic resonance spectrum of **C3A.** X-ray crystallographic analysis indicated that three anthracene moieties are inclined with respect to the cyclic skeleton and partly overlap each other. The fluorescence peak maximum of **C3A** (438 nm) showed a small red-shift compared with that of acyclic model compound (425 nm). Reduction of the amide carbonyl group in **C3A** gave the cyclic trimer **HC3A**, which has a tertiary amine unit. The fluorescence peak maximum of **HC3A** (489 nm) was largely red-shifted from that of **C3A** and exhibited strong solvent dependence. A linear correlation was observed between the Stokes shift ($\Delta\nu$), ranging from 2981 to 6646 cm^{-1}, and the Reichardt's solvent polarity parameter [$E_T(30)$].

Introduction

The well-defined three-dimensional spatial arrangement of π-conjugated chromophores has been attracting much attention with regard to the fundamental understanding of the relationship between this spatial arrangement and the optoelectronic properties of a compound.[1,2] This is because such organic molecules are mostly used not in an isolated state but in a condensed state (film or crystal) in optoelectronic devices such as light-emitting diodes,[3] field-effect transistors,[4] and photovoltaic cells.[5] In fluorescence resonance energy transfer (FRET) between energy-donor and energy-acceptor chromophores, the FRET efficiency can be described by the Förster equation.[6] The efficiency of this energy transfer is inversely proportional to the sixth power of the distance between the two chromophores and the relative orientation of their dipole moments. Accordingly, both the chemical structure and the three-dimensional arrangement have to be taken into account when developing new materials with optimal properties for optoelectronic applications. A number of cyclic oligomers, including [2.2]paracyclophane,[7–12] calix[4]arene,[13–15] bicyclo[4.4.1]undecane,[16–18] and pillar[5]arene,[19,20] have been used as scaffolds for the three-dimensional arrangement of π-conjugated systems. For example, Morisaki et al. and Bazan et al. independently reported that the [2.2]paracyclophane unit shows transannular through-space π–π interactions and is an excellent building block for the elongation of π-conjugated systems. It has also been demonstrated that an enantiopure ortho-difunctionalized [2.2]paracyclophane chiral skeleton can align π-conjugated oligomers to give optically active properties.[21] We previously investigated the alignment of pyrene using cyclic aromatic amide trimer, calix[3]amide, as the scaffold.[22] As a result of steric effects, the pyrenyl groups attached to the benzene ring were aligned in a screw-like fashion; this was confirmed by X-ray crystallographic analysis. However, the distance and orientation of π-conjugated chromophores on the benzene ring are difficult to control,

especially in the solution state, because calix[3]amide has a conformational flexibility derived from *syn* and *anti* isomers.[23] Recently, we achieved three-dimensional arrangement of bithiophenes with dynamic triple-stranded helicity using the planar chirality of calix[3]amide.[24] Although the interconversion between *syn* and *anti* isomers was nicely suppressed, the synthetic procedure consisted of multi-step reactions to be concerned with the low efficiency. We then envisaged that the install of π-conjugated chromophores directly in the cyclic structure would be better strategy to furnish the precision arrangement of π-conjugated chromophores and the aromatic tertiary amide unit must be an excellent linker to construct the molecule.

9,10-Diphenylanthracene (DPA) and its derivatives are highly fluorescent, and they are useful soft materials for the light-emitting application.[25,26] Accordingly, it is important to investigate the relationship between the three-dimensional arrangement and the optical properties. Yoshizawa et al. reported a tubular macrocycle containing four anthracene units connected by meta-phenylene linkers.[27] Despite the close arrangement of the chromophores, the compound showed neither excimer emission nor fluorescence quenching, as a result of the enforced orthogonal conformation. Toyota et al.[28] and Zhao et al.[29] synthesized aryleneethynylene macrocycles containing the 9,10-anthrylene unit, and demonstrated self-assembly behavior in the solution and liquid-crystalline phases. However, currently known macrocycles mostly have hydrocarbon frameworks.[30-32] The introduction of heteroatoms and push–pull interactions is expected to impart charge-transfer properties to cyclic oligomers bearing π-conjugated chromophores.[33]

In this paper, we will describe the synthesis of new cyclic aromatic amide trimer (**C3A**) and tetramer (**C4A**) containing the DPA unit. The conformations in the solution and solid states were studied using nuclear magnetic resonance (NMR) spectroscopy and X-ray crystallography, and ultraviolet (UV)/fluorescence spectroscopy were measured to discuss their optical properties. Reduction of the amide carbonyl group was

also performed to investigate the influence of the linker on the optical properties.

RESULTS AND DISCUSSION

Synthesis. Monomer **1**, containing amino and ester functional groups, was synthesized as shown in Scheme 1. 4-Iodoacetanilide was alkylated with NaH and 1-bromooctane to obtain **3** in 85% yield. The Suzuki coupling reaction of **3** with 10-bromoanthracene-9-boronic acid was performed using $Pd(PPh_3)_4$, giving **4** in 68% yield. The acetyl group in **4** was removed using concentrated HCl, and the obtained product **5** was subjected to a second Suzuki coupling reaction with 4-methoxycarbonylphenylboronic acid pinacol ester, giving **1** as a yellow powder in 82% yield. The cyclic oligomerization of **1** was performed using a 1 M tetrahydrofuran (THF) solution of lithium bis(trimethylsilyl)amide (LiHMDS) (Scheme 2). According to the method previously reported by Yokozawa et al.,[34] a THF solution of **1** was slowly added to LiHMDS (5 equiv relative to **1**) at room temperature and 0 °C (Method A). Although **1** was almost completely consumed irrespective of the reaction temperature (Figure 1, broken line), a proton signal assignable to the methyl ester was clearly detected in the ^{1}H NMR spectrum, implying the production of linear oligomers instead of cyclic oligomers. Higher-molecular-weight oligomers were obtained by carrying out the reaction at room temperature. In contrast, when the cyclic oligomerization was performed by dropwise addition of LiHMDS to a THF solution of **1** (Method B), no proton signal derived from the methyl ester was observed in the ^{1}H NMR spectrum. In the matrix-assisted laser desorption/ionization-time of flight (MALDI-TOF) mass spectrum of the crude products, cyclic oligomers (3 mer ~ 6 mer) were specifically detected. No significant temperature dependence was observed in the gel permeation chromatography (GPC) profiles between room temperature and 0 °C (Figure 1, solid

line). Cyclic trimer (**C3A**) and tetramer (**C4A**) were isolated, using preparative GPC, in 40% and 8% yields, respectively. Cyclic trimer **C3A** was preferentially obtained, as in the cyclic oligomerization of other aminobenzoic acid derivatives.[35–37] The carbonyl stretching vibrations of the amide bond were confirmed by infrared (IR) spectroscopy (**C3A** 1649 cm^{-1}, **C4A** 1645 cm^{-1}), and the cyclic architectures were verified by the MALDI-TOF mass spectra. Subsequently, reduction of the amide carbonyl group in **C3A** was carried out using $LiAlH_4$ and $AlCl_3$ in THF/Et_2O, giving the cyclic trimer **HC3A**, which has a methylene group between the benzene ring and the nitrogen atom, in 71% yield (Scheme 2). The peak derived from the amide carbonyl group completely disappeared in the IR spectrum, and the structure of **HC3A** was identified from the ^1H NMR spectrum and MALDI-TOF mass spectrum. Acyclic model compound **2** was also synthesized.

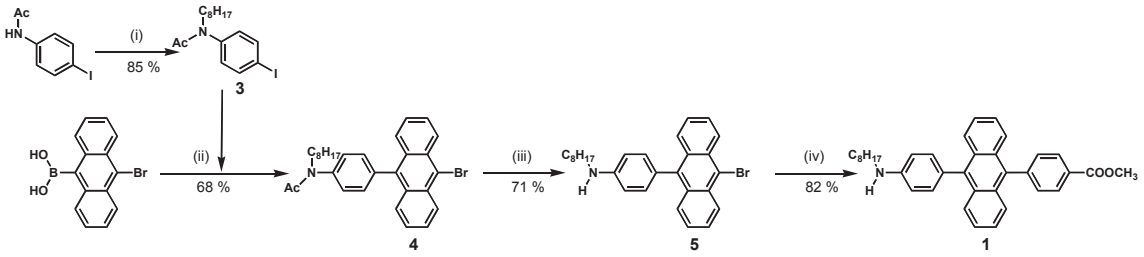

Scheme 1. Synthetic route to monomer **1**. Condition and reagents: i) NaH (55% oil suspension), 1-Bromooctane, DMF, 100 ˚C; ii) K_2CO_3, $Pd(PPh_3)_4$, THF, H_2O, reflux; iii) conc. HCl, Ethylene glycol, Dioxane, reflux; iv) 4-Methoxycarbonylphenyl boronic acid pinacol ester, K_2CO_3, $Pd(PPh_3)_4$, THF, H_2O, reflux.

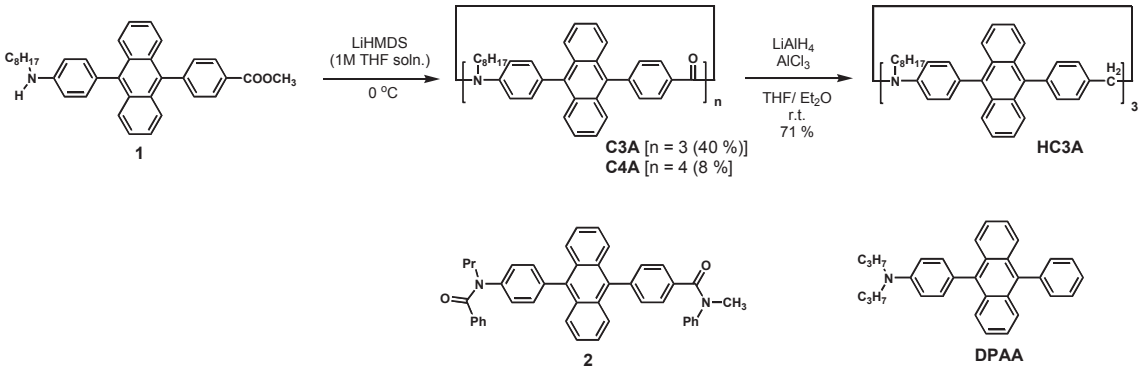

Scheme 2. Synthetic route to cyclic aromatic oligomers **C3A**, **C4A**, and **HC3A**. The chemical structure of acyclic model compounds **2** and **DPAA**.

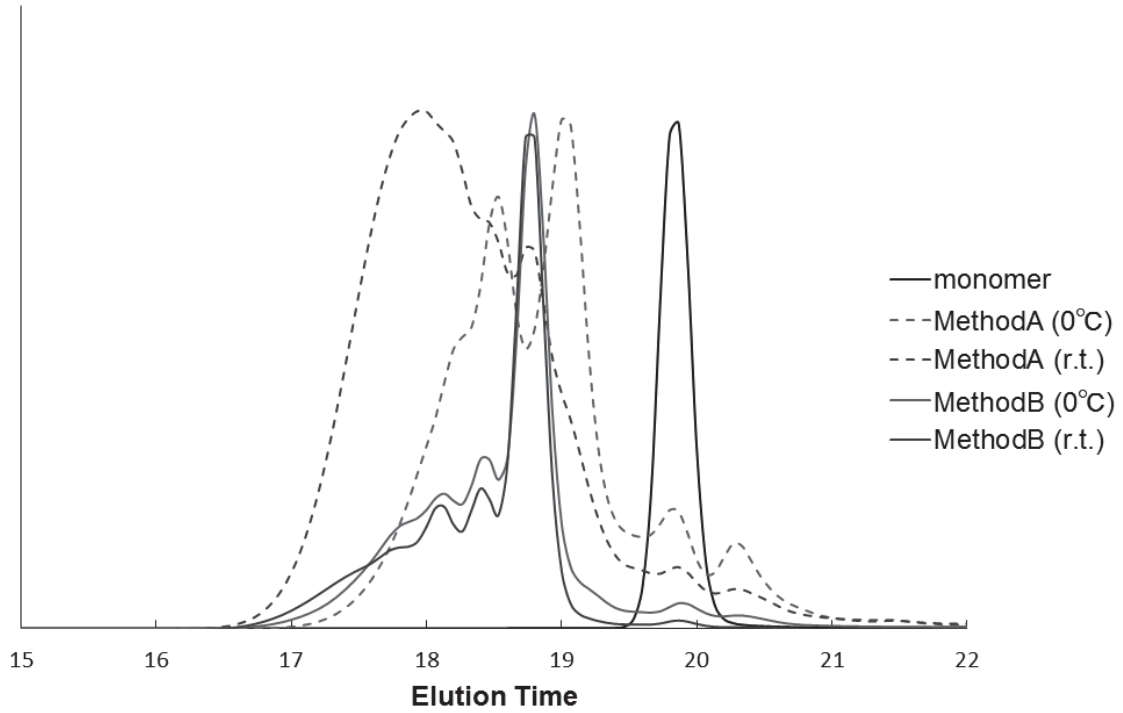

Figure 1. GPC (THF) profiles of reaction mixture.

Characterization. The ^{1}H NMR spectrum of **C3A** showed seven proton signals in the aromatic region, which were fully assigned using H–H correlation spectroscopy (COSY) and rotating overhauser enhancement and exchange spectroscopy (ROESY). It should be noted that two broad multiplet signals with a combined integral ratio of 12

appeared at 6.96–6.87 ppm at room temperature; these were assigned to the *f* and *g* protons of the anthracene ring (Figure 2). Since this upfield shift is not observed in acyclic model compound **2**, the shielding effect by the other anthracene rings located in close proximity is the most probable cause. Variable-temperature NMR studies showed that the corresponding proton signals broadened with decreasing temperature, and a signal with an integral ratio of 6 was observed at 6.4 ppm at 223 K (Figure 3). It can be deduced that the rotational motion of anthracene rings is suppressed at low temperatures, resulting in separate detection of intra-annular (*f* and *g*) and extra-annular (*f*″ and *g*′) protons. The signals from the *b* and *c* protons also broadened with decreasing temperature, but the proton signals derived from the benzene ring did not show obvious changes within the examined temperature range. Unfortunately, the calculation of the rotational energy barrier was difficult because the paired proton signal at the down field region was overlapped with other proton signals. In contrast, in the ^{1}H NMR spectrum of **C4A**, the corresponding proton signals of the anthracene ring were observed in the normal region (7.27–7.09 ppm). The difference between the chemical shifts in the spectra of **C3A** and **C4A** is probably originated from the conformations and ring sizes of the cyclic oligomers; this was further investigated using X-ray crystallography.

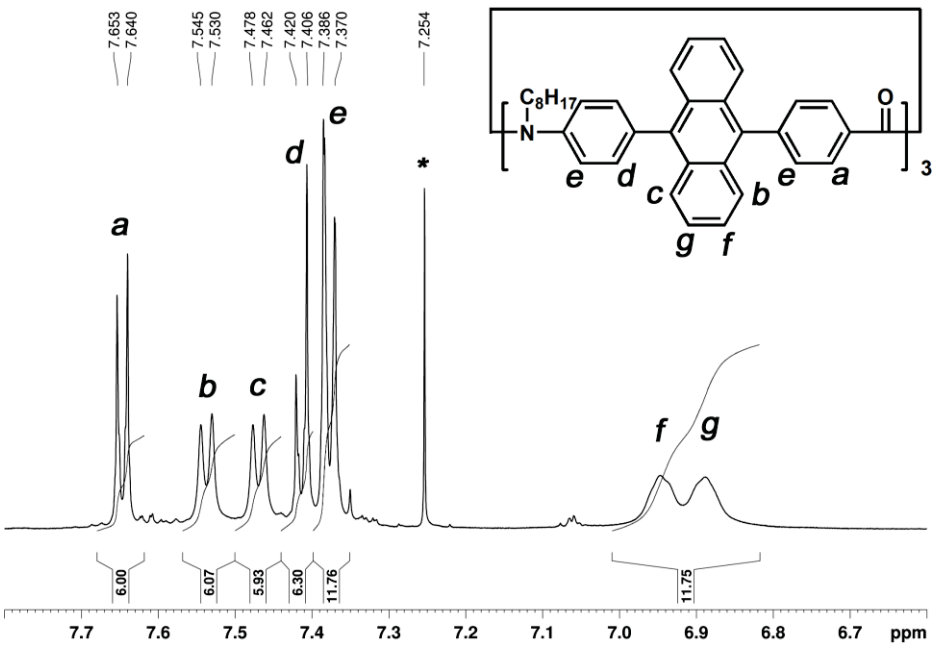

Figure 2. Expanded ^{1}H NMR spectrum of **C3A** in $CDCl_3$.

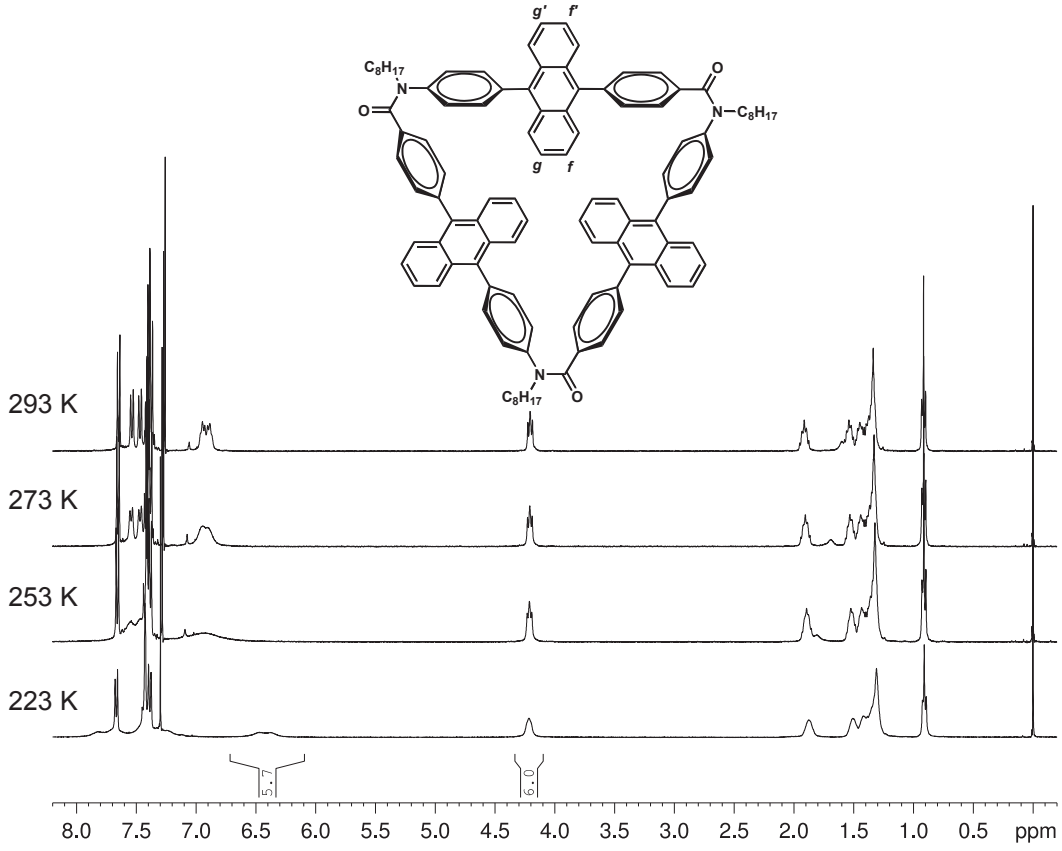

Figure 3. Variable-temperature ^{1}H NMR spectra of **C3A** in $CDCl_3$.

The relative positions of the three DPA groups were determined by X-ray crystallography, using cyclic aromatic amide oligomers with *n*-propyl substituents on the amide nitrogen (**C3A´** and **C4A´**) instead of **C3A** and **C4A**. Single crystals of **C3A´** and **C4A´** were obtained by recrystallization from $CHCl_3$ and hexane. Figure 4 shows the crystal structure of **C3A´**; three anthracene moieties are inclined with respect to the cyclic skeleton and partly overlap each other (Figure 4b). The phenyl and anthracene planes have a twisted conformation, with (N)Ph–Anth(Ph) and (Ph)Anth–Ph(CO) torsion angles of 78.2° and 87.2°, respectively, on average. It is of particular interest that **C3A´** forms a chiral crystal (space group: $P2_1$) as a result of fixing of the axis chirality, although **C3A´** is achiral in the solution state. In contrast, four anthracene moieties lie horizontally and a plane of mirror symmetry is observed in the case of **C4A´** (space group: *P*-1) (Figure 5). The crystals stacked along the *a*-axis and some of the neighboring column molecules filled the space between the molecules (Figure 5c).

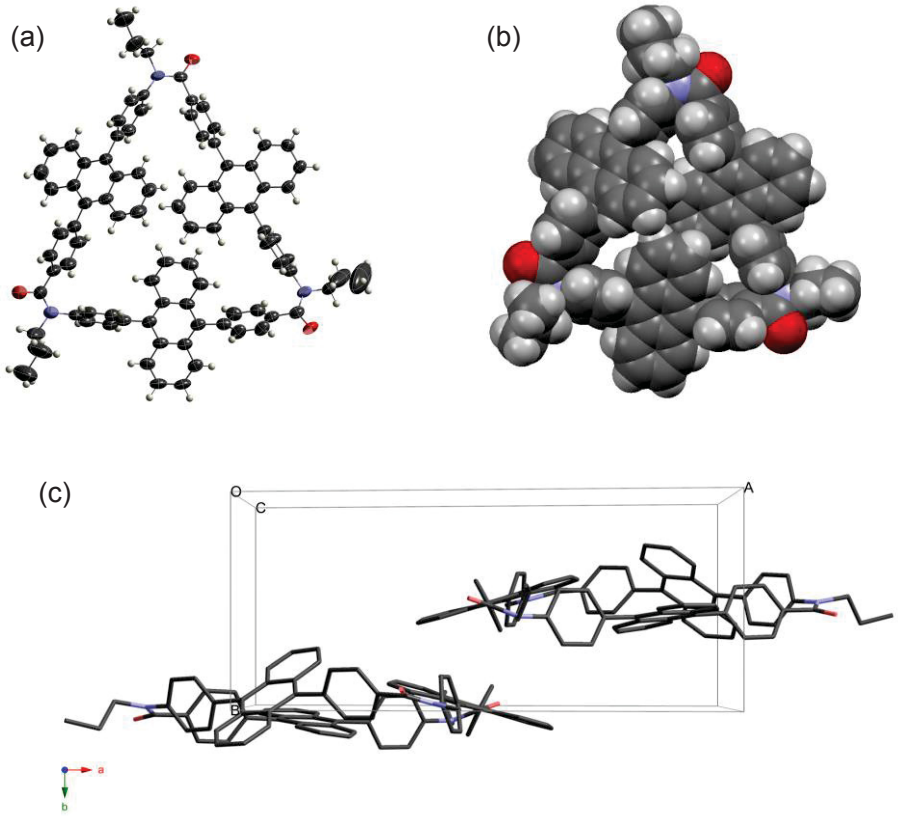

Figure 4. Crystal structure of **C3A´**. (a) Thermal ellipsoidal model. The ellipsoids are drawn at 50% probability level while isotropic hydrogen atoms are represented by spheres of arbitrary size. (b) Space-filling model. (c) Packing structure indicated by stick model along c axis. Labels, disordered atoms, and solvent molecules are omitted for clarity.

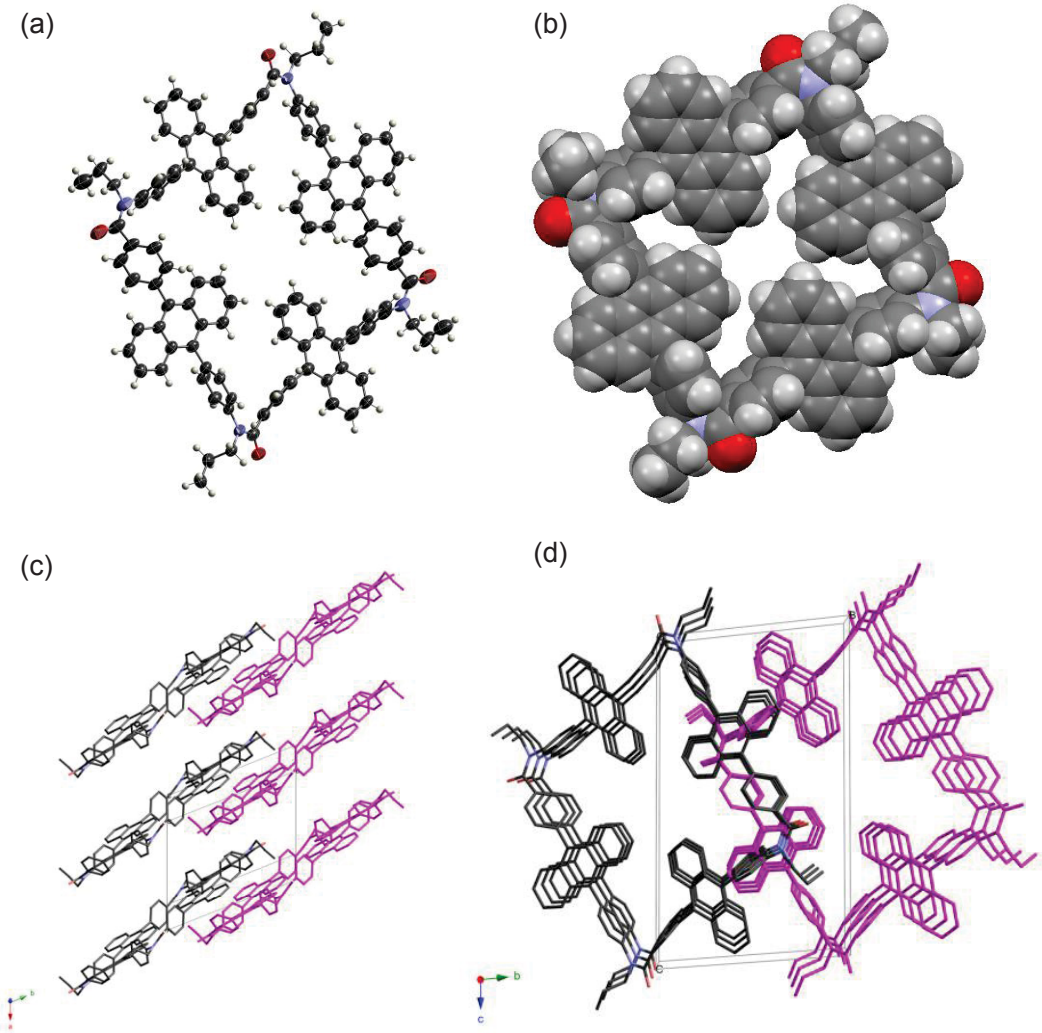

Figure 5. Crystal structure of **C4A´**. (a) Thermal ellipsoidal model. The ellipsoids are drawn at 50% probability level while isotropic hydrogen atoms are represented by spheres of arbitrary size. (b) Space-filling model. Pacing structure indicated by stick model along *c* axis (c) and *a* axis (d). Labels, disordered atoms and solvent molecules are omitted for clarity.

The UV and fluorescence spectra of **C3A, C4A** and **2** in dichloromethane (DCM) were recorded (Figure 6). The UV spectrum of **C3A** and **C4A** are similar to that of **2**. In contrast, the fluorescence peak maximum of **C3A** (λ_{max} = 438 nm) and **C4A** (λ_{max} = 439

nm) were slightly red-shifted compared with that of **2** (λ_{max} = 425 nm). The relative fluorescence quantum yields of **C3A** (15%) and **C4A** (6%) were lower than that of DPA (87%). The fluorescence spectra were independent of the solution concentration between 10^{-4} and 10^{-6} M. Consequently, the red-shifted fluorescence emission of **C3A** and **C4A** can be explained by intramolecular non-bonding interactions among three anthracene units (vide supra). The difference of the fluorescence spectra between **C3A** and **C4A** was not detected because the overlap of the π-cloud is not significant in **C3A**.

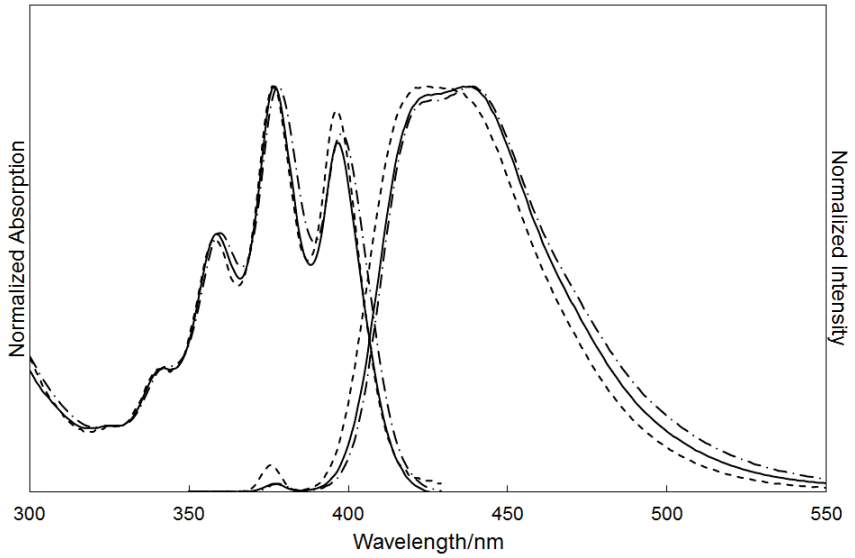

Figure 6. UV and fluorescence spectra of **C3A** (solid line), **C4A** (broken line), and **2** (dotted line) in DCM (r.t., 10^{-5} M).

The absorption and emission spectra of **C3A** and **HC3A** were then investigated to clarify the influence of linker on the optical properties of the molecules. In DCM, the UV spectrum of **HC3A** became broader and the fluorescence band (λ_{max} = 489 nm) was shifted to longer wavelength by 50 nm compared with that of **C3A** (438 nm) (Figure 7a). This red-shift could be related to twisted intramolecular charge transfer (TICT) from the electron-donating aniline moiety to the electron-accepting anthracene unit. To further

support this suggestion, the UV and fluorescence spectra were measured in various solvents. Both the UV and fluorescence spectra demonstrated a small solvent dependence in the case of **C3A**, indicating that the ground-state and excited-state structures of **C3A** were not affected by the solvent character. In sharp contrast, the fluorescence spectrum of **HC3A** became broader and gradually red-shifted with increasing solvent polarity (Figure 7b). As indicated in Figure 7c, the Stokes shift ($\Delta\nu$) showed a linear correlation with the Reichardt's solvent polarity parameter [$E_T(30)$].[38] According to the previous reports,[39–42] these phenomena are consistent with TICT from the aniline moiety to the anthracene unit in **HC3A**.

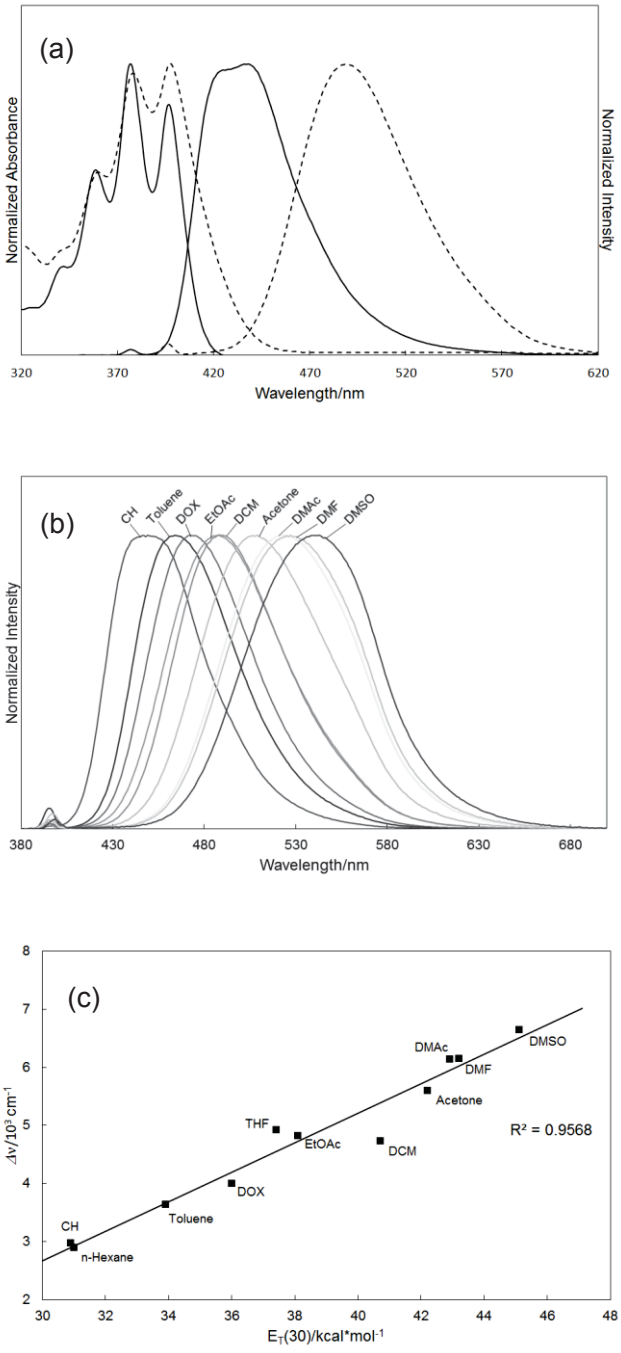

Figure 7. (a) UV and fluorescence spectra of **C3A** (solid line) and **HC3A** (broken line) in DCM (r.t., 10^{-5} M). (b) Solvent-dependent fluorescence spectra of **HC3A** (r.t., 10^{-5} M). (c) Plot between the Stokes shift of **HC3A** and $E_T(30)$ value. Abbreviation: CH; Cyclohexane, DOX; 1,4-Dioxane, EtOAc; Ethyl acetate, DCM; Dichloromethane, DMAc; *N,N*-Dimethylacetamide, DMF; *N,N*-Dimethylformamide, DMSO; Dimethyl sulfoxide.

Figure 8 shows the UV and fluorescence spectra of **HC3A** and a reference compound, *N,N*-dipropyl-4-(10-phenyl-9-anthracenyl)aniline (**DPAA**). The absorption peak maxima of **HC3A** and **DPAA** were similar in both cyclohexane and dimethyl sulfoxide (DMSO), but the tailings to the longer wavelength were detected in **HC3A**. In cyclohexane, which is less polar than DMSO, the fluorescence band of **HC3A** (λ_{max} = 449 nm) was shifted by 5 nm to a longer wavelength than that of **DPAA** (λ_{max} = 444 nm), as a result of intramolecular interactions among three anthracene moieties similarly to **C3A**. In contrast, in more polar DMSO, the fluorescence maximum of **HC3A** (λ_{max} = 543 nm) was blue-shifted by 16 nm compared with that of **DPAA** (λ_{max} = 559 nm). Accordingly, **HC3A** was less sensitive to solvent polarity than **DPAA** was. We suggest that TICT in the excited state of **HC3A** is relatively blocked as a result of restricted bond rotation because of the cyclic architecture. On protonation of the aniline moiety in **HC3A** with trifluoroacetic acid, a significant blue-shift of the fluorescence spectrum and an increase in the emission intensity were observed (Figure 9). It can be deduced that the electron density of the aniline moiety is decreased by protonation and, as a result, TICT from the aniline moiety to the anthracene unit is inhibited. Moreover, the original UV and fluorescence spectra were recovered by addition of excess triethylamine to the proton adduct of **HC3A**. The complete recovery of spectra indicates that the deprotonation was selectively occurred and no electronic interaction between triethylamine and anthracene[43] can be ignored.

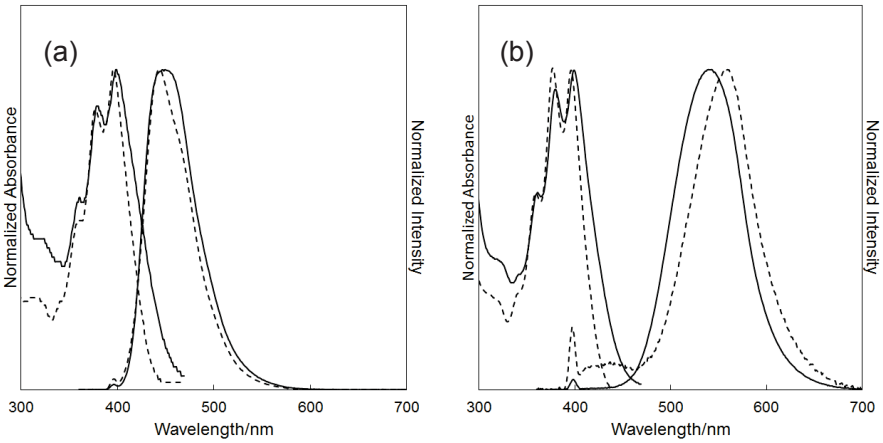

Figure 8. UV and fluorescence spectra of **HC3A** (solid line) and **DPAA** (broken line) (r.t., 10^{-5} M) in (a) CH and (b) DMSO.

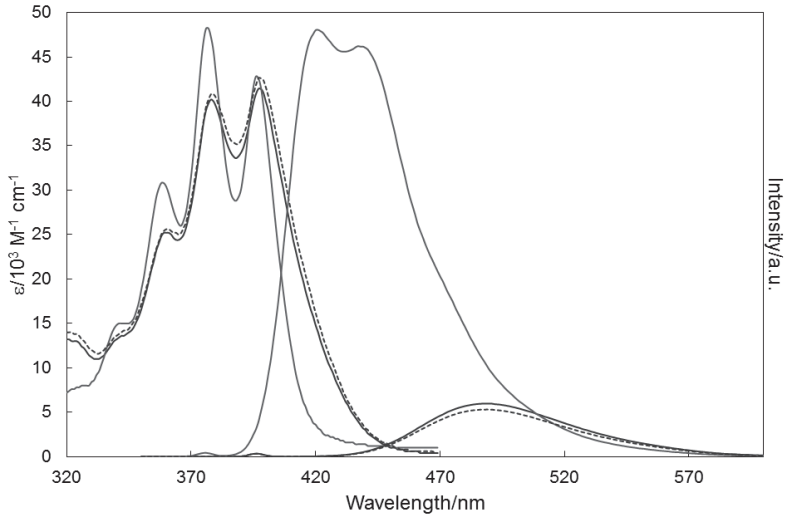

Figure 9. Changes in UV and fluorescence spectra of **HC3A** in DCM upon the addition of TFA and TEA; **HC3A** (black solid line), **HC3A**/TFA = 1/100 (gray solid line), and **HC3A**/TFA/TEA = 1/100/200 (black broken line).

CONCLUSION

In conclusion, we prepared a novel cyclic aromatic amide trimer (**C3A**) and tetramer (**C4A**) containing the DPA unit. The spectroscopic and X-ray crystallographic data for **C3A** show that three anthracene moieties are arranged in a triangular manner and partly stacked intramolecularly, in both the solution and solid states. Reduction of the carbonyl group in **C3A** gave the cyclic trimer **HC3A**, constructed from electron-donating aniline and electron-accepting anthracene units. The fluorescence spectrum of **C3A** showed a small red-shift from that of acyclic model compound **2**. The fluorescence spectrum of **HC3A** was largely red-shifted from that of **C3A** and the collection of spectra in various solvents suggested the occurrence of TICT from the aniline moiety to the anthracene unit.

Experimental section

Materials and instruments

All materials were obtained from commercial suppliers and used without purification. 4-iodoacetanilide[44] and *N*,*N*-dipropyl-4-(10-phenyl-9-anthracenyl)aniline (**DPAA**)[45] were synthesized following to the previous reports. ^{1}H and ^{13}C NMR spectra were investigated on Bruker (Billerica, MA, USA) Avance 200, 400, 500, and 600 FT-NMR spectrometers using tetramethylsilane (^{1}H NMR, δ 0.00) and solvent residual peaks as the internal standards (^{1}H NMR and ^{13}C NMR). IR spectra were recorded on a JASCO (Tokyo, Japan) FT-IR 460Plus spectrophotometer in the attenuated total reflectance (ATR) method. Melting points (M.p.) were determined on a Yanaco (Kyoto, Japan) micro melting point apparatus MP-500D. MALDI-TOF MS analyses were performed on a JEOL (Tokyo, Japan) JMS-S3000 in the spiral mode using dithranol as a matrix. Purifications with preparative GPC were carried out on a Japan analytical industry (Tokyo, Japan) LC-9210 system using tandem JAIGEL 1H, 2H, and 2.5H columns ($CHCl_3$ as an eluent, flow rate = 3.5 mL/min) equipped with an ultraviolet (UV) detector monitored at 254 nm. UV and fluorescence spectra were recorded on a Shimadzu (Kyoto, Japan) UV-1650PC spectrophotometer and a Shimadzu RF-5300PC spectrofluorometer, respectively, using a 10 mm quartz cell. Fluorescence quantum yields (QY) in solution were determined relative to quinine sulfate in 0.05 M H_2SO_4 having a QY of 0.55.

Monomer synthesis

N-Octyl-4-iodoacetanilide (3)

To a solution of 4-iodoacetanilide (3.2 g, 12 mmol) in DMF (60 mL) was added NaH (55% oil suspension) (0.58 g, 14 mmol) at 0 ˚C, and stirred at room temperature for 30 min. 1-Bromooctane (3.1 mL, 18 mmol) was added to the solution and the system was

heated to 100 ˚C for 24 h. The reaction mixture was poured into water and an aqueous phase was extracted with ethyl acetate. The combined extracts were dried over $MgSO_4$ and solvents were removed by the rotary evaporator. The crude product was purified by SiO_2 chromatography (DCM then DCM/ethyl acetate = 1/1) to obtain yellow liquid (3.8 g, 85%). ^{1}H NMR (δ, 200 MHz, ppm, $CDCl_3$) 7.75 (d, *J* = 7.9 Hz, 2H), 6.93 (d, *J* = 7.9 Hz, 2H), 3.65 (t, *J* = 7.4 Hz, 2H), 1.46 (m, 2H), 1.36–1.17 (10 H), 0.87 (t, *J* = 5.2 Hz, 3H). ^{13}C NMR (δ, 50 MHz, ppm, $CDCl_3$) 170.0, 142.9, 140.2, 137.5, 131.5, 129.0, 93.3, 49.0, 32.0, 29.3, 27.8, 22.8, 13.5. IR (cm^{-1}) 2923, 2854, 1658, 1581, 1484, 1400, 1288, 1058, 1008, 831, 717.

***N*-Octyl-4-(10-bromo-9-anthracenyl)acetanilide (4)**

To a mixture of **3** (0.65 g, 2.2 mmol) and 10-bromoanthracene-9-boronic acid (1.0 g, 2.7 mmol) in THF (20 mL) were added 2 M aq. K_2CO_3 (5.0 mL) and $Pd(PPh_3)_4$ (65 mg, 50 μmol), and the system was heated to reflux overnight. After an aqueous phase was extracted with ethyl acetate, the combined organic phase was washed with brine. After drying over $MgSO_4$, solvents were removed by the rotary evaporator. The crude product was purified by flash chromatography (acetone/hexane = 3/5) to obtain yellow powder (1.0 g, 92%).

M.p. 135–136 ˚C. ^{1}H NMR (δ, 200 MHz, ppm, $CDCl_3$) 8.64 (d, *J* = 9.7 Hz, 2H), 7.68–7.55 (4H), 7.51–7.34 (6H), 3.83 (t, *J* = 8.0 Hz, 2H), 2.03 (s, 3H), 1.73–1.60 (2H), 1.36–1.17 (10 H), 0.88 (t, *J* = 6.6 Hz, 3H). ^{13}C NMR (δ, 50 MHz, ppm, $CDCl_3$) 170.2, 142.8, 138.0, 136.3, 133.9, 131.0, 130.2 ,129.4, 128.2, 127.2, 126.7, 124.3, 123.3, 93.3, 49.0, 32.0, 29.3, 27.8, 22.8, 13.5. IR (cm^{-1}) 2958, 2920, 2853, 1638, 1592, 1511, 1402, 1296, 1026, 936, 879, 765, 751, 620.

***N*-Octyl-4-(10-bromo-9-anthracenyl)aniline (5)**

To a solution of **4** (1.3 g/ 2.6 mmol) in DOX (6 mL) were added ethyleneglycol (2 mL) and conc. HCl (8 mL), and the system was stirred for 48 h at 100 ˚C. The reaction mixture was neutralized using saturated aq. Na_2CO_3, and an aqueous phase was extracted with DCM. The combined organic phase was washed with brine. After drying over $MgSO_4$, solvents were removed by the rotary evaporator. The crude product was purified by column chromatography (ethyl acetate/hexane = 1/1) to obtain yellow powder (0.85 g, 71%).

M.p. 85–86 ˚C. ^{1}H NMR (δ, 200 MHz, ppm, $CDCl_3$) 8.57 (d, *J* = 8.8 Hz, 2H), 7.80 (d, *J* = 8.8 Hz, 2H), 7.55 (t, *J* = 7.9 Hz, 2H), 7.34 (d, *J* = 7.9 Hz, 2H), 7.12 (d, *J* = 8.3 Hz, 2H), 6.77 (d, *J* = 8.8 Hz, 2H), 3.79 (bs, 1H), 3.19 (t, *J* = 6.7 Hz, 2H), 1.69 (m, 2H), 1.36–1.17 (10 H), 0.90 (t, *J* = 6.3 Hz, 3H). ^{13}C NMR (δ, 50 MHz, ppm, $CDCl_3$) 147.9, 138.5, 133.1, 131.5, 130.2, 129.0, 128.2, 126.4, 125.4, 123.7, 122.0, 113.4, 44.1, 31.9, 29.6, 29.5, 29.4, 27.8, 22.8, 13.5. IR (cm^{-1}) 3943, 3443, 2946, 2916, 2847, 1604, 1518, 1464, 1437, 1341, 1289, 1258, 1179, 1029, 933, 874, 813, 756, 722, 654, 611.

Monomer (1)

To a mixture of **5** (0.78 g, 1.7 mmol) and 4-methoxycarbonylphenylboronic acid pinacol ester (0.71 g, 2.7 mmol) in THF (17 mL) were added 2 M aq. K_2CO_3 (6.8 mL) and $Pd(PPh_3)_4$ (52 mg, 40 μmol), and the system was heated to reflux overnight. After an aqueous phase was extracted with ethyl acetate, the combined organic phase was washed with brine. After drying over $MgSO_4$, solvents were removed by the rotary evaporator. The resulting solid residue was purified by recrystallization from DCM and hexane to yield yellow powder (0.82 g, 82%)

M.p. 192–193 ˚C. ^{1}H NMR (δ, 600 MHz, ppm, $CDCl_3$) 8.28 (d, *J* = 8.4 Hz, 2H), 7.86 (m, 2H), 7.61–7.55 (4H), 7.32, (m, 4H), 7.26 (d, *J* = 8.7 Hz, 2H), 6.82 (d, *J* = 8.7 Hz, 2H), 3.82 (bs, 1H), 3.24 (t, *J* = 6.9 Hz, 2H), 1.72 (m, *J* = 6.9 Hz, 2H) 1.48 (m, *J* = 6.9

Hz, 2H), 1.42–1.27 (8 H), 0.90 (t, J = 6.8 Hz, 3H). ^{13}C NMR (δ, 150 MHz, ppm, $CDCl_3$) 167.1, 147.9, 144.6, 138.5, 135.1, 132.1, 131.6, 130.3, 129.7, 129.6, 129.3, 127.5, 126.9, 126.3, 125.3, 124.8, 112.4, 52.2, 44.2, 31.9, 29.7, 29.5, 29.2, 27.2, 22.7, 14.2. IR (cm^{-1}) 3400, 2923, 2853, 1707, 1606, 1521, 1478, 1433, 1391, 1319, 1271, 1176, 1111, 1020, 942, 818, 765, 709, 670, 609. Anal. Calcd for $C_{36}H_{37}NO_2$: C, 83.85; H, 7.23; N, 2.72. Found: C, 83.65; H, 7.30; N, 2.65.

General procedure of cyclic oligomerization

Method A

To a THF solution of LiHMDS (1.0 M in THF, 0.5 mL) was added dropwise a THF solution of **1** (0.2 M, 0.5 mL), and the system was stirred for 6 h. After saturated. NH_4Cl was added, an aqueous phase was extracted with DCM. A combined organic phase was dried over $MgSO_4$ and solvents were removed by the rotary evaporator.

Method B

To a THF solution of **1** (0.1 M, 1.0 mL) was added dropwise a THF solution of LiHMDS (1.0 M in THF, 0.5 mL), and the system was stirred for 6 h. After saturated aq. NH_4Cl was added, an aqueous phase was extracted with DCM. A combined organic phase was dried over $MgSO_4$ and solvents were removed by the rotary evaporator. The crude product was purified by preparative GPC ($CHCl_3$ as an eluent) to obtain cyclic oligomers.

C3A

Yield, 40%. M.p. >300 ˚C. ^{1}H NMR (δ, 600 MHz, ppm, $CDCl_3$) 7.64 (d, J = 8.0 Hz, 6H), 7.54 (d, J = 8.9 Hz, 6H), 7.47 (d, J = 8.9 Hz, 6H), 7.41 (d, J = 8.2 Hz, 6H),

7.39–7.36 (12H), 6.94 (m, 6H), 6.89 (m, 6H), 4.21 (t, *J* = 7.8 Hz, 6H), 1.91 (m, 6H), 1.54 (m, 6H), 1.38 (m, 6H), 1.36–1.30 (18 H), 0.91 (t, *J* = 6.8 Hz, 9H). ^{13}C NMR (δ, 150 MHz, ppm, $CDCl_3$) 170.9, 143.5, 140.7, 137.9, 136.8, 136.6, 136.3, 132.4, 131.0, 130.0, 129.9, 129.4, 128.5, 126.9, 126.6, 126.0, 125.9, 50.5, 32.3, 29.9, 29.7, 28.5, 27.5, 23.1, 14.6. IR (cm^{-1}) 3904, 3059, 2925, 2852, 1648, 1603, 1511, 1438, 1377, 1293, 1177, 1020, 943, 828, 766, 670, 611. MALDI-TOF MS Calcd for $C_{105}H_{100}N_3O_3$ ($M+H^+$): 1451.78. Found: 1451.73. Anal. Calcd for $C_{105}H_{99}N_3O_3$: C, 86.92; H, 6.88; N, 2.90. Found: C, 86.33; H, 6.93; N, 2.77.

C4A

Yield 8%. M.p. >300 ˚C. ^{1}H NMR (δ, 600 MHz, ppm, $CDCl_3$) 7.67 (d, *J* = 7.9 Hz, 6H), 7.60 (d, *J* = 8.3 Hz, 6H), 7.57 (d, *J* = 8.3 Hz, 6 H), 7.43 (d, *J* = 8.3 Hz, 6H), 7.41 (d, *J* = 8.3 Hz, 6H), 7.35 (d, *J* = 8.3 Hz, 6H), 7.15 (t, *J* = 7.0 Hz, 6H), 7.11 (t, *J* = 7.0 Hz, 6H), 4.18 (t, *J* = 7.4 Hz, 6H), 1.90 (m, 6H), 1.52 (m, 6H), 1.43 (m, 6H), 1.37 (m, 6H), 1.36–1.17 (18 H), 0.90 (t, *J* = 7.0 Hz, 9H). IR (cm^{-1}) 3820, 3020, 2955, 2923, 2851, 1723, 1645, 1511, 1378, 1290, 1121, 1020, 764, 670, 612. MALDI-TOF MS Calcd for $C_{140}H_{133}N_4O_4$ ($M+H^+$): 1935.03. Found: 1934.50.

Reduction of amide carbonyl group

To ether (0.48 mL) solution of $LiAlH_4$ (9.0 mg/ 0.24 mmol) and $AlCl_3$ (32 mg/ 0.24 mmol) was added dropwise **C3A** (29 mg/ 0.02 mmol) in THF (0.24 mL) at 0˚C, and the system was stirred for 2 h at room temperature. The reaction mixture was quenched with cold H_2O (2 mL), cold 2M aq. NaOH (2 mL), and H_2O (6 mL). After an aqueous phase was extracted with DCM, the combined organic phase was washed with brine. After drying over $MgSO_4$, solvents were removed by the rotary evaporator. The crude

product was purified by preparative GPC ($CHCl_3$ as an eluent) to obtain **HC3A** (26 mg, 93%). M.p. 127–128 ˚C. ^{1}H NMR (δ, 600 MHz, ppm, $CDCl_3$) 7.69 (m, 6H), 7.54 (m, 6H), 7.50 (d, J = 7.5 Hz, 6H), 7.41 (d, J = 7.5 Hz, 6H), 7.25 (d, J = 7.9 Hz, 6 H), 7.97 (12 H), 6.90, (d, J = 7.43 Hz, 6H), 4.90 (s, 6H), 3.78 (t, J = 7.4 Hz, 6H), 1.97 (m, 6H), 1.50 (m, 6H), 1.46–1.31 (24 H), 0.95 (t, J = 6.1 Hz, 9H). ^{13}C NMR (δ, 150 MHz, ppm, $CDCl_3$) Not available due to low solubility. IR (cm^{-1}) 3063, 2928, 2853, 1606, 1518, 1395, 1183, 1027, 767, 672. MALDI-TOF MS Calcd for $C_{105}H_{105}N_3^{\cdot+}$ ($M^{\cdot+}$): 1407.83. Found: 1407.83.

X-ray crystallographic analysis

Crystallographic data were collected on a CCD diffractometer with Cu Kα (λ = 1.54178 Å) radiation. Data collections were carried out at low temperature using liquid nitrogen. All of the crystal structures were solved by direct methods with SHELXS-97 and refined with full-matrix least-squares SHELXL-97.[46] All non-hydrogen atoms were refined anisotropically and hydrogen atoms were included at their calculated positions.

Crystal data for **C3A'**: $C_{90}H_{69}N_3O_3 \cdot 5CHCl_3$, M_r = 1837.32, Monoclinic, $P2_1$, a = 22.2423(5), b = 9.3087(2), c = 22.5200(6) Å, β = 103.449(2)°, V = 4534.83(19) Å^3, Z = 2, D_c = 1.346 Mg m^{-3}, $2\theta_{max}$ = 135.74°, T = 173 K, 30648 reflections measured, 12985 unique (R_{int} = 0.0334), μ = 4.570 mm^{-1}. The final R_1 and wR_2 were 0.0856 and 0.2403 ($I > 2\sigma(I)$), 0.1008 and 0.2640 (all data). CCDC-961419. Some atoms of propyl groups and chloroform molecules are disordered to two positions respectively. The occupancies of the disordered atoms were refined.

Crystal data for **C4A'**: $C_{120}H_{92}N_4O_4 \cdot 6CHCl_3$, M_r = 2370.18, Triclinic, P-1, a = 10.5211(2), b = 13.4415(3), c = 21.8375(4) Å, α = 92.4470(10), β = 96.5220(10), γ = 111.4330(10)°, V = 2844.21(10) Å^3, Z = 1, D_c = 1.384 Mg m^{-3}, $2\theta_{max}$ = 136.06°, T = 120

K, 35078 reflections measured, 9867 unique (R_{int} = 0.0300), μ = 4.417 mm^{-1}. The final R_1 and wR_2 were 0.0905 and 0.2627 ($I > 2\sigma(I)$), 0.1174 and 0.2948 (all data). CCDC-961420. Some atoms of propyl groups and chloroform molecules are disordered to two positions respectively. The occupancies of the disordered atoms were refined.

References and notes

1) J.-L. Brédas, J. Cornil, D. Beljonne, D. A. dos Santos, and Z. Shuai, *Acc. Chem. Res*. **1999**, *32*, 267.

2) J.-L. Brédas, D. Beljonne, V. Coropceanu, and J. Cornil, *Chem. Rev.* **2004**, *104*, 4971.

3) J. H. Burroughes, D. D. C. Bradley, A. R. Brown, R. N. Marks, K. Mackay, R. H. Friend, P. L. Burns, and A. B. Holmes, *Nature* **1990**, *347*, 539.

4) H. Sirringhaus, N. Tessler, and R. H. Friend, *Science* **1998**, *280*, 1741.

5) N. S. Sariciftci, L. Smilowitz, A. J. Heeger, and F. Wudl, *Science* **1992**, *258*, 1474.

6) T. Förster, *Ann. Phys.* **1948**, *2*, 55.

7) G. C. Bazan, W. J. Oldham, Jr., R. J. Lachicotte, S. Tretiak, V. Chernyak, and S. Mukamel, *J. Am. Chem. Soc.* **1998**, *120*, 9188.

8) J. W. Hong, B. S. Gaylord, and G. C. Bazan, *J. Am. Chem. Soc.* **2002**, *124*, 11868.

9) J. W. Hong, H. Y. Woo, B. Liu, and G. C. Bazan, *J. Am. Chem. Soc*. **2005**, *127*, 7435.

10) Y. Morisaki, and Y. Chujo, *Macromolecules* **2002**, *35*, 587.

11) Y. Morisaki, and Y. Chujo, *Macromolecules* **2003**, *36*, 9319.

12) Y. Morisaki, F. Fujimura, and Y. Chujo, *Organometallics* **2003**, *22*, 3553.

13) X. H. Sun, C. S. Chan, M. S. Wong, and W. Y. Wong, *Tetrahedron* **2006**, *62*, 7846.

14) C. Song, and T. M. Swager, *Org. Lett.* **2008**, *10*, 3575.

15) A. Molad, I. Goldberg, and A. Vigalok, *J. Am. Chem. Soc.* **2012**, *134*, 7290.

16) S. Mataka, K. Takahashi, T. Mimura, T. Hirota, K. Takuma, H. Kobayashi, and M. Tashiro, *J. Org. Chem.* **1987**, *52*, 2653.

17) K. M. Knoblock, C. J. Silvestri, and D. M. Collard, *J. Am. Chem. Soc.* **2006**, *128*, 13680.

18) V. J. Chebny, R. Shukla, S. V. Lindeman, and R. Rathore, *Org. Lett.* **2009**, *11*, 1939.

19) T. Ogoshi, K. Umeda, T. Yamagishi, nad Y. Nakamoto, *Chem. Commun*. **2009**, 4874.

20) T. Ogoshi, R. Shiga, M. Hashizume, and T. Yamagishi, *Chem. Commun.* **2011**, *47*, 6927.

21) Y. Morisaki, R. Hifumi, L. Lin, K. Inoshita, and Y. Chujo, *Polym. Chem.* **2012**, *3*, 2727.

22) R. Yamakado, S. Matsuoka, M. Suzuki, K. Takagi, K. Katagiri, and I. Azumaya, *Tetrahedron* **2013**, *69*, 1516.

23) K. Takagi, S. Sugimoto, R. Yamakado, and K. Nobuke, *J. Org. Chem.* **2011**, *76*, 2471.

24) R. Yamakado, K. Mikami, K. Takagi, I. Azumaya, S. Sugimoto, S. Matsuoka, M. Suzuki, K. Katagiri, M. Uchiyama, and A. Muranaka, *Chem. Eur. J*. **2013**, *19*, 11853.

25) S. S. Babu, M. J. Hollamby, J. Aimi, H. Ozawa, A. Saeki, S. Seki, K. Kobayashi, K. Hagiwara, M. Yoshizawa, H. Möhwald, and T. Nakanishi, *Nature Commun*. **2013**, *4*, 1969.

26) Y. Fujiwara, R. Ozawa, D. Onuma, K. Suzuki, K. Yoza, and K. Kobayashi, *J. Org. Chem.* **2013**, *78*, 2206.

27) K. Hagiwara, Y. Sei, M. Akita, and M. Yoshizawa, *Chem. Commun*. **2012**, *48*, 7678.

28) K. Miyamoto, T. Iwanaga, S. Toyota, *Chem. Lett*. **2010**, *39*, 288.

29) S. Chen, Q. Yan, T. Li, and D. Zhao, *Org. Lett*. **2010,** *12*, 4784.

30) G. Venkataramana, P. Dongare, L. N. Dawe, D. X. Thompson, Y. Zhao, and G. Bodwell, *Org. Lett.* **2011**, *13*, 2240.

31) V. H. Gessner and T. D. Tilley, *Org. Lett.* **2011**, *13*, 1154.

32) T. Li, K. Yue, Q. Yan, H. Huang, H. Wu, N. Zhu, and D. Zhao, *Soft Matter.* **2012**, *8*, 2405.

33) W. C. W. Leu, A. E. Fritz, M. Diganantonio, and C. S. Hartley, *J. Org. Chem.* **2012**,

77, 2285.

34) A. Yokoyama, T. Maruyama, K. Tagami, H. Masu, K. Katagiri, I. Azumaya, and T. Yokozawa, *Org. Lett*. **2008**, *10*, 3207.

35) I. Azumaya, H. Kagechika, K. Yamaguchi, and K. Shudo, *Tetrahedron Lett*. **1996**, *37*, 5003.

36) H. Kakuta, I. Azumaya, H. Masu, M. Matsumura, K. Yamaguchi, H. Kagechika, and A. Tanatani, *Tetrahedron* **2010**, *66*, 8254.

37) N. Fujimoto, M. Matsumura, I. Azumaya, S. Nishiyama, H. Masu, H. Kagechika, and A. Tanatani, *Chem. Commun*. **2012**, *48*, 4809.

38) C. Reichardt, *Chem. Rev.* **1994**, *94*, 2319.

39) A. Simiarzuk, Z. R. Grabowski, A. Krówczyñski, M. Asher, and M. Ottolenghi, *Chem. Phys. Lett.* **1977**, *51*, 315.

40) J. Herbich, A. Kapturkiewicz, and W. Rettig, *Chem. Phys*. **1991**, *158*, 143.

41) Z. R. Grabowski, K. Rotkiewicz, W. Rettig, *Chem. Rev*. **2003**, *103,* 3899.

42) Z. Li, H. Ishizuka, Y. Sei, M. Akita, and M. Yoshizawa, *Chem. Asian J.* **2012**, *7*, 1789.

43) T. Nakayama, T. Hamana, P. Jane, S. Akimoto, I. Yamazaki, and K. Hamanoue, *J. Phys. Chem*. **1996**, *100*, 18431.

44) P. Hrobárik, V. Hrobáriková, I. Sigmundová, P. Zahradnik, M. Fakis, I. Polyzos, and P. Persephonis, *J. Org. Chem.* **2011**, *76*, 8726.

45) M. Kawai, K. Itaya, and S. Toshima, *J. Phys. Chem*. **1980**, *84*, 2368.

46) A short history of SHELX. G. M. Sheldrick, *Acta Cryst*. **2008**, A64, 112.

Chapter 6

Summary

In this thesis, the author has described programmable assembly of π-conjugated systems utilizing the stereochemistry of aromatic tertiary amide units as new scaffolds for the three-dimensional arrangement of π-conjugated molecules.

In Chapter 2, preparation of molecular cage by coordination of calix[3]amide bearing pyridine with palladium complexes is described. The cyclization of methyl 3-nonylamino-5-(pyridin-4-yl)benzoate was carried out with LiHMDS. The conformation of the cyclic trimers was analyzed by VT-NMR measurements. The proportion of the *syn* conformer was increased with increasing polarity of solvents. The 2:3 mixture of calix[3]amide bearing pyridine and [Pd(dppp)$(OTf)_2$] in $CDCl_3/CD_3OD$ = 5/1 (in volume) gave the molecular cage, whose structure was supported by ESI-MS, DOSY, ^{1}H NMR, and ^{31}P NMR spectra. In contrast, the formation of polymeric mixture was observed in $CDCl_3$, in which the *trans* conformer is predominant. Accordingly, the conformation change of calix[3]amide triggered by solvent character has a large impact on the formation of the molecular cage.

In Chapter 3, the author describes the screw-shaped alignment of pyrene using calix[3]amide. Calix[3]amides bearing three pyrenes was synthesized by the condensation reaction using Ph_3PCl_2. Pyrenyl groups were found to be aligned in the screw-like fashion by calix[3]amide as confirmed by the X-ray crystallography. Aromatic proton signals observed at the up-field region (6.1 – 6.9 ppm) in the ^{1}H NMR spectrum at 233 K indicated that pyrenyl groups are aligned in close proximity in the THF solution. The pyrenyl groups are arranged closely but cannot form the face-to-face stacked structure, so that the fluorescence emission from the associate state (excimer emission) was not observed. In contrast, the compound having the flexible spacer between pyrene and calix[3]amide showed excimer emission.

In Chapter 4, three-dimensional arrangement of π-conjugated molecules with triple-stranded helicity has been achieved using the planar chirality of calix[3]amide. The cyclic oligomerization was carried out by the dropwise addition of LiHMDS to a dilute THF solution of the bis(nonylaminobenzoate) derivative. As expected, three optical isomers, generated by the direction of the amide bond of calix[3]amide, was detected in the ratio of 1:2:1 by chiral HPLC. The absolute configuration of the calix[3]amide and the preferred helicity of the bithiophene units were determined by the combination of experimental and theoretical studies. It is worth mentioning that ECD and VCD analyses were mutually complementary in aiding the interpretation of the chiral structure in the present system; the ECD spectroscopy was sensitive to the helicity of the bithiophene chromophores, whereas the VCD spectroscopy was sensitive to the planar chirality of the calix[3]amide.

In Chapter 5, the author describes the synthesis and optical properties of cyclic trimer bearing 9,10-diphenylanthracene based on an aromatic tertiary amide. The cyclic aromatic amide oligomers containing highly fluorescent 9,10-diphenylanthracene units were prepared by condensation of the monomer with amino and ester functional groups using LiHMDS. The spectroscopic and X-ray crystallographic data for the trimer show that three anthracene moieties are arranged in a triangular manner and partly stacked intramolecularly, in both the solution and solid states. The amide trimer showed a small red-shift in the fluorescence spectrum as compared with the acyclic model compound. Reduction of the amide carbonyl groups in the trimer gave cyclic trimer **HC3A**, which has tertiary amine units. The fluorescence peak maximum of **HC3A** was largely red-shifted from that of amide trimer and exhibited strong solvent dependence. A linear

correlation was observed between the Stokes shift ($\Delta\nu$), ranging from 2981 to 6646 cm^{-1}, and the Reichardt's solvent polarity parameter [$E_T(30)$]. This phenomenon suggested the occurrence of TICT from the aniline moiety to the anthracene unit.

As summarized above, this thesis deals with the programmable assembly of pi-conjugated systems based on the stereochemistry of the aromatic tertiary amides. The systematic investigation on the conformation and the optical properties of the π-conjugated moieties based on the cyclic aromatic triamide gave much valuable information for their three-dimensional arrangement. Various arrangements of π-conjugated moieties will be realized without any difficulties, since the present method can be tolerant of various substituents on the monomer. Furthermore, chiral arrangement of π-conjugated moieties is simply prepared, because the cyclic oligo amide has planner chirality without chiral substituents. The author hopes the study described in this thesis will be widely referred and matured in the future.

List of Publication

Chapter 2

Preparation of Molecular Cage by Coordination of *m*-Calix[3]amide Bearing Pyridine with Palladium Complex, Ryohei Yamakado, Shin-ichi Matsuoka, Masato Suzuki, Yasuhiro Funahashi, and Koji Takagi, *Chemistry Letters*, **2012**, 41, 249 – 251.

Chapter 3

A screw-shaped alignment of pyrene using *m*-calix[3]amide, Ryohei Yamakado, Shin-ichi Matsuoka, Masato Suzuki, Koji Takagi, Kosuke Katagiri, Isao Azumaya, *Tetrahedron*, **2013**, 69, 1516 – 1520.

Chapter 4

Helicity Induction in Three π-Conjugated Chromophores by Planner Chirality of Calixamide, Ryohei Yamakado, Koichiro Mikami, Koji Takagi, Isao Azumaya, Shinri Sugimoto, Shin-ichi Matsuoka, Masato Suzuki, Kosuke Katagiri, Masanobu Uchiyama, and Atsuya Muranaka, *Chemistry a European Journal*, **2013**, 19, 11853 – 11857.

Chapter 5

Synthesis and Optical Properties of Cyclic Trimer bearing 9,10-Diphenylanthracene Based on an Aromatic Tertiary Amide Unit Ryohei Yamakado, Shin-ichi Matsuoka, Masato Suzuki, Daisuke Takeuchi, Hyuma Masu, Isao Azumaya, and Koji Takagi, *RSC Advances* submitted.

Other Publication

Self-Assembly of Oligothiophene Chromophores by *m*-Calix[3]amide Scaffold, Koji Takagi, Shinri Sugimoto, Ryohei Yamakado, and Katsuya Nobuke, *The Journal of Organic Chemistry*, **2011**, 2471 – 2478.

3 位をビチオフェンで修飾した 4-オクチルアミノ安息香酸メチル類の重縮合と光学特性、信家克哉、山門陵平、高木幸治、*高分子論文集*、**2011**, 68, 33 – 38.

Synthesis and optical properties of poly(*p*-benzamide)s bearing oligothiophene on the amide nitrogen atom through an alkylene spacer, Koji Takagi, Katsuya Nobuke, Yuma Nishikawa, and Ryohei Yamakado, *Polymer Journal*, **2013**, in press

List of Presentation

1. Synthesis of cyclic *m*-aromatic amide oligomer having heterocycles at meta-position and optical properties, Ryohei Yamakado, Shinri Sugimoto, and Koji Takagi, in 58th SPSJ Annual Meeting, 1Pd016, Kobe, May, 2009.
2. Synthesis of cyclic *m*-aromatic amide oligomer having pi-conjugated system at meta-position and optical properties, Ryohei Yamakado, Shinri Sugimoto, and Koji Takagi, in 58th SPSJ Symposium on Macromolecules, 3Pc007, Kumamoto, September, 2009.
3. Synthesis and characteristic of cyclic *m*-aromatic amide oligomer having functional group at meta-position, Ryohei Yamakado, Shinri Sugimoto, and Koji Takagi, in The 1st FAPS Polymer Congress, 21PG1-062b, Nagoya, October, 2009.
4. Synthesis and characterization of *m*-calixamide having pi-conjugated system, Ryohei Yamakado, Shin-ichi Matsuoka, Masato Suzuki, and Koji Takagi, in The 90th Annual Meeting of CSJ, 3E3-15, Osaka, March, 2010.
5. Aggregation of chromophores based on calix[3]amide and optical properties, Ryohei Yamakado, Shin-ichi Matsuoka, Masato Suzuki, and Koji Takagi, in 59th SPSJ Annual Meeting, 3C05, Yokohama, May, 2010.
6. Synthesis and characterization of *m*-calix[3]amide having π-conjugated system, Ryohei Yamakado, Shin-ichi Matsuoka, Masato Suzuki, and Koji Takagi, in 2010 International Chemical Congress of Pacific Basin Societies, 21PG1-062b, Hawaii, December, 2010.
7. Synthesis and characterization of calix[3]amide bearing pyridine for building molecular capsules, Ryohei Yamakado, Shin-ichi Matsuoka, Masato Suzuki, and Koji Takagi, in The 91st Annual Meeting of CSJ, 3E3-36, Yokohama, March, 2011.
8. Synthesis of molecular capsule through complexation of calix[3]amide having pyridine with palladium ion, Ryohei Yamakado, Shin-ichi Matsuoka, Masato Suzuki, and Koji Takagi, in 60th SPSJ Annual Meeting, 1L17, Osaka, May, 2011.

9. Synthesis of calix[3]amide having pyrene as chromophore and optical properties there of, Ryohei Yamakado, Shin-ichi Matsuoka, Masato Suzuki, and Koji Takagi, in 60th SPSJ Annual Meeting, 1Pf024, Osaka, May, 2011.
10. Alignment of π-conjugated systems based on calix[3]amide skeleton, Ryohei Yamakado, Shin-ichi Matsuoka, Masato Suzuki, and Koji Takagi, in 22nd Symposium on Pysical Organic Chemistry, 1P098, Tsukuba, September, 2011.
11. Synthesis and characterization of twin *m*-calix[3]amide connected by bithiophenes, Ryohei Yamakado, Shinri Sugimoto, Shin-ichi Matsuoka, Masato Suzuki, and Koji Takagi, in The 92nd Annual Meeting of CSJ, 1M3-25, Yokohama, March, 2012.
12. Synthesis of substituted poly (*m*-benzamide)s for alignment of pyrene, Ryohei Yamakado, Haruka Egoshi, Yuma Nishikawa, Katsuya Nobuke, Shin-ichi Matsuoka, Masato Suzuki, and Koji Takagi, in 61st SPSJ Annual Meeting, 1Pe005, Yokohama, May, 2012.
13. Synthesis of polybenzamides bearing π-conjugated system: Alignment of π-conjugated systems and optical properties, Ryohei Yamakado, Yuma Nishikawa, Shin-ichi Matsuoka, Masato Suzuki, Koji Takagi, Polycondensation 2012, San Francisco, September, 2012
14. Synthesis and optical properties of novel cyclic aromatic amides by the cyclization of anthracene derivatives functionalized at the 9,10-positions, Ryohei Yamakado, Shin-ichi Matsuoka, Masato Suzuki, Koji Takagi, Daisuke Takeuchi, and Isao Azumaya, in 62nd SPSJ Symposium on Macromolecules, Kanazawa, 2013.
15. 第三級芳香族アミド骨格を用いたπ共役系分子の環状集合化および不斉誘起に関する研究, Ryohei Yamakado, Shin-ichi Matsuoka, Masato Suzuki, Koji Takagi, 3rd CSJ Chemistry Festa, Tokyo, 2013.

Acknowledgements

The studies described in this thesis have been carried out under the direction of Associate Professor Koji Takagi at the Department of Materials Science and Engineering, Graduate School of Engineering, Nagoya Institute of Technology, during 2008 – 2014.

The author wishes to express his sincere thanks to Associate Professor Koji Takagi for his valuable guidance, inspiration, assistance, and trenchant advice at times throughout this study. The author is also extremely grateful to Prof. Masato Suzuki and Dr. Shin-ichi Matsuoka for their constant advice, very useful discussion, sharp insights, and very kind encouragement.

The author would like to make the special acknowledgement to Prof. Isao Azumaya (Faculty of Pharmaceutical Science, Toho University) to give valuable discussions, advices, and hearty encouragement. The author thanks to Prof. Yoshihito Inai, Dr. Akinori Takasu (Department of Frontier Materials), and Dr. Daisuke Takeuchi (Chemical Resources Laboratory, Tokyo Institute of Technology) for precious advices, suggestion, and warm encouragement. The author grateful to Prof. Masanobu Uchiyama, Dr. Koichiro Mikami (Graduate School of Pharmaceutical Sciences, The University of Tokyo), and Dr. Atsuya Muranaka (Advenced Elements Chemistry Research Team and Element Research Laboratory, RIKEN) for theoretical calculation. The author also make acknowledgement to Prof. Yasuhiro Funahashi (Department of Chemistry, Osaka University), Dr. Hyuma Masu (Center for Analytical Instrumentation, Chiba University) and Dr. Kosuke Katagiri (Faculty of Pharmaceutical Science at Kagawa Campus, Tokushima Bunri University) for single crystal X-ray diffraction.

Furthermore, it is pressure to express the author's wholehearted appreciates to his all colleagues who spend grateful and precious time with him at Suzuki-Takagi-Matsuoka laboratory, especially to Mr. Shinri Sugimoto, Mr. Naoto Okumura, Mr. Katsuya Nobuke, Mr.

Takashi Atsumi, Mr. Yohei Ito, Mr. Eiki Kawagita, Ms. Haruka Egoshi and Ms. Yuma Nishikawa for their valuable discussion, advice, information, technical helps and enjoyable times.

Finally, the author expresses his heartfelt thanks to his parent, Mr. Yoshihiko Yamakado and Mrs. Satomi Yamakado, and his sister, Ms. Chiaki Yamakado.

Ryohei Yamakado

山門 陵平

March 2014